

**MAGNETICALLY CONFINED KINETIC-ENERGY
STORAGE RING: A NEW
FUNDAMENTAL ENERGY-STORAGE CONCEPT**

by

John R. Hull and Malvern K. Iles



**RETURN TO REFERENCE FILE
TECHNICAL PUBLICATIONS
DEPARTMENT**

ARGONNE NATIONAL LABORATORY, ARGONNE, ILLINOIS

Operated by THE UNIVERSITY OF CHICAGO

for the U. S. DEPARTMENT OF ENERGY

under Contract W-31-109-Eng-38

Argonne National Laboratory, with facilities in the states of Illinois and Idaho, is owned by the United States government, and operated by The University of Chicago under the provisions of a contract with the Department of Energy.

DISCLAIMER

This report was prepared as an account of work sponsored by an agency of the United States Government. Neither the United States Government nor any agency thereof, nor any of their employees, makes any warranty, express or implied, or assumes any legal liability or responsibility for the accuracy, completeness, or usefulness of any information, apparatus, product, or process disclosed, or represents that its use would not infringe privately owned rights. Reference herein to any specific commercial product, process, or service by trade name, trademark, manufacturer, or otherwise, does not necessarily constitute or imply its endorsement, recommendation, or favoring by the United States Government or any agency thereof. The views and opinions of authors expressed herein do not necessarily state or reflect those of the United States Government or any agency thereof.

Printed in the United States of America
Available from
National Technical Information Service
U. S. Department of Commerce
5285 Port Royal Road
Springfield, VA 22161

NTIS price codes *
Printed copy: A06
Microfiche copy: A01

ANL-84-19

ARGONNE NATIONAL LABORATORY
9700 South Cass Avenue
Argonne, Illinois 60439

MAGNETICALLY CONFINED KINETIC-ENERGY STORAGE RING:
A NEW FUNDAMENTAL ENERGY-STORAGE CONCEPT

by

John R. Hull
Components Technology Division, ANL

and

Malvern K. Iles
Ames Laboratory
Iowa State University
Ames, Iowa

February 1984

CONTENTS

ABSTRACT.....	1
1. INTRODUCTION.....	1
1.1 General MCKESR Description.....	1
1.2 Applications.....	3
1.3 Major Design Options.....	3
1.4 Example Design.....	5
2. BACKGROUND.....	9
2.1 Alternative Energy-Storage Technologies.....	9
2.1.1 Pumped Hydroelectric Storage.....	9
2.1.2 Underground Pumped Hydroelectric Storage.....	9
2.1.3 Compressed-Air Storage.....	9
2.1.4 Batteries.....	10
2.1.5 Superconducting Magnetic-Energy Storage.....	10
2.1.6 Flywheels.....	10
2.2 Analogies with Other Technologies.....	11
2.2.1 Superconducting Magnetic-Energy Storage.....	11
2.2.2 Flywheels.....	12
2.2.3 Synchrotrons.....	12
2.2.4 Levitated Trains.....	13
2.3 Cost Comparison with Alternative Energy-Storage Technologies	13
2.4 Development History of MCKESR.....	13
2.5 References.....	16
3. BASIC PHYSICS OF THE ROTATIONAL RING.....	18
3.1 Rotating Point Particle.....	18

3.2 Basic Ring Relationships.....	18
3.2.1 Magnetic Pressure.....	20
3.2.2 Current Density.....	22
3.3 Levitation.....	23
3.4 Discussion.....	23
4. LEVITATION METHODS.....	25
4.1 Introduction.....	25
4.1.1 Repulsive Levitation due to Eddy Currents.....	26
4.1.2 Superconducting Ring.....	26
4.1.3 Mixed Mu Levitation.....	28
4.2 Superconducting Ring.....	28
4.2.1 Synchrotron Analog.....	28
4.2.2 Solid Ring.....	31
4.2.3 Modular Ring.....	33
4.3 Nonsuperconducting Rings.....	35
4.3.1 Introduction.....	35
4.3.2 Repulsive Image-Force Levitation Systems.....	36
4.3.2.1 Calculation of Losses.....	36
4.3.2.2 Thin-Track Approximation.....	37
4.3.2.3 Thick-Track Approximation.....	38
4.3.2.4 Discussion.....	38
4.3.3 Repulsive Null-Flux Levitation Systems.....	38
4.3.4 Attractive Levitation Systems.....	40
4.3.5 Stability of Attractive Levitation Systems.....	41
4.3.5.1 Attractive Systems.....	41
4.3.5.2 Repulsive Levitation Stabilizers.....	42
4.3.5.3 Dynamic Stabilization.....	43
4.4 Radially Stable Attractive Levitation.....	44
4.4.1 Physics of Interacting Current Loops.....	44
4.4.2 Application to MCKESR.....	49
4.5 Torque on the MCKESR due to Earth's Rotation.....	49
4.6 References.....	52
4.7 Partial Bibliography of Magnetic Levitation.....	54

5.	SOURCES OF RING HEATING.....	63
	5.1 Heat Production from Skin Friction.....	63
	5.1.1 Continuum Region	64
	5.1.2 Free-Molecule Region.....	64
	5.1.3 Accommodation Coefficient.....	65
	5.1.4 Transition Region.....	65
	5.1.5 Results.....	66
	5.2 Tunnel Vacuum.....	66
	5.3 Eddy-Current Heating.....	68
	5.3.1 Levitation-Field Inhomogeneities.....	68
	5.3.2 Precession.....	69
	5.4 References.....	69
6.	RING-COOLING METHODS.....	71
	6.1 Radiant Cooling.....	71
	6.2 Inertial Cooling.....	72
	6.2.1 Lattice Heat Capacity at Low Temperatures.....	73
	6.2.2 Magnetic Heat Capacity.....	74
	6.3 Magnetic Refrigeration.....	74
	6.3.1 Thermal Diode.....	74
	6.3.2 Refrigeration Cycle.....	77
	6.3.3 Other Features.....	78
	6.4 Thermoelectric or Thermomagnetic Cooling.....	78
	6.5 Stirling-Cycle Refrigerators.....	82
	6.6 Transfer of Liquid Helium.....	82
	6.7 References.....	82
7.	POWER INPUT AND OUTPUT.....	83
	7.1 Synchronous Motor.....	83
	7.2 Power Conditioning.....	85
	7.3 References.....	85

8.	CONTROL OF PERSISTENT CURRENTS.....	86
	8.1 Magnetic Induction.....	86
	8.2 Flux Pump.....	86
	8.3 References.....	88
9.	PLANT DESIGN.....	89
	9.1 General Plant Design.....	89
	9.2 Containment Shell.....	89
	9.2.1 Dewar-Wall Heat Loss.....	89
	9.2.2 Virial Theorem.....	92
	9.3 Rock Mechanics.....	93
	9.4 Thermal Contraction.....	93
	9.5 Safety.....	93
	9.6 References.....	94
10.	PERFORMANCE ANALYSIS.....	95
	10.1 Efficiency.....	95
	10.2 Cost Analysis.....	96
	10.3 References.....	98
11.	FUTURE DEVELOPMENT.....	99
	11.1 Critical Research Needs.....	99
	11.2 Possible Technological Niches.....	100
	11.3 References.....	101

FIGURES

1.1	Solid-Ring Design in Weak-Focusing Synchrotron Magnetic Field....	7
1.2	Ring Design in Quadrupole-Type Magnetic Field.....	8
2.1	Specific Energy and Capital Cost: MCKESR vs. Other Energy-Storage Technologies.....	14
3.1	Ring Cross-Section.....	19
3.2	Angular Wedge of Ring.....	21
4.1	Repulsive Levitation Method for Nonsuperconducting Ring.....	27
4.2	Attractive Levitation of Nonsuperconducting Magnetic Ring Using Superconducting Shields for Vertical Stabilization.....	29
4.3	Power Input and Output Method for a Modular Ring in a Weak-Focusing Synchrotron Confinement Field.....	34
4.4	Coordinate System of Two Interacting Current Loops.....	45
4.5	Acceleration Force Between Two Interacting Current Loops as a Function of their Separation Distance.....	47
4.6	Restoring-Force Constant for Two Interacting Current Loops as a Function of their Separation Distance.....	48
4.7	Coordinate System for Calculation of Torque on MCKESR Due to Earth's rotation.....	51
5.1	Skin-Friction Heating as a Function of Pressure for Several Velocities.....	67
6.1	Superconducting-Ring Cross-Section with Magnetic Refrigeration	75
6.2	Magnetic Refrigeration Cycle.....	76
6.3	Entropy vs. Temperature for Gadolinium Sulfate Octahydrate for Several Applied Magnetic-Field Strengths.....	79
6.4	Entropy vs. Temperature for Gadolinium Hydroxide for several Applied Magnetic-Field Strengths.....	80

7.1	Relationship between Applied Magnetic Field and Current Slab in Synchronous-Motor Power-I/O Method.....	84
8.1	Flux-Pump Method of Creating and Maintaining Persistent Current in a Superconducting Ring.....	87
9.1	General MCKESR Plant Layout.....	90
9.2	Trench Cross-Section.....	91

TABLES

1.1	Major Magnetic-Confinement Options for MCKESR.....	4
3.1	MCKESR Parameters for a Single Ring.....	24
5.1	Physical Properties of Helium.....	63
5.2	Skin-Friction Heating Q for Several Ring Configurations.....	66
6.1	Power Radiated from Ring Surface.....	72
6.2	Coefficient of Performance for Thermoelectric or Thermomagnetic Cooling.....	81
10.1	Estimated Daily Losses for a 7000 MWh, 1000 MW MCKESR Plant Operating on a Diurnal Basis.....	95
10.2	Capital-Cost Estimate of 7000 MWh, 1000 MW MCKESR Facility.....	97

MAGNETICALLY CONFINED KINETIC-ENERGY STORAGE RING:
A NEW FUNDAMENTAL ENERGY-STORAGE CONCEPT

by

John R. Hull and Malvern K. Iles

ABSTRACT

The magnetically confined kinetic-energy storage ring (MCKESR) is a new, fundamental type of energy-storage device. Energy is stored as kinetic energy in mass circulated at high velocity around a circular loop. The constraining force necessary to keep the circulating ring from flying apart is provided by radial, inwardly directed forces exerted along the perimeter of the loop by magnetic fields. The magnets and ring are contained in a tunnel, which may be buried in the ground. Levitational support against gravity is also provided by magnetic fields. Energy insertion or extraction is similar to that for a synchronous motor.

Many MCKESR designs are possible. The rotating ring may be either superconducting or made from magnetic material, and can attain very high velocities, resulting in a large energy-storage density. Major advantages of the MCKESR concept are that large devices are feasible and that costs are inversely related to size. A MCKESR of 500-1000 m radius, having a tunnel bore of approximately 1 m, would provide complete diurnal load-leveling capability for a large (1000 MW) electrical-power generating plant.

The MCKESR is still in the preliminary conceptual stage of development. Although several technical challenges must be overcome before the MCKESR is proven technically feasible, it appears that construction of such a device does not require any major breakthroughs in technology. The MCKESR has close analogs with several other technologies, including the flywheel, superconducting magnetic-energy storage, the synchrotron particle accelerator, and the magnetically levitated train. The cost of a 7000 MWh MCKESR device for utility load-leveling applications is estimated to be \$40/kWh. For this size of unit, the MCKESR is cost-competitive with pumped hydroelectric storage.

1. INTRODUCTION

1.1 GENERAL MCKESR DESCRIPTION

The magnetically confined kinetic-energy storage ring (MCKESR) is a new, fundamental type of energy-storage device. Energy is stored as kinetic energy in mass circulated at high velocity around a circular loop. The constraining force necessary to keep the circulating mass (often called a "ring" in this report) from flying apart is provided by radial, inwardly directed forces

exerted along the perimeter of the loop by magnetic fields. The magnets and ring are contained in a tunnel, which may be buried in the ground. Levitational support against gravity is also provided by magnetic fields. Energy insertion or extraction is similar to that for a synchronous motor.

The ring must be able to generate the necessary magnetic fields or must be composed of a material that will respond to a magnetic field (e.g., by generating eddy currents). The same is true of the support structure (sometimes called the "tunnel" in this report) that provides levitation or constraint. The magnetic fields can be generated with permanent magnets, electromagnets, or superconducting magnets; the last are usually preferred.

The moving ring of the MCKESR can attain very high velocities, resulting in a large energy-storage density. Major advantages of the MCKESR concept are that large devices are feasible and that costs are inversely related to size. A MCKESR of 500-1000 m radius, having a tunnel bore of approximately 1 m, would provide complete diurnal load-leveling capability for a large (1000 MW) electrical-power generating plant.

The MCKESR is still in the preliminary conceptual stage of development. Although several technical challenges must be overcome before the MCKESR is proven feasible, it appears that construction of such a device does not require any major breakthroughs in technology.

The MCKESR has close analogs with several other technologies, as follows:

- o The flywheel (energy is stored as kinetic energy of a rotating mass),
- o Superconducting magnetic-energy storage (the force ultimately constraining the magnets of the system is provided by a large inert mass, such as bedrock),
- o The synchrotron particle accelerator (for one major design option the magnetic forces constraining the rotating ring, as well as the power input and output method, are similar to that of a synchrotron), and
- o The magnetically levitated train (running in a circle on a banked track).

The MCKESR also has major differences from each of the four technologies mentioned and is therefore properly defined as a new, fundamental type of energy-storage device. The analogs listed are discussed further in Sec. 2.2.

Although an accurate economic analysis of the MCKESR cannot be made until the technology is developed further, a rough estimate of the MCKESR capital cost can be made by comparing it with the cost for superconducting magnetic-energy storage (SMES). Most of the expensive items (e.g., superconductor fabrication, vacuum and Dewar enclosure, excavation, etc.) are similar in type for both technologies. The cost of a 5000 MWh SMES system has recently been estimated at \$240/kWh. A MCKESR plant of the same capacity would be approximately 20 times smaller, with a capital cost of \$12/kWh; this cost is roughly equal to that for pumped hydroelectric storage. The advantage of the MCKESR plant over the hydroelectric plant is that the MCKESR can be sited in almost any part of the country. MCKESR costs are discussed further in Sec. 10.2.

1.2 APPLICATIONS

The most obvious application for the MCKESR is for diurnal load-leveling for electric utilities. This would make use of large-radius ($R = 1000$ m) devices, for which the cost of the stored energy is lowest. The storage rings would be charged up during the night or whenever the demand load was less than the baseload capacity. The rings would be discharged during the periods when demand exceeded capacity. This application is extremely attractive, because it allows the utilities to use low-cost baseload power plants, such as nuclear reactors. Use of expensive peaking plants would be minimal. These utility-size MCKESR devices could also be used as a spinning reserve for the utilities, making use of the fast charge/discharge capability.

A possible application for smaller MCKESR units ($R = 50$ m) is in energy-intensive industrial batch processes that have time scales on the order of several hours (e.g., in steel mills). Use of such a device by private industry would prevent large demand charges for such applications. Another application for these size units is wayside energy storage for electric trains, recovering energy from the trains traveling downgrade.

A possible application involving even smaller storage units ($R = 10$ m) requires rapid charge and discharge. This application is the provision of power to pulsed magnets used in particle accelerators and magnetic-confinement fusion reactors. Power could also be provided to large lasers.

A final possible application, not directly involving energy storage, is to use a smaller-size MCKESR ($R = 10$ - 50 m) as a basic-research facility. The combination of high vacuum, low temperature, high speeds, large magnetic fields, and high g-forces offers conditions found nowhere else. This application is discussed further in Sec. 11.2.

1.3 MAJOR DESIGN OPTIONS

The major design options available for the MCKESR depend mainly on the method chosen to magnetically confine the moving ring and are outlined in Table 1.1. Some of the magnetic-levitation methods are discussed in detail in Chapter 4. In this report, levitation is defined as confinement against radial centrifugal forces, as well as suspension against gravity.

A superconducting ring can employ the largest magnetic-field strengths and will have the highest energy-storage density. The magnetic confinement of a superconducting ring is patterned after synchrotron particle accelerators. Because of the necessity of keeping the superconducting ring at cryogenic temperatures, cooling of the ring is likely to be difficult. For this reason, the weak-focusing alternative is probably preferable to strong-focusing, because less eddy-current heating is expected to occur.

Table 1.1 Major Magnetic-Confinement Options for MCKESR

-
1. Superconducting Ring
 - (a) Weak-Focusing Synchrotron
 - (b) Strong-Focusing Synchrotron
 2. Nonsuperconducting Ring
 - (a) Repulsive Levitation
 - (b) Attractive Levitation
 - o Active Feedback
 - o Superconducting Shields
 - o Vertical Repulsive Levitation
 - o Alternating-Gradient Synchrotron
-

A nonsuperconducting ring has the advantage that the ring temperature is not critical. Ring cooling is relatively easy; the ring radiates heat to the tunnel wall, where the heat is removed by a conventional cryogenic refrigeration system. Repulsive levitation has the advantage that large magnetic fields can be used. Unfortunately, the large eddy-current heating losses make this option unsuitable for diurnal load leveling in electric utilities; however, repulsive levitation may have promise for short-storage-time applications where efficiency is not so critical. Attractive levitation has the inherent disadvantage that saturation of the magnetic material in the ring limits the available magnetic-levitation pressure. However, in terms of cost, the relative simplicity of the ring design may compensate for this limitation. A number of ways are known to stabilize a ring by attractive levitation (see detailed discussion in Chapter 4).

There are many other major design-option categories in addition to magnetic confinement. Many of these are discussed later in this report. One important option is modularity of the ring. A solid ring will produce the most uniform mechanical stress on the system, whereas a modular ring (where the moving ring is composed of discrete and spatially separated segments) offers many unique design opportunities, including factory fabrication and easier maintenance.

In this report most of the attention is focused on rings of rather small cross-sectional area, because the technical challenges for these higher-speed rings are the most formidable and would require the most advanced research. Also, the economics of small rings looks better than that of large rings, at least in a preliminary analysis. In the long run, it may prove that larger, slower-moving rings are to be preferred. Larger rings would have less difficult technical problems. After all, a large ring is really not much more than a magnetically levitated train moving in a circle, a technology that is

almost standard today. Clearly, "maglev" trains can be made to run faster in an evacuated tunnel than they do on a wind-swept track. The purpose of examining small rings is to see just how far this technology can be extended. Somewhere between the very-high-speed rings discussed in this report and the maglev train reside the limits of technical feasibility for the MCKESR.

1.4 EXAMPLE DESIGN

There are many possible designs for the MCKESR, and many concepts have already been identified that should be feasible in an actual device. Several of these concepts are summarized here:

1. The compressional and levitational magnetic fields would be produced by superconductors located in the tunnel in a configuration similar to that of a weak-focusing synchrotron. These magnetic fields would interact with a superconducting cable, carrying a large current and located in the ring, to produce the compressional and levitational forces. A schematic diagram of a cross-section of a possible configuration of this type is shown in Fig. 1.1. (Many schemes using repulsive and attractive levitation -- as shown, for example, in Fig. 1.2 -- are also possible.) The compressional magnetic field would slowly increase as the ring velocity increases. The nearly d.c. currents result in very low eddy-current losses, as well as inherent stability of the loop upon loss of control circuitry. Betatron oscillations, which are present in particle accelerators, should mostly damp out while the ring is at low velocity, due to eddy currents induced in the conducting matrix of the ring's superconducting cables. The current in the superconducting cables can be maintained by induction by the tunnel magnetic fields or with a flux pump.

2. Energy insertion and extraction is similar to that for a synchronous motor. Dipole magnets located around the tunnel interact with superconducting coils in the ring to accelerate and decelerate the ring. The use of low magnetic-field strengths and magnetic fields synchronized with the rotating ring ensure that heating losses will be small.

3. The circulating mass need not be a continuous loop. It could consist of unconnected modules ("blocks"), thus facilitating the use of mass-production techniques for fabrication and minimizing the problems of thermal contraction as the device cools to operating temperature. The energy input and extraction method, similar to that used in a synchrotron particle accelerator, automatically ensures that the blocks will not touch one another. The shaping of the superconducting coils in each block results in a mutually repulsive force between the blocks to prevent bumping during "coasting" periods.

4. The circulating mass assists evacuation by "pumping" gas molecules to the outside rim of the tunnel. The high vacuum thus achieved would result in low skin-friction heating. The moving ring

can be continually cooled without contact with the tunnel walls, by a combination of a thermal diode and a magnetic-refrigeration cycle. The thermal diode pumps heat from the superconducting part of the ring to the refrigerator, which is located on the inside part of the ring. A cycling, external magnetic field turns off the diode by heating up the magnetic material in the refrigerator, which then radiates heat to the tunnel wall.

5. If an extra degree of safety is necessary, a catcher magnet can be located outside the main confinement magnets. The safety fields would be provided by d.c. superconducting coils that are spatially inhomogeneous in the circumferential direction, located outside the regular confining magnets. These safety coils would induce eddy currents in the conducting part of the ring, and the resulting repulsive force would keep the ring constrained. The effect is identical to that used for repulsive magnetic levitation of trains. Such a scheme could also be used for the main confinement magnets; the ring would then consist of a simple conductor that need not be cryogenic. However, the drag force in this case would be high enough that the energy-storage time would be approximately an hour at best.

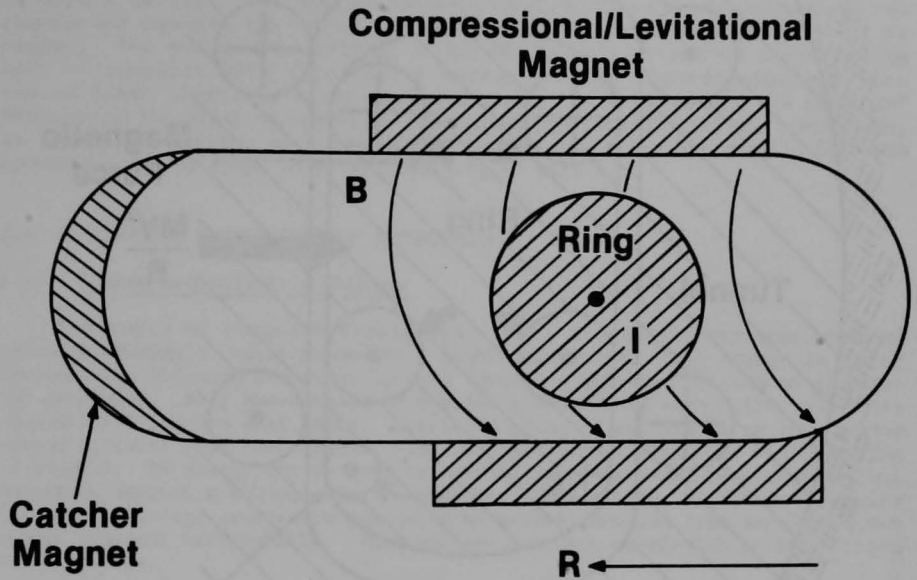


Fig. 1.1 Solid-Ring Design in Weak-Focusing Synchrotron Magnetic Field (A dot in the ring indicates that current, I , is coming out of the page.)

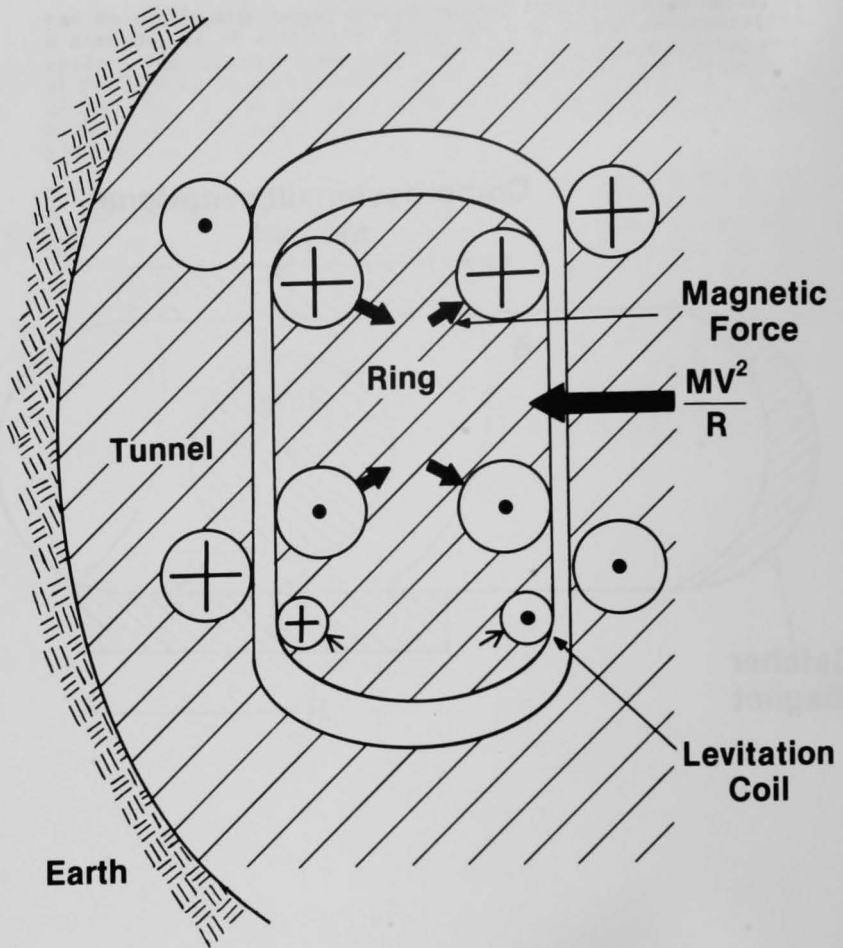


Fig. 1.2 Ring Design in Quadrupole-Type Magnetic Field (The dots in the circles indicate current coming out of the page. A cross indicates current going into the page. Several major forces are indicated by arrows. In a practical design, the currents in the tunnel and the ring would be more spread out to provide greater stability.)

2. BACKGROUND

Energy storage is necessary to offset the mismatch between times when energy demand is present and times when an energy source is available. An important class of energy-storage devices is that which returns the stored energy in the form of electricity. The energy storage device discussed in this report, the magnetically confined kinetic-energy storage ring (MCKESR), is such a device. The MCKESR converts electricity to mechanical energy for storage and converts the mechanical energy back to electricity when energy is needed. The economic feasibility of the MCKESR will ultimately depend on how well it competes with alternative energy-storage technologies and with conventional electricity generating systems. In this section the prominent features of the existing competing energy-storage technologies are summarized, so that a comparison with the MCKESR can be made. Further details for each technology may be found in References 1-12 in Sec. 2.5.

2.1 ALTERNATIVE ENERGY-STORAGE TECHNOLOGIES

2.1.1 Pumped Hydroelectric Storage

The basis of pumped hydroelectric (PH) storage is the gravitational potential energy of water pumped to a higher elevation. This energy is later recovered by allowing the water to drop through a turbine, driving an electrical generator. Many aboveground PH storage systems have been built, and their characteristics are well known. Utilities using PH systems as an inexpensive method to level peak-load demands have realized energy-recovery efficiencies of 65-80%. PH energy can be used for either long- or short-term storage, but economics imposes a minimum size limitation. In addition, PH systems require two large storage reservoirs separated by several hundred feet vertically but nearly adjacent horizontally. This imposes a severe constraint on the siting of PH systems.

2.1.2 Underground Pumped Hydroelectric Storage

Underground pumped hydroelectric (UPH) storage is like PH storage, except that the lower reservoir is below the ground. More geographic locations are candidate sites for UPH than for PH systems. Practical cavern excavation and tunneling methods already exist for construction of the lower reservoir, and high-lift pump-turbine technology is also available. UPH storage has not yet seen commercial application but may be economical in some applications.

2.1.3 Compressed-Air Storage

Compressed-air (CA) energy storage uses a mechanically driven compressor to force air into a reservoir under pressure. When a source of mechanical energy is available, the reservoir is pressurized. When energy is needed, the pressurized air is available for producing mechanical energy. Underground reservoirs (e.g., aquifers, salt cavities, and mined hard-rock caverns) are

used for CA systems. There are several prototype CA systems in operation, but economics seems to favor combining the CA with a combustion turbine to increase the output of the turbine by eliminating the need to drive a compressor.

2.1.4 Batteries

With energy storage in batteries, and also in fuel cells, electricity flow is used to drive a reversible chemical reaction. When energy from storage is needed, the reaction is allowed to go in the reverse direction, generating electricity. The storage battery is characterized by a lack of moving parts, rapid electrical response, compactness, and modularity. Batteries are a mature, but currently expensive, technology. Their modularity makes them suitable for both small and large applications. They are best suited for shorter-term storage, because most battery types will slowly self-discharge.

2.1.5 Superconducting Magnetic-Energy Storage

Superconducting magnetic-energy storage (SMES) uses the large magnetic fields of a d.c. superconducting coil for energy storage. Rectified current is charged into the coil until the rated value is reached. When the coil is not being charged, it is isolated from the charging circuit, and the stored current will flow permanently inside the closed coil network. SMES is a promising technology, but cost, development of suitable switches, and confinement pressure remain as problems.

2.1.6 Flywheels

A flywheel is a massive wheel that stores rotational kinetic energy. Flywheels have traditionally been used to smooth out power output from cyclic engines and to compensate for uneven loads. When coupled to an electrical system, a flywheel is generally powered by a connecting shaft from its center to a dynamo, which acts either as a motor, increasing the rotational velocity, or as a generator, in which case the flywheel slows down as it supplies electrical energy. Flywheels are capable of energy-recovery efficiencies of 80-90% and energy densities of 70-90 kJ/kg. The energy density is limited by the strength of the flywheel material, which limits the maximum rotational speed. The flywheel is especially suited for rapid charge and discharge. It is currently under consideration by electric utilities for use in off-peak electricity storage and by electric-vehicle manufacturers as a supplement or alternative to batteries.

Flywheels have a number of advantages over competing storage technologies: simplicity, low maintenance, long shelf life, high power density, rapid charge/discharge capability, flexibility (input/output can be electrical [a.c. or d.c.], hydraulic, mechanical, or any combination), unlimited depth of discharge, and unlimited number of cycles.

The major disadvantage of flywheels that currently keeps them from being economically competitive is a speed/size limitation. Flywheels are self-contained and are held together by their own tensile strength. As the flywheel speeds up, the centrifugal forces tending to pull the flywheel apart increase. Beyond a critical rotational velocity, the flywheel no longer has the tensile strength needed to hold itself together; it flies apart, rapidly dissipating the kinetic energy as well as destroying the flywheel. The high energy densities achieved to date have been made possible by the use of high strength-to-density composite fiber materials in optimized designs. In general, these materials require a high technology base to manufacture and are expensive. The flywheel also has several other shortcomings, including the constant hazard of catastrophic failure and its limited storage duration. Current development is directed toward lowering the cost of this otherwise mature technology.

2.2 ANALOGIES WITH OTHER TECHNOLOGIES

2.2.1 Superconducting Magnetic-Energy Storage

As pointed out in Sec. 1.1, there is a close analogy between MCKESR and SMES. Both technologies make extensive use of magnetic fields generated by superconductors. In both technologies the device is contained in a Dewar vessel that is buried in the ground, and in both cases the force ultimately constraining the magnets is provided by the large inert mass of surrounding earth. The amount of rock needed to contain a given amount of stored energy is the same for both systems. The two technologies share the major design problem of the transmission of the magnetic forces from the magnets to bedrock at an acceptable rate of heat transfer through an insulating structure that spans a temperature interval from 4 K to 300 K. It is fortunate for MCKESR that so many of the design problems are so similar to those of SMES. This allows MCKESR investigators to take advantage of the many man-years of research invested in SMES to solve these problems. The technology borrowed from SMES is discussed in more detail in later sections of this report.

Besides the additional complication of a rotating ring, there is an important difference between SMES and MCKESR. For a given amount of superconducting mass and magnetic-field strength, rotational kinetic energy is a more efficient energy-storage method than a magnetic field. This is indicated by the scaling laws as a function of radius R . For a fixed cross-sectional area of conductor, the energy stored in an inductor is approximately proportional to $R \ln(R)$. As demonstrated in Chapter 3, for MCKESR the energy stored is proportional to R^2 . Because the energy-storage density of the MCKESR is much higher than that of SMES (based on mass of superconductor or volume of tunnel), the most expensive component of the technologies, the superconducting windings (including both ring and magnets), is needed in much smaller quantities in the MCKESR. Thus, even though the costs of the inexpensive items (such as rock bolts) are the same, the MCKESR is much less expensive per unit of stored energy than SMES.

The magnetic fields in the tunnel of the MCKESR are comparable to those for SMES, but in the MCKESR system the magnetic-field energy is only a small fraction of the kinetic energy. The magnet design of the MCKESR should be no more difficult than for SMES, because the tunnel magnets and the ring currents are nearly constant in time. It may be necessary to develop a flux pump to maintain the large persistent currents in the ring, but this device need not switch large amounts of current in a short time, as would be the case for SMES.

2.2.2 Flywheels

Like the MCKESR, the flywheel consists of a mass rotating about an axis and stores energy in the form of rotational kinetic energy. The rotational kinetic energy may be easily and efficiently transformed to and from electrical energy. At this point the similarity ends. By the intrinsic nature of the flywheel, it holds itself together by its own tensile strength. The MCKESR does not. The key concept for the MCKESR is that the forces that keep the rotating device from flying apart are external to the device. For that reason, the MCKESR offers a significant improvement over the flywheel, because much higher energy densities are obtainable. The maximum rim velocity of the flywheel decreases as the flywheel radius increases. With the MCKESR, however, the maximum velocity increases as the radius increases.

Unlike a flywheel, MCKESR makes optimal use of its rotational mass. Because all the mass in the MCKESR is at the perimeter, the maximum kinetic energy is stored for a given rotational velocity. In a flywheel, the mass near the rotational axis is inefficient in storing the kinetic energy. If the rotating ring were connected to a shaft at the center of the MCKESR, then power could be inserted or extracted mechanically through the shaft. In this case, the MCKESR would be nothing more than a flywheel with a superconducting current at the rim to help hold it together. Such a design is not very attractive. The radius of such a device must be relatively small to keep the stress in the shaft connection low and to limit the size of the vacuum chamber. Because of this size limitation, the magnetic constraint does not radically increase the performance of the flywheel. In addition, extending the ring of the MCKESR radially inward would eliminate its primary advantage, namely that the cost of energy stored is inversely proportional to size.

2.2.3 Synchrotrons

With a superconducting ring, the MCKESR is approximately equivalent to a synchrotron, accelerating mass slugs containing superconducting currents rather than charged particles. Magnet designs for stability of rotating objects are well known, and it is profitable to borrow as much as possible from this well developed technology. If a modular ring is used, the synchrotron oscillation principle can be used to keep the modules from bumping. The major difference between the MCKESR and a standard synchrotron is that the charged particles (i.e., superconducting currents) are mechanically and electrically linked. This analogy is discussed further in Sec. 4.2.1.

2.2.4 Levitated Trains

A device that is similar in some respects to the MCKESR is the Kinetic Ring Energy Storage System (KRESS), proposed by Russell and Chew¹³. This device transmits the gravitational and inertial forces to the ground by means of a distributed support system using rolling wheels on rails. In essence, the KRESS is a train traveling around a beveled circular track. Power is injected into or extracted from the ring by using motors coupled to the ring through wheels or gears. This proposed device is limited in speed by rolling friction and could profit from adoption of magnetic levitation.

With a nonsuperconducting ring, many of the levitation techniques (e.g., repulsive levitation and attractive levitation with active-feedback stabilization) applicable to MCKESR are similar to those used for magnetically levitated trains. Such trains are now entering commercialization with open-air speeds on the order of 100 m/s. If we enclose such a train in an evacuated tunnel and run it in a circle, we have a MCKESR. If we make the train components very small (i.e., into a solid ring), we can run it very fast. Big or small ring cross-section, the potential for energy storage at low cost exists. Further, the technology can be advanced in a relatively easy way from an established industrial and technical base.

2.3 COST COMPARISON WITH ALTERNATIVE ENERGY-STORAGE TECHNOLOGIES

The specific energy and cost of the MCKESR are compared with those of other energy-storage technologies in Fig. 2-1. The ring design is that described in Sec. 3.4. The volume of the MCKESR was taken as 50 times that of the ring volume. Cost was estimated on a dollar-per-kilogram basis. The more detailed cost analysis in Sec. 10.2 also supports the estimate for the MCKESR in Fig. 2.1.

It can be readily appreciated from examination of Fig. 2.1 that the MCKESR appears to be superior to the alternative technologies both in terms of specific energy and in terms of cost. It is still much too early to have a good cost estimate, but one expects the MCKESR to be less expensive than alternative technologies due to its large specific energy.

2.4 DEVELOPMENT HISTORY OF MCKESR

The MCKESR concept was invented by Malvern K. Iles and John R. Hull during the latter half of 1981. Although the development of the MCKESR to date has received contributions from a large number of individuals, most of the concepts presented in this report were developed by these two scientists.

The inspiration for the invention came about after Iles attended the first space-shuttle launch¹⁴ and obtained a copy of a paper describing a launch loop system by Keith Lofstrom of Tektronics Corporation¹⁵. The essential idea in the launch loop¹⁶ is that a massive ring rotates in a vertical plane such that the centrifugal force of the ring counters the gravitational force in the upper part of its orbit. The ring diameter is such

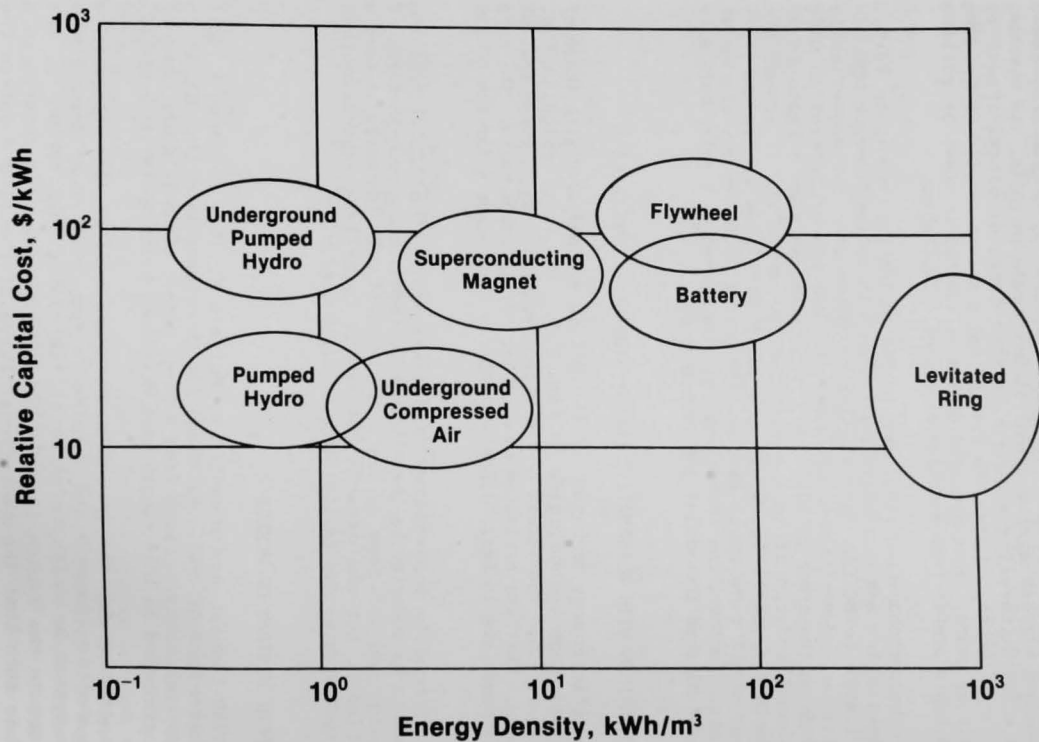


Fig. 2.1 Specific Energy and Capital Cost: MCKESR vs. Other Energy-Storage Technologies

that the upper part of the ring is in low Earth orbit. One uses the ring support structure to hoist elevators, thus providing a way to move people and other fragile items into space without the use of rockets.

At the same time, Hull was writing an energy-storage handbook¹ and came across the idea of trains running in circular paths for energy storage¹³. During 1981 these ideas were discussed, and the essentials of the MCKESR idea evolved at this time.

Some time before Christmas, 1981, the idea was sketched out to William Schertz of ANL, who encouraged its further development. This resulted in a preliminary patent disclosure in January, 1982¹⁷. Here the basic features of the device were described: confinement magnets, levitation magnets, and the use of an induction-type motor for energy insertion and extraction. The basic scaling laws were also worked out, with the surprising feature that the cost of energy stored decreased with increasing ring radius. The details of the device were not considered, but all forms of magnetic field were considered: permanent magnets, d.c. electromagnets, and superconducting magnets. At this time, MCKESR was envisioned as trainlike and rather slow-moving, much like the KRESS¹³. In one configuration, the system was envisioned as an aluminum ring confined by concrete sewer pipe.

With awareness of new mass-driver technology¹⁸, it appeared that coils could be wound poloidally around the ring and tunnel, and that these coils would provide both acceleration and confinement (with levitation thrown in as a side benefit of the latter effect). A patent disclosure of March 4, 1982, explained this new technique for confinement.

During the history of MCKESR, Schertz has contributed many technical, as well as managerial, insights that have had a major impact on its successful development. In late summer, 1982, he suggested that the MCKESR would make an excellent subject for a proposal for ANL internal discretionary funds. In an effort to muster support for the MCKESR idea, Schertz contacted several recognized researchers at ANL for comments and criticism. The first people contacted were Robert Kustom and Richard Smith. Kustom immediately pointed out that the poloidally wound configuration would not work well. Not only was the magnetic energy used inefficiently for confinement, but pulsing the coils would use up too much energy in the form of a.c. losses. Kustom came up with the superconducting-magnet concept of the previous (January) patent disclosure and suggested a way to implement the induction motor, using the synchrotron oscillation principle. His synchronous-motor power input/output (I/O) method is the one discussed in this report. Most important, he stressed the close analogy between the MCKESR and the synchrotron.

In order to get more expert input, the idea was explained to Paul Nelson of ANL. Nelson pointed out that with a relatively low specific energy, the idea would probably not be economically competitive. This suggested that the size of the ring should be small and that it should run very fast, obtaining very high specific energy. Nelson also pointed out that, because the ring could be modular, a more encompassing and appropriate name for the device was the Magnetically Levitating Loop (MLL).

Nelson appointed a panel to investigate the idea further. The panel members included J. Asbury, J. Hull, R. Kustom, W. Schertz, and R. Smith. After many discussions and calculations by the panel members, the MLL concept was advanced further, and a proposal for program discretionary funds was submitted to ANL management in September, 1982. An award of \$25 thousand was given for further development in FY1983. Using these funds, the MLL concept was further advanced, a research proposal was drafted by J. Hull and W. Schertz, and a preliminary report was written by J. Hull. Elements from the proposal and preliminary report are combined in this report. Seminars describing the device were given at ANL, Iowa State University, and the University of Wisconsin. Since these seminars, Roger Boom at the University of Wisconsin has contributed greatly to the application of SMES technology to the MCKESR concept.

In May, 1983, Iles died, leaving the project bereft of one of its greatest inspirational sources. The name of the technology has reverted to MCKESR, the name he preferred.

2.5 REFERENCES

1. J. R. Hull, R. L. Cole, and A. B. Hull, Energy Storage Criteria Handbook, Naval Civil Engineering Laboratory Report CR082.034, Oct. 1982.
2. M. Masuda and T. Shinotomi, "Superconducting magnetic energy storage," Cryogenics 17, 607-612, 1977.
3. R. F. Post and S. F. Post, "Flywheels," Sci. Am. 229(6), 17-23, 1973.
4. D. W. Rabenhorst and R. J. Taylor, "Design Considerations for a 100-Megajoule/500-Megawatt Superflywheel," Report APL/JHU TG 1229, Dec. 1973.
5. Anonymous, "Compressed-Air Energy Storage in a Salt Dome," Report EPRI EM-2210, April 1982.
6. Anonymous, "Compressed-Air Energy Storage Using an Aquifer," Report EPRI EM-2351, Dec. 1982.
7. D. W. Boyd, O. E. Buckley, and C.E. Cark, "Compressed-Air Energy Storage: Commercialization Potential and EPRI Roles in the Process," Report EPRI EM-2780, Dec. 1982.
8. D. Creamer and C. F. X. Cadou, "Increased Efficiency of Hydroelectric Power," Report EPRI EM-2407, June 1982.
9. J. Bast, "Development of Advanced Batteries for Utility Applications," Report EPRI EM-2579, Sept. 1982.

10. W. J. Stolte, "Feasibility Assessment of Customer-Side-of-the-Meter Applications for Battery Energy Storage," Report EPRI EM-2769, Dec. 1982.
11. S. T. Lee, R. S. Albert, and D. T. Imamura, "Evaluation of Superconducting Magnetic Energy Storage Systems," Report EPRI EM-2861, Feb. 1983.
12. H. H. Kolm and R. D. Thornton, "Electromagnetic Flight," Scientific American 229(4), 17-25, 1973.
13. F. M. Russell and S. H. Chew, "Kinetic Ring Energy Storage System," International Conf. on Energy Storage", pp. 373-384, Brighton, UK, April 29 -May 1, 1981.
14. M. K. Iles, "Fear and Loathing on the Launch Pad," Iowa State University Daily, August 1981.
15. K. H. Lofstrom, "The Launch Loop: A Low Cost Earth-to-High Orbit Launch System," Submitted to Lewis Advanced Space Propulsion Competition, May 1981.
16. K. H. Lofstrom, "The Launch Loop," Analog 103, pp. 67-80, Dec. 1983.
17. J. R. Hull and M. K. Iles, "Levitated Kinetic Storage Loop," Invention Report ANL-IN-82-4, Jan. 1982.
18. G. K. O'Neill, "Recent Developments in Mass Drivers," Space Studies Institute, 1982.

3. BASIC PHYSICS OF THE ROTATIONAL RING

3.1 ROTATING POINT PARTICLE

Consider a point particle of mass m , rotating in a circle of radius R about the origin. The rotational velocity is ω . The linear velocity of the point, or rim velocity, is

$$v = R \omega . \quad (3.1)$$

The kinetic energy is

$$KE = 1/2 m v^2 = 1/2 m R^2 \omega^2 = 1/2 I \omega^2, \quad (3.2)$$

where

$$I = m R^2 \quad (3.3)$$

is the moment of inertia. The centripetal force necessary to keep a particle in orbit is

$$F = \frac{m v^2}{R} = m R \omega^2. \quad (3.4)$$

Let W be the radial width of a ring cross-section. If W is negligible compared with R , then to first order, the equations of a point particle apply to the ring.

3.2 BASIC RING RELATIONSHIPS

The basic ring relationships are examined in terms of two types of technologies. In the first, it is assumed that magnetic pressure is the critical factor. In the second, it is assumed that the current density of the persistent ring currents is the critical factor.

If the ring material has density ρ and cross-sectional area A , with

$$A = W Z , \quad (3.5)$$

where Z is the vertical height of the ring cross-section, and W is the width of the ring in the radial direction (as shown in Fig. 3.1), then the total mass of the ring is

$$M = 2 \pi \rho R A = 2 \pi \rho R W Z . \quad (3.6)$$

From Eqs. 3.2 and 3.6, the kinetic energy of the ring is

$$KE = \pi \rho W Z R v^2 = \pi \rho W Z R^3 \omega^2. \quad (3.7)$$

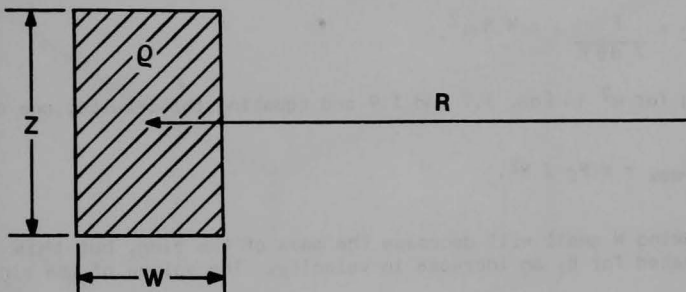


Fig. 3.1 Ring Cross-Section

3.2.1 Magnetic Pressure

It is assumed that the maximum force per unit area on the periphery of the ring is fixed and determined by the maximum pressure that can be developed by the magnetic fields. Consider an angular wedge of ring, as shown in Fig. 3.2. The centrifugal force on the wedge is

$$F = m R \omega^2 = \rho Z W d\theta R^2 \omega^2. \quad (3.8)$$

The compressional pressure from the magnetic fields is P_C and is related to the centripetal force by

$$P_C = \frac{F}{Z d\theta R} = \rho W R \omega^2. \quad (3.9)$$

Solving for ω^2 in Eqs. 3.7 and 3.9 and equating the results, one obtains

$$KE_{\max} = \pi P_C Z R^2. \quad (3.10)$$

Making W small will decrease the mass of the ring, but this decrease is compensated for by an increase in velocity. The volume of the ring is

$$V = 2 \pi R Z W, \quad (3.11)$$

and the energy density h (in J/m^3) is given by

$$h = \frac{KE}{V} = \frac{P_C R}{2 W}. \quad (3.12)$$

As a first approximation, the cost of the ring and magnets is likely to be proportional to Z , W , and R . The cost per unit energy stored, then, is proportional to $1/R$; the bigger the radius, the better. It is also worthwhile to make W as small as possible, because KE_{\max} does not depend on W but cost does.

The confinement pressure can be estimated in terms of the available magnetic fields by the equation

$$P_C = \frac{B_e B_r}{\mu_0}, \quad (3.13)$$

where B_e is the external applied magnetic field, B_r is the magnetic field due to the ring, and $\mu_0 = 4 \pi \times 10^{-7} \text{ N/A}^2$ is the permeability of free space.

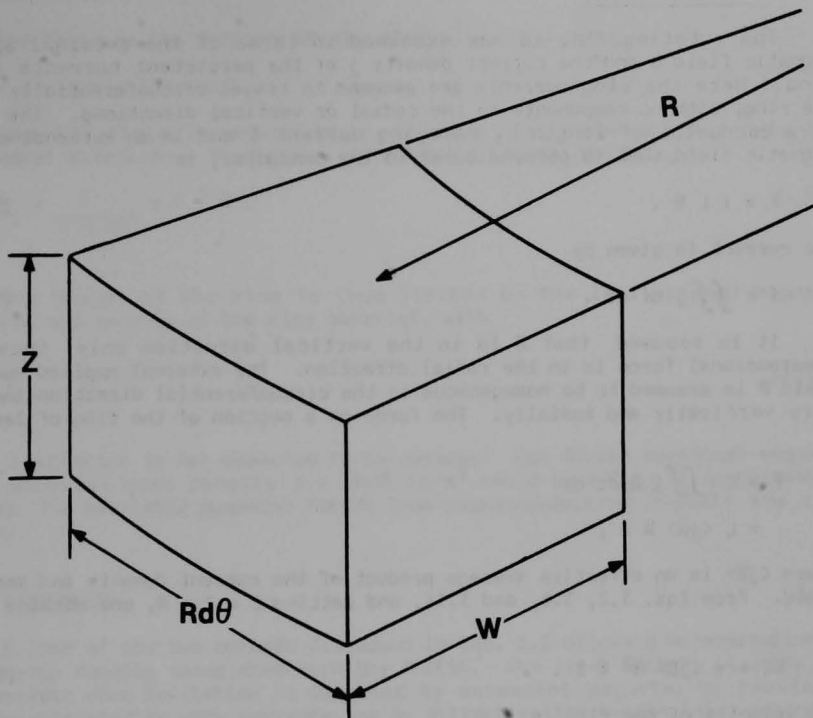


Fig. 3.2 Angular Wedge of Ring

3.2.2 Current Density

The rotating ring is now examined in terms of the external applied magnetic field B and the current density j of the persistent currents in the ring. Here the ring currents are assumed to travel circumferentially around the ring, with no components in the radial or vertical directions. The force on a conductor of length L , carrying current I and in an external applied magnetic field that is perpendicular to the conductor, is

$$F = I L B . \quad (3.14)$$

The current is given by

$$I = \iint j \, dr \, dz . \quad (3.15)$$

It is assumed that B is in the vertical direction only; thus, the compressional force is in the radial direction. The external applied magnetic field B is assumed to be homogeneous in the circumferential direction but may vary vertically and radially. The force on a section of the ring of length L is

$$\begin{aligned} F &= L \iint j B \, dr \, dz \\ &= L \langle jB \rangle W Z , \end{aligned} \quad (3.16)$$

where $\langle jB \rangle$ is an effective average product of the current density and magnetic field. From Eqs. 3.2, 3.4, and 3.16, and setting $L = 2 \pi R$, one obtains

$$KE = \pi \langle jB \rangle R^2 W Z . \quad (3.17)$$

The velocity of the ring is

$$v = \left(\frac{\langle jB \rangle R}{\rho} \right)^{1/2} . \quad (3.18)$$

Comparison of Eq. 3.17 with Eq. 3.10 indicates that the effective magnetic pressure is given by

$$P_C = \langle jB \rangle W . \quad (3.19)$$

If it is assumed that $\langle jB \rangle$ is independent of W and Z , there is now no incentive to make the ring thin. The energy density is given by

$$h = \frac{\langle jB \rangle R}{2} . \quad (3.20)$$

3.3 LEVITATION

The force in the z-direction due to gravity on a wedge of the ring is

$$F = m g = \rho Z W R d\theta g . \quad (3.21)$$

The magnetic field is assumed to be uniformly distributed across the ring in the radial direction. The levitation pressure is then given by

$$P_L = \frac{F}{W R d\theta} = \rho Z g . \quad (3.22)$$

The height of the ring is thus limited by the levitational magnetic pressure and density of the ring material, with

$$Z_{\max} = \frac{P_L}{\rho g} . \quad (3.23)$$

This limitation is not expected to be serious. For Alnico permanent magnets, ring material with density $\rho = 5000 \text{ kg/m}^3$ would have Z_{\max} of approximately 20 cm. The available magnetic fields from superconducting magnets are much higher.

3.4 DISCUSSION

Either of the two methods discussed in Sec. 3.2 allows a determination of the energy density associated with the MCKESR. The first method, using P_C , is appropriate when levitation is supplied by permanent magnets, by repulsive forces generated by eddy currents, or by attractive levitation using a ring of magnetic material. The second method, using $\langle jB \rangle$, is appropriate when the ring contains persistent superconducting currents.

As a numerical example, using the second method, assume a MCKESR design with

$$\begin{aligned} R &= 1000 \text{ m,} \\ Z &= 10 \text{ cm,} \\ W &= 10 \text{ cm,} \\ B &= 4 \text{ T, and} \\ j &= 10^4 \text{ A/cm}^2 = 10^8 \text{ A/m}^2. \end{aligned}$$

The latter two values are readily obtainable with present superconducting-magnet technology. These values yield

$$h = 2 \times 10^{11} \text{ J/m}^3 = 5.6 \times 10^4 \text{ kWh/m}^3,$$

$$KE = 1.26 \times 10^{13} \text{ J} = 3500 \text{ MWh.}$$

One ring of this design can store 3.5 h of output from a 1000 MW electric-power generating plant. With an assumed ring density of 8000 kg/m^3 , the mass of the ring is 480,000 kg, and the velocity of the ring in the fully charged condition is 7070 m/s.

The effect of changing the radius and the density in this design is shown in Table 3.1.

As a comparison, with $B_e = 4$ T and $B_r = 1.5$ T in Eq. 3.13, and $R = 1000$ m and $W = 10$ cm in Eq. 3.12,

$$h = 2.4 \times 10^{10} \text{ J/m}^3 = 6.7 \times 10^3 \text{ kWh/m}^3.$$

Table 3.1 MCKESR Parameters for a Single Ring ($B = 4$ T,
 $j = 10^4$ A/cm², $Z = 10$ cm, $W = 10$ cm)

Ring Radius	Ring Density	Ring Velocity	Specific Energy	Energy Stored
(m)	(kg/m ³)	(m/s)	(kWh/kg)	(MWh)
100	2000	4,470	2.76	36
500	2000	10,000	13.89	872
1000	2000	14,140	27.78	3,489
2000	2000	20,000	55.56	13,956
500	4000	7,070	6.94	872
1000	4000	10,000	13.89	3,489
1000	8000	7,070	6.94	3,489

4. LEVITATION METHODS

This chapter describes several different levitation methods that may prove useful in a MCKESR system. In addition to levitational support against gravity, levitation is also defined to mean the production of the confinement force to counter the outward centrifugal force (i.e., levitation in the horizontal, radially inward direction).

4.1 INTRODUCTION

Electromagnetic levitation has received the most attention in the application of high-speed ground transportation. Nine basic electromagnetic methods of supporting moving or rotating masses have been identified¹:

1. Levitation using forces of repulsion between permanent magnets.
2. Levitation using forces of repulsion between diamagnetic materials.
3. Levitation using superconducting magnets.
4. Levitation by forces of repulsion due to eddy currents induced in a conducting surface or body.
5. Levitation using the force that acts on a current-carrying linear conductor in a magnetic field.
6. Suspension using a tuned inductance-capacitance-resistance (LCR) circuit and the electrostatic force of attraction between two plates.
7. Suspension using a tuned LCR circuit and the magnetic force of attraction between an electromagnet and a ferromagnetic body.
8. Suspension using controlled d.c. electromagnets and the force of attraction between magnetized bodies.
9. Mixed μ system of levitation, where μ is the permeability of the material.

Any of the nine methods, individually or in combination, could be used with the MCKESR, but Methods 3, 5, and (possibly) 9 offer the greatest potential for low-cost energy storage.

Method 1 is a well understood approach, but permanent magnets have a relatively low magnetic pressure and therefore result in a low energy-storage density. Likewise, the pressure generated by diamagnetic materials, even Type I superconductors (Method 2), is too low to be of interest for energy storage.

Method 6 requires relatively high voltages to generate a significant pressure and has the same instability problems as Method 7. The basic idea of Method 7 is that by placing the inherently unstable attractive system in a tuned LCR circuit, static stability can be achieved. For example, in Method 7, when the bar magnet moves away from the electromagnet, the system moves toward resonance and the attractive force increases. The reverse is true for motion toward the electromagnet. The difficulty is that the LCR circuits possess large time constants, so that once disturbed from equilibrium, the system suffers divergent oscillations¹. Methods 6, 7, and 8 all require an active feedback mechanism to maintain stability. This need for active control does not totally rule these methods out for the MCKESR, but it does leave them secondary (less desirable) choices.

4.1.1 Repulsive Levitation due to Eddy Currents

Method 4 offers stable levitation without the need for active control. In this case, a magnetic field that is periodic in the circumferential direction around the loop generates eddy currents in the conducting skin of the ring. A simple design for this configuration is shown in Fig. 4.1. The primary advantage of this design is that the ring need not be cooled. The temperature of the ring may be allowed to rise to an equilibrium value, and the heat generated by the eddy currents will be radiated to the tunnel walls. As will be discussed in Chapter 6, cooling a moving ring is a most challenging technical problem. The disadvantage of Method 4 is that the drag force created by the eddy currents dissipates the kinetic energy stored in the ring in a period on the order of an hour. This calculation is detailed in Sec. 4.3.2. This disadvantage eliminates the method for use in diurnal load leveling for utilities, but it may be useful for applications where the required storage time is much smaller. The method may also be useful in the design of a catcher magnet, as discussed in Sec. 9.5.

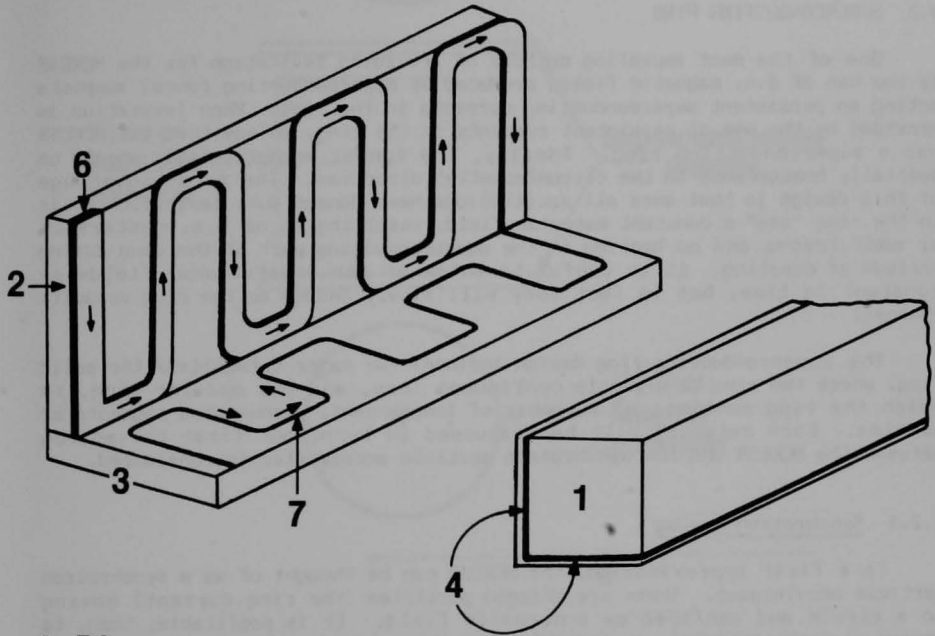
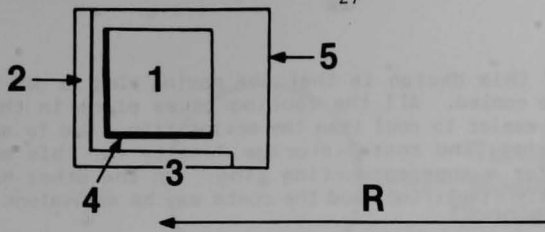
4.1.2 Superconducting Ring

The use of a superconducting ring in Methods 3 and 5 appears to offer the greatest potential for low-cost energy storage, mainly because the energy storage density is highest. Fig. 1.2 illustrates one example of Method 3; however, in a practical design, the current-carrying conductors would be distributed over the ring and tunnel wall to give greater dynamic stability. There are many possible designs of the magnetic fields for this method, and the optimization of these fields will be an important research task. Fig. 1.1, which illustrates Method 5, shows a weak-focusing synchrotron field. A strong-focusing, alternate-gradient field is also a possible design, however, such a field will induce greater eddy-current ring heating because of the intrinsic inhomogeneity of the field.

Although offering the greatest potential, methods 3 and 5 also represent the greatest technical challenges. By far the biggest challenges are cryogenic stability of the ring and control of the persistent superconducting currents. The mechanical integrity of the ring is also an important design problem.

4.1.3 Mixed Mu Levitation

Method 9 is an extremely desirable method if the static experiments^{2,3} demonstrated in the laboratory can be scaled up to a moving ring. A possible design of such a system is indicated in Fig. 4.2. A detailed analysis of the dynamic stability of the attractive system is provided in Sec. 4.4. The basic idea is to operate the MCKESR in the stable regime of the attractive system in the radial direction. The attractive system is then unstable in the vertical direction. Stability in the vertical direction is achieved by the use of the superconducting shields, which for short time constants act as a diamagnetic material. Stability in the vertical direction could also be achieved by other means, such as active feedback or repulsive levitation.



1. Ring
2. Tunnel-compressional magnet.
3. Tunnel-levitational magnet.
4. Ring-conducting skin.
5. Tunnel-vacuum wall.
6. Compressional magnet coils (arrow shows current direction).
7. Levitational magnet coils (arrow shows current direction).

Fig. 4.1 Repulsive Levitation Method for Nonsuperconducting Ring

The advantage of this design is that the moving ring is not superconducting and need not be cooled. All the cooling takes place in the tunnel walls, which are much easier to cool than the moving ring. Due to saturation of the magnetic material, the energy-storage density for this method is somewhat lower than for a superconducting ring. On the other hand, the overall design is greatly simplified, and the costs may be equivalent to those of a superconducting ring.

4.2 SUPERCONDUCTING RING

One of the most appealing methods of providing levitation for the MCKESR is the use of d.c. magnetic fields produced by superconducting tunnel magnets acting on persistent superconducting currents in the ring. When levitation is provided by the use of persistent currents in the ring, we say that the MCKESR has a superconducting ring. Ideally, the tunnel magnetic field should be spatially homogeneous in the circumferential direction. The great advantage of this design is that once all oscillations have damped out, levitation coils in the ring "see" a constant magnetic field, resulting in no a.c. hysteresis or eddy losses and no heating in the superconducting part of the ring during periods of coasting. It is useful to think of the levitational fields as constant in time, but in fact they will slowly change as the ring velocity changes.

The superconducting-ring design includes two major categories: the solid ring, where the ring is a single continuous loop, and the modular ring, in which the ring consists of a number of independent, unconnected segments or modules. Each category will be discussed in turn, but first the analog between the MCKESR and the synchrotron particle accelerator is considered.

4.2.1 Synchrotron Analog

To a first approximation, the MCKESR can be thought of as a synchrotron particle accelerator. There are charged particles (the ring current) moving in a circle and confined by a magnetic field. It is profitable, then, to borrow as much technology as possible from this already well developed field. References 4 and 5 contain many of the details of accelerator design and particle stability. In this section, several key ideas and some differences between the MCKESR and the synchrotron are brought into focus.

There are two basic types of circular synchrotron particle accelerators^{4,5}, weak-focusing and strong-focusing. The strong-focusing machines employ alternating gradients in the magnetic field to keep the particles in a stable orbit. For the MCKESR, this means that the magnetic field is not homogeneous in the circumferential direction. This is expected to continually induce eddy currents in the superconducting ring, which in turn produces ring heating. Removal of heat from a rapidly rotating ring that is at cryogenic temperatures is difficult, and ring heating must be kept to a minimum. The magnetic field in a weak-focusing machine is homogeneous in the circumferential direction and, to a first approximation, produces no heating. While the strong-focusing concept is not totally ruled out for future investigation, the weak-focusing configuration appears to be the one of choice.

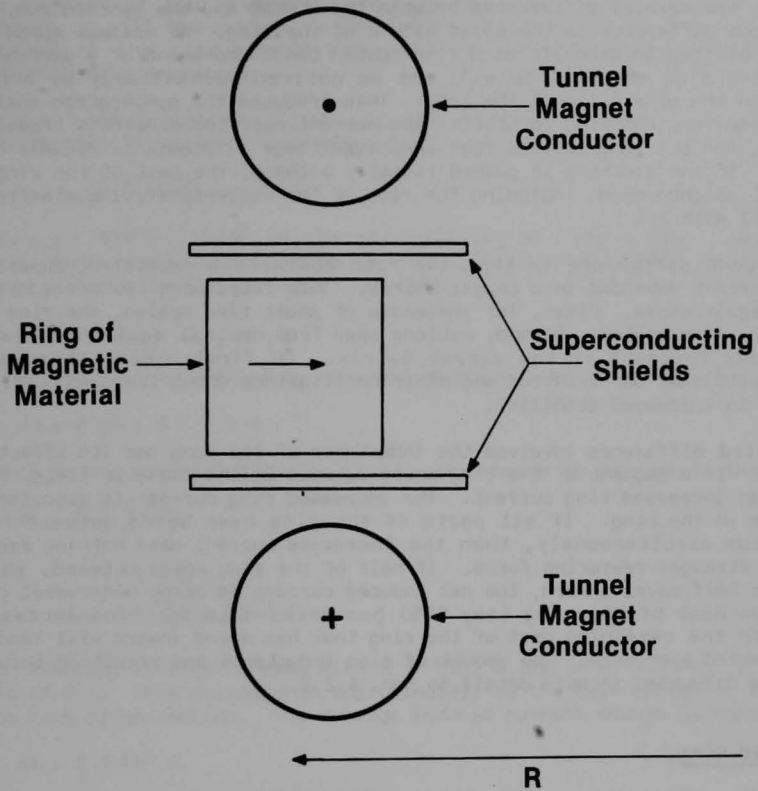


Fig. 4.2 Attractive Levitation of Nonsuperconducting Magnetic Ring Using Superconducting Shields for Vertical Stabilization

There are several differences between the MCKESR and the synchrotron. The most obvious difference is the solid nature of the ring. At maximum speed the ring can be treated globally as a limp rubber band. Movement of a section of ring on one side of the loop will not be noticed mechanically by a ring section on the other side of the loop. This produces the synchrotron analog. Locally, however, the ring is stiff. The current-carrying electrons travel in filaments, and the ring lattice that comprises these filaments is rigidly held together. If one electron is pushed radially outward, the rest of the ring in the local neighborhood, including the rest of the current-carrying electrons, must travel with it.

A second difference is that the ring contains a persistent superconducting current embedded in a copper matrix. This introduces two effects not seen in accelerators. First, for phenomena of short time scales, the ring may be slightly diamagnetic. Second, motions away from orbital equilibrium will induce eddy currents in the copper matrix. To first order, these eddy currents will damp out betatron and other oscillations about the equilibrium, resulting in increased stability.

A third difference involves the inductance of the ring and its effect on stability. If a segment of the ring moves outward in the magnetic field, this induces an increased ring current. The increased ring current is experienced everywhere in the ring. If all parts of the ring have moved outward from equilibrium simultaneously, then the increased current does nothing except produce a stronger restoring force. If half of the ring moves outward, while the other half moves inward, the net induced current is zero. The worst case occurs when most of the ring (say 90%) has moved outward. The increased current in the remaining part of the ring that has moved inward will tend to move it inward even more. The amount of ring inductance and resulting induced current is discussed in more detail in Sec. 4.2.2.

4.2.2 Solid Ring

In the solid-ring design, the superconducting ring consists of one continuous loop. This concept has the simplest magnet design and has several attractive operational and safety features, but it offers the manufacturing challenge of fabricating the ring on site as one continuous piece. In addition, this design requires a separate circuit to transfer energy in and out of the ring.

A schematic diagram of a possible solid-ring design was shown in Fig. 1.1. For a fixed radius, the vertical field is constant in the circumferential direction. For a fixed vertical height, the radial field is constant in the circumferential directions and nearly constant in the radial direction.

To first approximation, the ring must stay at a fixed radius for all ring velocities. Therefore, as the ring speeds up, the vertical field must increase so that the compressional force balances the centrifugal force. To first order, the radial field should be constant in time to counter the constant gravitational force. However, because some of the vertical field

will consist of flux lines linked with the loop, when the vertical field increases so will the current in the rotating loop. The ring current will increase as the ring speeds up, and the radial magnetic field must be correspondingly decreased.

The self-inductance L of a circular ring of radius R and circular cross-section of diameter d is given by⁶

$$L = \mu_0 R \left[\ln\left(\frac{4R}{d}\right) - 7/4 \right], \quad (4.1)$$

where $\mu_0 = 4\pi \times 10^{-7} \text{ N/A}^2$ is the permeability of free space. Assuming no eddy-current losses, the change in flux ϕ contained inside the ring will induce a change in ring current I , given by

$$L dI = d\phi. \quad (4.2)$$

If the ring expands outward by one ring diameter, the change in flux is

$$d\phi = B dA = B 2 \pi R d, \quad (4.3)$$

where B is the external magnetic field. The change in current is then

$$\begin{aligned} dI &= \frac{B 2 \pi R d}{L} \\ &= \frac{2 \pi B d}{\mu_0 \ln\left[\left(\frac{4R}{d}\right) - 7/4\right]}. \end{aligned} \quad (4.4)$$

As an example, consider a ring with $R = 1000 \text{ m}$ and $d = 12 \text{ cm}$ in a magnetic field of 4 T . This corresponds approximately to the base design of a 10 cm by 10 cm ring cross-section. The average induced current change is then

$$dI = 2.3 \times 10^5 \text{ A}.$$

Because the base current for this design is 10^6 A , this amounts to about a 25% increase. In practice, more current will be induced in the outer portion of the ring, and the initial current distribution must take this into account. If a flux pump is used to control the ring current, it must be capable of distinguishing the spatial location of the individual cables.

Under normal circumstances, the eddy-current losses caused by expansion of the ring in the magnetic field should be small. If the ring is brought to a fully charged condition in approximately two hours, this is equivalent to pulsing the ring in a magnetic field at the rate of approximately $5 \times 10^{-4} \text{ T/s}$. From Eq. 4.1, the self-inductance of the ring is

$$L = 1.3 \times 10^{-2} \text{ H}.$$

The stored magnetic energy of the ring is

$$E_B = 1/2 L I^2. \quad (4.5)$$

For the present design, Eq. 4.5 yields the following value for stored energy:

$$E_B = 6.5 \times 10^9 \text{ J.}$$

Note that this is 0.05% of the kinetic energy of the ring. The fraction of power dissipated in a circuit goes as $B \text{ dB/dt}$. The present state of the art is a fractional energy loss of 0.001 for $\text{dB/dt} = 10 \text{ T/s}$ in a 1 to 5 T field. The fraction of energy lost in the current example is then 5×10^{-8} . This is equivalent to 325 J, less than 0.1 W for the period of time that the ring is brought up to maximum speed.

One effect due to ring inductance depends on how the strands of superconducting filament are wound on the ring. If the strands are wound as circular loops, with each loop of different radius, then the ring will be unstable. The current loops to the outside of the ring are linked by more flux than are the loops to the inside, and a correspondingly larger current is induced in the outside loops when the magnetic field changes. The resulting nonuniform current distribution in the ring will result in instability in the vertical direction. The outer loops will tend to move upward, while the inner loops will tend to move downward, assuming that on the average the ring is stable in the vertical direction. At a minimum, the ring will roll about the azimuthal axis. Each strand would experience a changing magnetic field and consequent heating.

One method of preventing this effect is to wind the strands of superconductor spirally about the circumferential axis. The idea is that each strand should "see" the same average flux within one "stiffness length" of the ring. Then the induced current will be the same in each strand. This type of winding is usually necessary in superconducting-magnet design anyway, for cryogenic stability of high current densities in large magnetic fields.

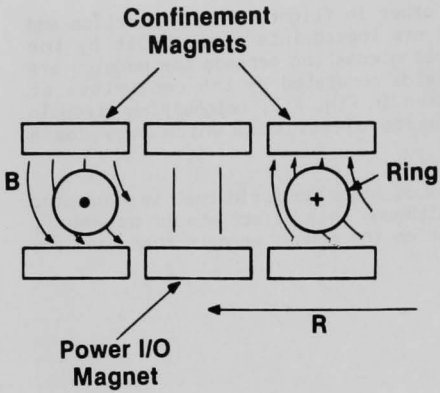
4.2.3 Modular Ring

In a modular-ring design, the superconducting ring consists of a number of independent, unconnected modules. The modularity makes ring fabrication and service easier. Compared to the solid ring, the only design compromise arises from the need to provide a return path for the current within the module. This necessitates the use of a somewhat more complicated tunnel magnetic field than that proposed in the previous section. Fig. 4.3 shows a schematic diagram of a possible design.

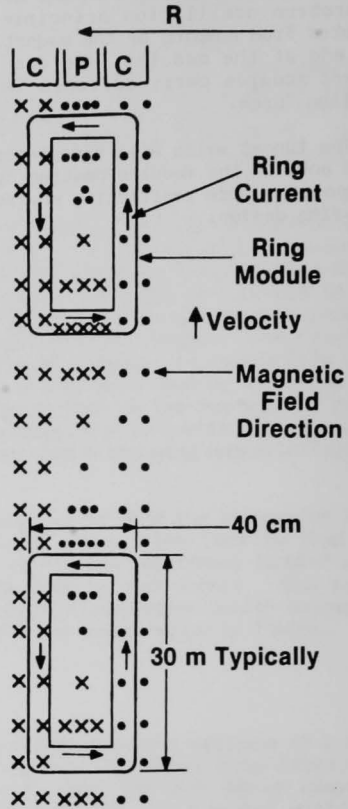
The current in the modular ring does not travel completely around the circumference of the MCKESR. Thus, to first order, there is no induced current change in the ring modules as the ring expands outward. The stability requirements are more complicated in this design, because one must now take into account the torque around the circumferential axis, as well as the movement in the vertical and radial direction.

The ring modules will not bump each other in flight. Power insertion and extraction is managed so that the modules are locked into their orbit by the synchrotron oscillation principle. During coasting periods the modules are prevented from bumping by the magnetic fields generated by the conductors at each end of the modules. As can be seen in Fig. 4.3, neighboring wires in adjacent modules carry currents in opposite directions, which provides a repelling force.

The tunnel walls will experience an a.c. magnetic field that is generated by the ends of the modules passing by. Although this effect should be small, it imposes a more restrictive environment on the tunnel magnets than does the solid-ring design.



a. Cross-sectional View



b. Top View Showing Ring Modules Under Acceleration

Fig. 4.3 Power Input and Output Method for a Modular Ring in a Weak-Focusing Synchrotron Confinement Field (At the top of (b), C refers to confinement and P to power input and output.)

4.3 NONSUPERCONDUCTING RINGS

4.3.1 Introduction

One of the early MCKESR design concepts envisioned a nonsuperconducting ring rotating in a strong magnetic field. The magnetic field would be produced, preferably, by superconducting magnets in the tunnel wall. These magnets would be typical of those used for magnetic levitation of trains with spatially varying fields constant in time. The confining force on the ring is produced by inducing eddy currents in the conducting part of the ring as the ring moves past the magnetic field. The currents are induced because the magnetic fields are not homogeneous (as were the fields for a superconducting ring). In a repulsive levitation system, the ring could be made out of any good conductor, or it could consist of a conductor laminated onto a large nonconducting mass. In an attractive levitation system, the ring could be made from a highly magnetic material. The nonsuperconducting-ring concept has the advantage that no cooling of the ring is necessary. The temperature of the ring is allowed to "float", and the heat generated by the eddy currents is radiated to the tunnel walls, where it is removed. The design criterion here is that it is much easier to actively cool the stationary tunnel wall than the rapidly moving ring.

In this section the expected heat loss associated with a nonsuperconducting ring is calculated, and the results of the calculation are used to examine the feasibility of the concept. It will be shown that the simple repulsive and attractive systems considered in this section dissipate the stored energy too quickly to be considered for diurnal storage. However, the methods described may be feasible for storage times of less than an hour. More advanced attractive levitation systems are discussed in Sec. 4.4.

Heat losses from a conducting ribbon moving past a set of magnets should be identical with those of a set of magnets moving past a conducting ring. The latter is exactly the case of a magnetically levitated train, and we can use some of the results produced from this area of research. We assume here that the heat generated by eddy currents can be totally accounted for by the drag force on the ring. We then need to know the lift and drag forces produced for a given ring velocity, magnetic field, magnet spacing, ring conductivity, etc. In general, the equations are quite cumbersome and require a numerical solution. However, for certain limiting conditions the equations may be simplified⁷, and the limiting conditions are satisfactory for our purposes.

The system is characterized by the following parameters:

- L, the spatial period of the magnetic-coil array, or rather the dominant wavelength of a Fourier decomposition of the field in the circumferential direction around the ring;
- μ , the permeability of the ring;
- σ , the electrical conductivity of the ring; and
- v, the relative velocity between the ring and the magnets.

It is convenient to introduce the following parameters:

$$\begin{aligned} k &= 2 \pi / L \\ v_0 &= 2 k / (\mu_0 \sigma) \\ \beta &= v / v_0 \end{aligned}$$

For repulsive systems, $\mu = \mu_0$, where μ_0 is the permeability of free space. For attractive levitation systems, μ is on the order of $1000 \mu_0$.

The levitational "lift" force F_L and the drag force F_D are presented in terms of these parameters and the image force F_I . F_I is the force per unit area that would be produced by the actual magnet with its mirror image, if the mirror surface were identical to the rail surface. The term F_I is the force that the magnet can produce and is closely related to the P_C term of previous calculations.

4.3.2 Repulsive Image-Force Levitation Systems

A prominent feature of repulsive levitation is that the levitational force increases, and the drag force decreases, as speed increases. The fact that the levitational force is zero for zero velocity in repulsive systems is of small consequence for the MCKESR, because the centripetal force is also zero.

4.3.2.1 Calculation of Losses

Three limiting cases of repulsive systems ($\mu = \mu_0 = 4 \pi \times 10^{-7} \text{ N/A}^2$) are considered.

Case 1. Low speed ($\beta \ll 1$), with $kT \ll 1/\beta$:

$$\frac{F_L}{F_I} = \beta^2 \left(1 - \frac{2kT}{\sinh(2kT)} \frac{1 + \cosh(2kT)}{1 + \cosh(2kT) + \sinh(2kT)} \right) \frac{\sinh(2kT)}{1 + \cosh(2kT) + \sinh(2kT)} \quad (4.6)$$

$$\frac{F_D}{F_I} = \beta \frac{\sinh(2kT)}{1 + \cosh(2kT) + \sinh(2kT)} \quad (4.7)$$

The lift force is quadratic with velocity in this case. Therefore, at low speeds the confinement force will match the v^2/R centrifugal force. The drag force is linear with velocity, and so the power loss, $P_D = F_D v$, will be a constant fraction of the energy stored.

Case 2. High speed ($\beta \gg 1$), with nonzero track thickness $(kT)^2 \gg 1/\beta$:

$$F_L/F_I = 1 - 1/\beta^{1/2} \quad (4.8)$$

$$F_D/F_I = 1/\beta^{1/2} \quad (4.9)$$

For large β , the levitational force becomes constant. The maximum energy stored is then limited by F_I . The drag force decreases with velocity, and so the power dissipated should go as $v^{1/2}$. The fraction of energy dissipated goes as $1/v^{3/2}$. This is a good scaling relation.

Case 3. Thin track ($kT \ll 1$ and $(kT)^2 \ll 1/\beta$):

The following equations are valid at all speeds, but the second condition will eventually break down for some large β .

$$\frac{F_L}{F_I} = \frac{(\beta k T)^2}{1 + (\beta k T)^2} \quad (4.10)$$

$$\frac{F_D}{F_I} = \frac{\beta k T}{1 + (\beta k T)^2} \quad (4.11)$$

The scaling relationship here is even more desirable than that of Case 2, for now the drag force goes as $1/v$ for high speeds. Power loss would then be constant, independent of speed. The maximum speed, determined by v^2/R , is still determined by the maximum F_I that can be produced, as well as by the size of the ring.

4.3.2.2 Thin-Track Approximation

Examination of Eqs. 4.10 and 4.11 indicates that $\beta k T$ should be as large as possible, in order to reduce drag and still maintain enough levitational force to contain the ring at maximum velocity. (For $\beta k T < 1$, $F_L < 0.5 F_I$.)

From the definition of β ,

$$\beta k T = \frac{\mu_0 \sigma T v}{2} . \quad (4.12)$$

Because v is already fixed, it is desirable to make T as large as possible to maximize $\beta k T$. However, the requirements of the thin-track approximation [$(kT)^2 \ll 1/\beta$] must also be satisfied; therefore it must follow that

$$k^2 T^2 \ll \frac{2 k}{\mu_0 \sigma v} \quad \text{and} \quad T^2 \ll \frac{2}{\mu_0 \sigma v k} . \quad (4.13)$$

To maximize T , k must be minimized (maximize $L = 2 \pi / k$). While there is considerable flexibility in the value of T , there is a constraint because of L , and $L = 30$ m is arbitrarily assumed as a maximum value. Then

$$T = \frac{1}{5} \left(\frac{L}{\mu_0 \sigma v} \right)^{1/2} , \quad (4.14)$$

with the result that

$$\beta k T = \frac{1}{10} (\mu_0 \sigma L v)^{1/2} . \quad (4.15)$$

One concludes that the best design is that which has the highest electrical conductivity and largest magnet spacing. It is interesting to note that the superconducting-ring design maximizes both of these parameters. From Eq. 4.11, it follows that for large $\beta k T$, the drag force goes as $1/\beta k T$. Because $P_D = F_D v$, the power loss per unit length is then given by

$$P_D = 10 \left(\frac{v}{\mu_0 \sigma L} \right)^{1/2} F_I Z . \quad (4.16)$$

4.3.2.3 Thick-Track Approximation

In this approximation, it follows from Eq. 4.9 that the drag force is proportional to $1/\beta^{1/2}$. The results are independent of the track thickness T . From the definition of β , the power loss per unit length of ring is

$$P_D = \frac{v}{\beta^{1/2}} F_I Z = \left(\frac{4 \pi v}{\mu_0 \sigma L} \right)^{1/2} F_I Z. \quad (4.17)$$

This is essentially the same result as for the thin-track approximation, but with P_D reduced by almost a factor of 3.

4.3.2.4 Discussion

The losses associated with repulsive levitation systems can be summarized by writing the decay time τ in terms of the relevant parameters. Starting with $\tau = KE/P_D$, and using $2 KE = F_I Z R$, Eq. 4.17 above, and Eq. 3.7 divided by $2 \pi R$,

$$\tau^4 = \frac{\mu_0^2 \sigma^2 L^2 W R^3 \rho}{256 \pi^2 F_I}. \quad (4.18)$$

This indicates that storage times are longer for larger-radius devices of heavier and more conductive material. Because of the W term in the numerator, large ring cross-sections also appear to be favored. Unfortunately, storage times decrease with increasing magnetic pressure F_I .

As a numerical example, consider a density $\rho = 8000 \text{ kg/m}^3$, $\sigma = 10^{10} \text{ mho/m}$, $W = 10 \text{ m}$, $L = 40 \text{ m}$, $R = 1 \text{ km}$, and $F_I = 8 \times 10^5 \text{ N/m}^2$. This set of parameters results in a decay time of $\tau = 10^4 \text{ s}$, about 3 h. If $Z = 10 \text{ m}$ also, then the device is virtually equivalent to a large maglev train running about in the tunnel, with $KE = 2.4 \times 10^{13} \text{ J}$ and $v = 100 \text{ m/s}$. These calculations indicate that nonsuperconducting repulsive levitation systems dissipate too much energy to be seriously considered for use in low-loss energy-storage devices.

4.3.3 Repulsive Null-Flux Levitation Systems

A levitational method that has proven very valuable in train transportation is the null-flux system of Powell and Danby⁸. When used in train transportation, a conducting-sheet track lies between two rows of oppositely polarized train magnet coils⁹. When the thickness of the track is less than the skin depth, contributions of the top and bottom magnets tend to cancel. Because the drag force is proportional to B_z^2 while the lift force is proportional to δB_x (z -direction vertical and x direction horizontal in this example), the drag-to-lift ratio can be made arbitrarily small if cancellation is made nearly complete. This null-flux method has been popular in maglev-train research because of the low drag force. It would be the levitation method of choice for very-high-speed trains running in evacuated tunnels.

For the MCKESR, the null-flux levitation method would need oppositely polarized magnet coils on the inside and outside tunnel walls. The ring would consist of a thin conducting ribbon running between the two sets of magnets. The levitational and drag forces are given by Ref. 9:

$$F_L = F_I \frac{(\beta k T)^2}{1 + (\beta k T)^2} k \Delta h, \quad (4.19)$$

$$F_D = F_I (\beta k T) \left[\frac{k^2 (\Delta h)^2}{1 + (\beta k T)^2} + \frac{k^2 T^2}{12} \right], \quad (4.20)$$

where Δh is the spatial translation of the ring from the midpoint between the two sets of magnets and $T = W$ is the thickness of the ring. If $kT \ll 1$, the drag-to-lift ratio is

$$\frac{F_D}{F_L} = \frac{\Delta h}{\beta T} + \frac{\beta k^2 T^3}{12 \Delta h}. \quad (4.21)$$

This can be minimized with respect to Δh as

$$(F_D/F_L)_{\min} = kT / 3^{1/2}. \quad (4.22)$$

The power loss per unit length of ring is

$$P_D = \frac{2 \pi W}{3^{1/2} L} F_L Z v. \quad (4.23)$$

Note that the power loss depends on F_L , which may be very different from F_I . Following a similar analysis to that of Sec. 4.3.2.4, the decay time for the optimal design and speed is found from

$$\tau^2 = \frac{3 R L^2 \rho}{16 \pi^2 F_I W}. \quad (4.24)$$

Unlike the image-force levitation methods, it is beneficial here to make the thickness of the ring as small as possible. In any event, it must be smaller than the skin depth, to take advantage of the null-flux condition.

As a numerical example, consider a density $\rho = 8000 \text{ kg/m}^3$, $W = 1 \text{ mm}$, $L = 40 \text{ m}$, $R = 1 \text{ km}$, and $F_I = 8 \times 10^5 \text{ N/m}^2$. This set of parameters results in $(F_D/F_L) = 10^{-4}$ and a decay time of $\tau = 600 \text{ s}$, much worse than the image-force methods. The velocity of the ring is $v = 10^4 \text{ m/s}$. For $Z = 1 \text{ m}$, $KE = 2.5 \times 10^{12} \text{ J}$.

In contrast to the train application, the null-flux levitation method does not scale well for MCKESR. For a train, F_L depends only on the weight of the train and cargo. F_L is independent of velocity, and Δh is constant. Drag force can be made low. In MCKESR, F_L must go as v^2 to balance the centrifugal force, and Δh must increase with v . The ratio (F_D/F_L) contains the term $\Delta h/v$. This term goes to zero in the train application, but it must go as v in MCKESR.

4.3.4 Attractive Image-Force Levitation Systems

In an attractive levitation system, a material of high magnetic permeability would be attached to the inside surface of the ring and would experience an attractive force, with magnets located on the inside wall of the tunnel. A prominent feature of attractive levitation systems is that the levitational force decreases and the drag force increases with increasing velocity. However, as shown below, it is very easy to operate in the low velocity limit, so that the drag forces are negligible. The other problem, which we investigate in Sec. 4.3.5, is that attractive levitation systems are inherently unstable.

A disadvantage of attractive levitation systems compared to repulsive systems is the limited attractive force due to saturation in the magnetic material. Even with very-high-field superconducting tunnel magnets, the magnetic field in the ring material is limited to the saturation value. The reduction in confining force results in a lower specific energy for the system. The specific energy of attractive systems would be approximately four to ten times lower than for repulsive systems.

Attractive levitation systems have a magnetic permeability $\mu = \mu_r \mu_0$, where μ_r is on the order of 1000. In the low-speed limit⁷, $\beta \ll 1/\mu_r$. Consider the case of moderate track thickness, which imposes the additional constraint $1/\mu_r \ll kI \ll 1/(\beta \mu_r)$. Because

$$\beta = \left(\frac{\mu_0 \sigma}{2k} \right) v ,$$

increasing the electrical resistivity (decreasing the conductivity, σ) will yield a small value of β . Nonconducting but highly magnetic materials need to be used. The lift and drag forces are, respectively,

$$\frac{F_L}{F_I} = -1 + \frac{2}{\mu_r} \left(\frac{1 + \cosh(2kT)}{\sinh(2kT)} \right) \quad (4.25)$$

and

$$\frac{F_D}{F_I} = 2\beta \frac{1 + \cosh(2kT)}{\sinh(2kT)} \left(1 - \frac{2kT}{\sinh(2kT)} \right) \quad (4.26)$$

Inspection of Eq. 4.26 indicates that kI should be as small as possible to reduce drag. For $kI \ll 1$, the decay time is given by

$$\tau = \frac{3}{4} \frac{\rho}{\mu_0} \frac{W}{\sigma T F_I} . \quad (4.27)$$

As a numerical example, consider $\rho = 8000 \text{ kg/m}^3$, $W = 1 \text{ m}$, $\sigma = 0.1 \text{ mho/m}$, $l = 10 \text{ cm}$, and $F_I = 5 \times 10^5 \text{ N/m}^2$. This set of parameters results in a decay time of $\tau = 10^7 \text{ s}$, approximately two weeks. If $Z = 1 \text{ m}$ and $R = 1 \text{ km}$, then $KE_{\text{max}} = 1.5 \times 10^{12} \text{ J}$. This result might be acceptable, and the power loss could undoubtedly be made lower by further decreasing the conductivity. One concludes that attractive levitation systems with nonsuperconducting rings are probably feasible if a method can be found to make them stable without introducing additional heating terms.

4.3.5 Stability of Attractive Levitation Systems

In this section methods of stabilizing attractive levitation systems are considered. The additional heating introduced by each method is also investigated.

4.3.5.1 Attractive Systems

The image force per unit area, F_I , used in the previous sections has a spatial dependence given by⁹

$$F_I = \frac{1}{2 \pi \mu_0} B_0^2 \exp(-2kh) , \quad (4.28)$$

where B_0 is the root-mean-square (rms) value of the magnetic induction in the plane of the magnet, and h is in the direction perpendicular to the surface of the ring. In all calculations, the magnet is assumed to lie entirely in a plane.

Consider a ring rotating with speed v at a distance from the tunnel wall. Choose a coordinate system so that at equilibrium $h = 0$ and h is positive outward. The equilibrium radius is R_0 . The centrifugal force is

$$F_C = \frac{m v^2}{R_0 + h} . \quad (4.29)$$

The force due to the attractive magnets is

$$F_I = F_A \exp(-2kh) , \quad (4.30)$$

where F_A is a constant. At equilibrium, $F_I = F_C$; therefore,

$$F_A = m v^2 / R_0 .$$

For small h the total force can be approximated as

$$\begin{aligned} F_{\text{TOT}} &= F_C + F_I \\ &= F_A (2k - 1/R_0) h . \end{aligned} \quad (4.31)$$

This is similar to the equation for a spring

$$F = -\alpha h ,$$

where

$$\alpha = (1/R_0) - 2k .$$

For the system to be in stable equilibrium, $\alpha > 0$, or

$$1/R_0 > 2k \quad (\text{i.e., } R_0 < L/4) . \quad (4.32)$$

Because this condition is impossible with d.c. fields, stability for an attractive levitation system by itself is impossible. The case of attractive levitation magnets on both the inside and outside of the ring is also unstable.

4.3.5.2 Repulsive Levitation Stabilizers

An attractive levitation system can be made stable by using repulsive magnets on the outside of the ring. It is hoped that if the stabilizing field can be made small, there will not be the large drag-force losses that were found in the previous section. We assume the following conditions: (1) the outside surface of the ring is very conductive, and (2) the ring is wide enough that the field from the inner tunnel wall acts minimally at the outside of the ring, and the field from the outer tunnel wall acts minimally at the inside surface of the ring. It will be shown that the conditions imposed by stability considerations reintroduce the large drag forces in all practical situations.

To investigate the stability of our proposed system, a repulsive component must be added to Eq. 4.31:

$$F_{TOT} = \frac{m v^2}{R_0} - \frac{m v^2}{R_0^2} h - F_A + 2k_A h F_A - F_R - 2k_R F_R h . \quad (4.33)$$

At equilibrium ($h=0$), $F_{TOT} = 0$, and

$$\frac{m v^2}{R_0} - F_A - F_R = 0 .$$

If $F_{TOT} = -\alpha h$,

$$\alpha = \frac{F_A + F_R}{R_0} + 2k_R F_R - 2k_A F_A .$$

For stability, $\alpha > 0$; therefore, where $k = 2\pi/L$, one obtains

$$\frac{(F_A + F_R)LAR}{4\pi R_0} > F_A L_R - F_R L_A . \quad (4.34)$$

Because $F_A \ll F_R$, Eq. 4.34 reduces to

$$\frac{F_R}{F_A} > \frac{L_R}{L_A} - \frac{L_R}{4\pi R_0} . \quad (4.35)$$

If $L_A = 30$ m, compared to $R_0 = 1000$ m, Eq. 4.35 may be reduced to

$$\frac{F_R}{F_A} > \frac{L_R}{L_A} . \quad (4.36)$$

Set

$$F_R = \frac{L_R}{L_A} F_A .$$

Both L_A and F_A are fixed by the constraint of supplying a large attractive force. Take $L_A = 30$ m, and $F_A = 10^6$ N. Unfortunately, there is a lower limit to the practical value of L_R . First, the current density J cannot be made too large and still change quickly. The reason is that the smallest L_R occurs when J alternates direction in adjacent strands of wire. The maximum of J is fixed by the wire diameter, which here is proportional to L_R . The second, and most important, constraint is that the field dies off as $\exp(h/L_R)$ (h negative away from the magnet). If L_R is too small, then J must be very large to produce reasonable fields at a significant distance away from the tunnel wall. In addition, there must be some clearance between the ring and the tunnel wall. For a best-case value, choose $L_R = 3$ mm. The image force is then

$$F_R = 100 \text{ N} .$$

For $v = 5000$ m/s and $\sigma = 2 \times 10^7$ mho/m, $\beta = 30$. Using Eq. 4.9,

$$F_D = 18 \text{ N}, \quad P_D = 9 \times 10^4 \text{ W}, \quad \tau = 2.7 \times 10^3 \text{ sec} .$$

This is still very lossy. From Eqs. 4.18 and 4.36, one can show that the decay time scales as

$$\tau^4 \propto \frac{\sigma^2 L_R L_A W}{P_C} , \quad (4.37)$$

where P_C is the attractive magnetic pressure, but σ is the conductivity of the repulsive material. Because this is maximized by large L_R (and a corresponding large F_R), the best situation is no better than that for repulsive levitation itself. One is then forced to conclude that the use of repulsive stabilization in attractive levitation systems introduces too much heat loss to be viable.

4.3.5.3 Dynamic Stabilization

Dynamic stabilization of attractive levitation systems has been successfully demonstrated for maglev trains¹⁰. This type of stabilization requires some sort of feedback mechanism between the position of the ring and the strength of the magnetic field. It is not clear at this time whether such feedback will result in successful stabilization at the speeds envisioned for the storage ring. One possible technique is the application of a small a.c. magnetic field superimposed on the d.c. attractive field. The frequency would equal that of the resonant frequency of the ring, and control would be accomplished by changing the phase of the field oscillation relative to the oscillation of the ring.

4.4 RADIALLY STABLE ATTRACTIVE LEVITATION

A levitational method that may prove viable for the MCKESR is the use of attractive levitation that is stable in the radial direction, but unstable in the vertical direction. Stability in the vertical direction would then be provided by a different technique. Laboratory experiments have successfully demonstrated this levitational method for a stationary object by using superconducting shields for stabilization¹¹⁻¹³. The use of this method in the MCKESR is indicated schematically in Fig. 4.3. The system can be approximated by a pair of interacting current loops, and the discussion will be aided by a digression to consider the details of that interaction.

4.4.1 Physics of Interacting Current Loops

Consider two single-turn interacting current loops, as shown in Fig. 4.4. Both loops are square and are oriented so as to lie in the yz plane, such that the center of each square is on the x-axis. Loop 1, located at the origin, has sides of length $2L_1$ and has current I_1 . Loop 2, located a distance x from the origin, has sides of length $2L_2$ and has current I_2 . The relative direction of the current in the coils is taken so as to produce an attractive force.

Assume loop 1 is rigidly fixed and calculate the force acting on loop 2. This is easily calculated by using the Biot-Savart law, together with the Lorentz force produced by a magnetic field on a linear conductor. The force in the x-direction, F_x , is given by

$$F_x = \frac{2 \mu_0}{\pi} I_1 I_2 \times K_x(x, L_1, L_2), \quad (4.38)$$

where the force constant $K_x(x, L_1, L_2)$ is

$$K_x = \frac{[x^2 + 2(L_1 - L_2)^2]^{1/2} - [x^2 + (L_1 + L_2)^2 + (L_1 - L_2)^2]^{1/2}}{x^2 + (L_1 - L_2)^2} + \frac{[x^2 + 2(L_1 + L_2)^2]^{1/2} - [x^2 + (L_1 + L_2)^2 + (L_1 - L_2)^2]^{1/2}}{x^2 + (L_1 + L_2)^2} \quad (4.39)$$

Note that K_x is always negative, indicating a restoring force towards the origin. For small displacements from the x-axis in the z-direction, F_x is approximately the same as that given by Eqs. 4.38 and 4.39. The force in the z-direction, F_z , is given by

$$F_z = \frac{2 \mu_0}{\pi} I_1 I_2 z K_z(x, L_1, L_2), \quad (4.40)$$

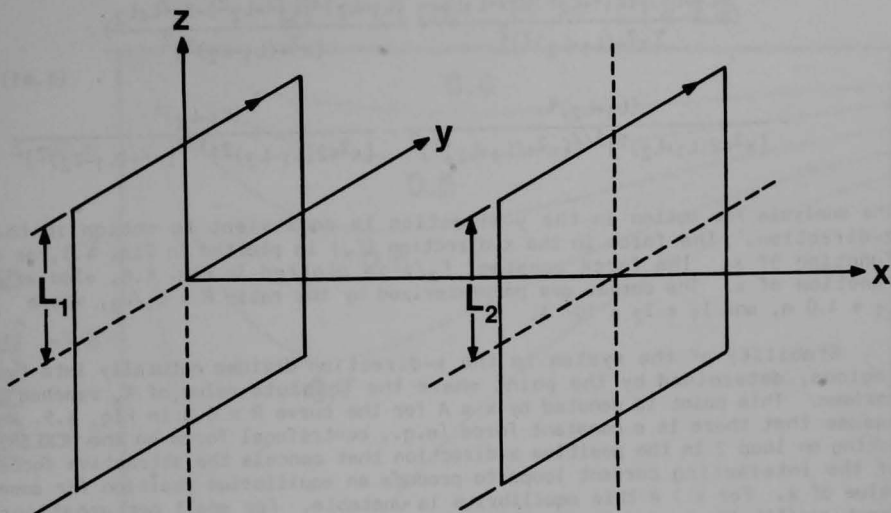


Fig. 4.4 Coordinate System of Two Interacting Current Loops

where the force constant $K_z(x, L_1, L_2)$ is given by

$$K_z = [x^2 + (L_1+L_2)^2 + (L_1-L_2)^2]^{-1/2} \\ \left(\frac{(L_1+L_2)^2(L_1^2+L_2^2)+2x^2L_1L_2}{[x^2+(L_1+L_2)^2]^2} + \frac{(L_1-L_2)^2(L_1^2+L_2^2)-2x^2L_1L_2}{[x^2+(L_1-L_2)^2]^2} \right) \quad (4.41) \\ - \frac{(L_1+L_2)^4}{[x^2+2(L_1+L_2)^2]^{1/2}[x^2+(L_1+L_2)^2]^2} - \frac{(L_1-L_2)^4}{[x^2+2(L_1-L_2)^2]^{1/2}[x^2+(L_1-L_2)^2]^2} .$$

The analysis for motion in the y-direction is equivalent to motion in the z-direction. The force in the x-direction (F_x) is plotted in Fig. 4.5, as a function of x. The force constant F_z/z is plotted in Fig. 4.6, also as a function of x. The curves are parameterized by the ratio $R = L_1/L_2$, where $L_1 = 1.0$ m, and $I_1 = I_2 = 10^3$ A.

Stability of the system in the x-direction divides naturally into two regions, determined by the point where the absolute value of K_x reaches a maximum. This point is denoted by $x = A$ for the curve $R = 0.8$ in Fig. 4.5. We assume that there is a constant force (e.g., centrifugal force on the MCKESR) acting on loop 2 in the positive x-direction that cancels the attractive force of the interacting current loops to produce an equilibrium position for some value of x. For $x > A$ this equilibrium is unstable. For small perturbations about equilibrium toward the origin, the attractive force increases, and for a small displacement from equilibrium away from the origin, the attractive force decreases. Loop 2 will continue to move in the direction of the displacement. For $x < A$, the equilibrium position is stable. Any displacement from equilibrium in the x-direction results in a net restoring force. Thus, to maintain stable equilibrium in the x-direction, we must operate in the region $x < A$.

Because K_z is essentially the negative of a spring constant, stability in the z-direction revolves about the point where K_z crosses the origin. When K_z is positive, the system is unstable. Comparison of Figs. 4.5 and 4.6 indicates that the zero of K_z always occurs for values of x that are greater than that for which the maximum for the absolute value of K_x occurs. Because K_z is positive near the origin, the result is that the system must always be unstable in the z-direction, if it is stable in the x-direction.

One concludes that without additional stabilizing forces, the system of two interacting current loops cannot be stable. If the system is stable in one direction, it will not be stable in the other direction. It is also worth noting that as L_1 approaches L_2 both force constants increase in magnitude, and both the position where K_z crosses zero and where the absolute value of K_x is a maximum move closer to the origin and closer to each other.

ACCELERATION FORCE
LOOP CURRENTS = 1000 A EACH
 $L_1 = 1\text{ m}, R = L_1 / L_2$

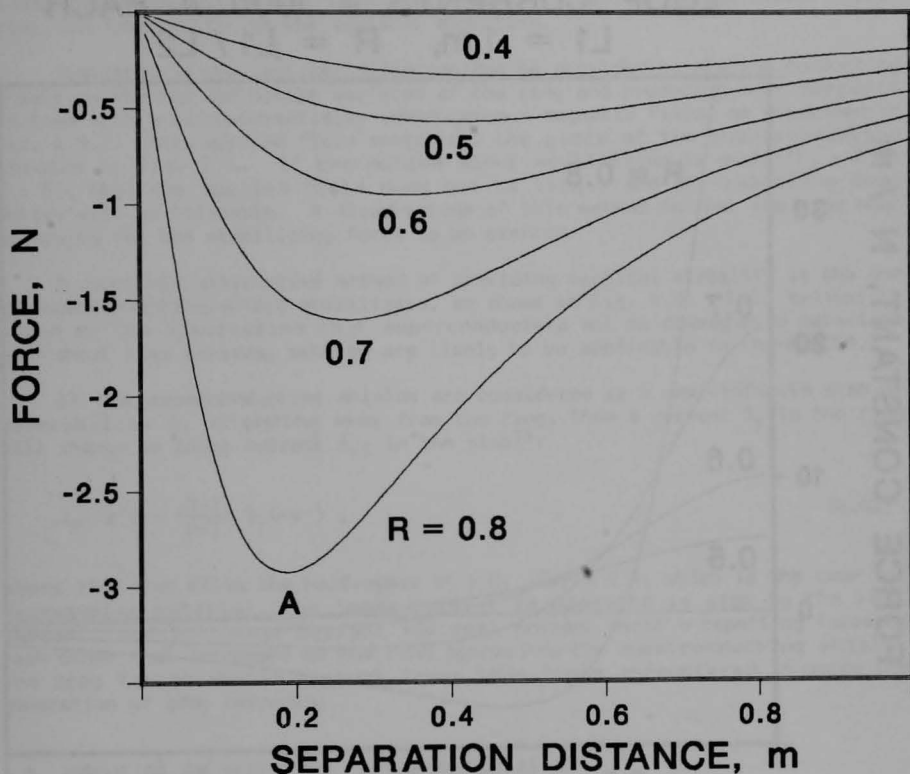


Fig. 4.5 Acceleration Force Between Two Interacting Current Loops as a Function of their Separation Distance

RESTORING FORCE CONSTANT
 LOOP CURRENTS = 1000 A EACH
 $L1 = 1\text{ m}$, $R = L1 / L2$

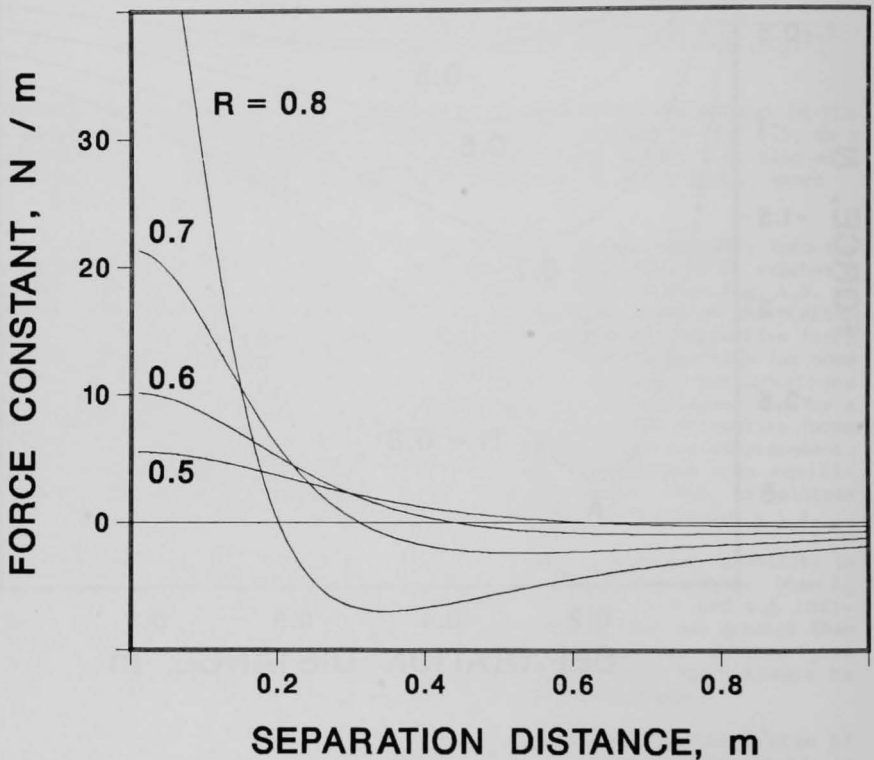


Fig. 4.6 Restoring-Force Constant for Two Interacting Current Loops as a Function of their Separation Distance

4.4.2 Application to MCKESR

In Fig. 4.3, if one replaces the magnetic moment of the ring with a current loop (L_2), essentially the same situation as was described above exists. The only difference is that there are no vertical current elements in either loop, and there is no motion in the y-direction. The positive r-direction in Fig. 4.3 is, of course, now synonymous with the positive x-direction in Fig. 4.4. If $x < A$, there is stability in the radial direction, but instability in the vertical direction.

Stability in the vertical direction can be provided by placing conducting sheets on the top and bottom surfaces of the ring and producing eddy currents in them with a circumferentially inhomogeneous magnetic field, as described in Sec. 4.3.2. This applied field would take the place of the superconducting shields in Fig. 4.3. If the motion about equilibrium is small ($F_z = 0$ at $z = 0$), then the applied field need not be large, and the resulting drag forces will be tolerable. A disadvantage of this method is that the ring must be moving for the stabilizing force to be exerted.

A possible alternative method of providing vertical stability is the use of superconducting-shield stabilizers, as shown in Fig. 4.3. This method is based on the observation that superconductors act as diamagnetic materials over short time periods, such as are likely to be applicable in the MCKESR.

If the superconducting shields are considered as a semi-infinite slab of permeability μ , extending away from the ring, then a current J_y in the ring will induce an image current J_{yI} in the slab¹⁴:

$$J_{yI}(z') = \left(\frac{\mu-1}{\mu+1} \right) J_y(-z'), \quad (4.42)$$

where the slab fills the half-space $z' > 0$. For $\mu < 1$, which is the case for diamagnetic material, the image current is opposite in sign to the real current, and the image current and real current exert a repelling force on each other that increases as the ring approaches the superconducting shield. The drag forces should be much lower than those encountered in using the generation of eddy currents.

4.5 TORQUE ON THE MCKESR DUE TO EARTH'S ROTATION

The angular momentum L of the MCKESR is

$$L = M R v, \quad (4.43)$$

where M is the total mass of the rotating ring, R is the major radius, and v is the ring velocity. The angular momentum is a vector that tends to remain pointing in some initial direction with respect to the fixed stars. In order to keep the angular momentum fixed with respect to the earth's coordinate system, a torque N must be applied, given by

$$\vec{N} = d\vec{L}/dt = \vec{\Omega}_e \times \vec{L} , \quad (4.44)$$

where $\Omega_e = 7.27 \times 10^{-5}$ rad/s is the angular velocity of the earth's rotation. For the worst case, with the MCKESR on the earth's equator, Eqs. 4.43 and 4.44 combine to give

$$N = \Omega_e M R v . \quad (4.45)$$

In order to apply this torque, consider the situation in Fig. 4.7, where the y-axis is the axis of rotation. Given a symmetry about both axes, the torque is given by

$$N = 4 \int_0^{\pi/2} R d\theta (f \cos \theta)(R \cos \theta) , \quad (4.46)$$

where f is the z-direction force per meter of circumference at $x=R, y=0$. The $\cos\theta$ term inside the parentheses with f arises because the z-direction restoring force is assumed to be proportional to the z-direction displacement away from equilibrium. Thus, $x=R, y=0$ is the location of the maximum displacement from equilibrium, and f is the maximum force per unit length. The integration of Eq. 4.46 yields

$$N = \pi R^2 f . \quad (4.47)$$

Equating Eqs. 4.45 and 4.47, one obtains

$$f = (\Omega_e M v) / (\pi R) . \quad (4.48)$$

Because M scales directly with R , while v scales as the square root of R , f scales as the square root of R . Precession is likely to be the largest problem for a large-radius device. For the numbers of the $R = 1000$ m base design,

$$f = (7.27 \times 10^{-5} \text{ rad/s})(5 \times 10^5 \text{ kg})(7090 \text{ m/s}) / (3.14)(1000 \text{ m}) = 82 \text{ N/m} .$$

The gravitational force exerted on one meter of ring circumference is:

$$W = M g = 784 \text{ N} .$$

This requires that the restoring force in the vertical direction must have a range on both sides of equilibrium that is more than 10% of the equilibrium value. This requirement is reduced by a factor of ten for the $R = 10$ m design.

The above analysis assumed that the ring was a rigid body. As discussed in Sec. 4.2, it is more reasonable to consider a large ring as analogous to a limp rubber band. The mechanical effect of one section of the ring on another section would be limited to several "stiffness lengths."

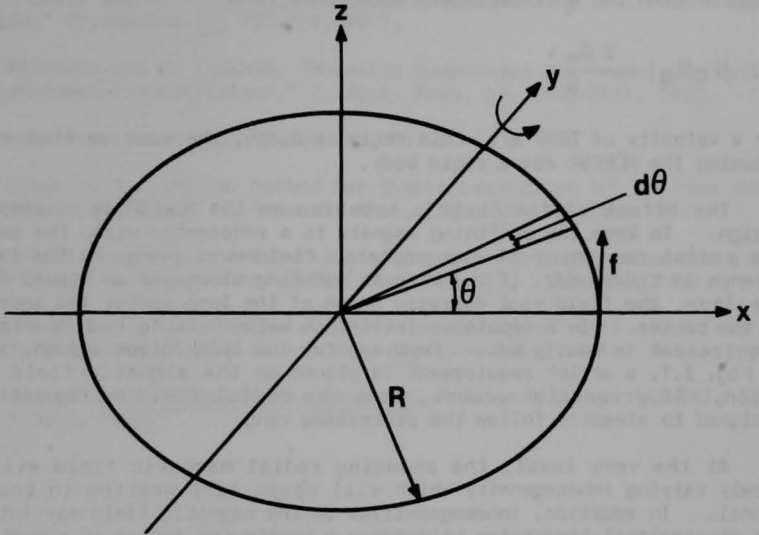


Fig. 4.7 Coordinate System for Calculation of Torque on MCKESR Due to Earth's Rotation

The force exerted on a segment of the ring due to the Earth's rotation can be calculated from the equation for the coriolis force. For the worst case (a ring located on the equator), the maximum force is given by

$$F_C = -2 m \Omega_e v . \quad (4.49)$$

Compared with the gravitational force, this is

$$|F_C/F_g| = \frac{2 \Omega_e v}{g} . \quad (4.50)$$

For a velocity of 7090 m/s, this ratio is 0.105, the same as that calculated assuming the MCKESR was a rigid body.

The effect of the Earth's rotation on the MCKESR is to complicate the design. To keep the confining magnets to a reasonable size, the magnitude of the radial component of the magnetic field must change as the loop circumference is traversed. If the ring is rotating clockwise as viewed from above the loop, the field must decrease north of the loop center and increase south of the center. In a repulsive levitation method using eddy currents, this requirement is easily met. However, for the synchrotron design, illustrated in Fig. 2.1, a strict requirement is placed on the magnetic field configuration. If precession occurs, then the radial field configuration must be designed to steadily follow the precessing ring.

At the very least, the changing radial magnetic field will act as a slowly varying inhomogeneity which will cause eddy heating in the ring and tunnel. In addition, inhomogeneities in the magnetic field may interact with the precessional tendencies to produce a continuing source of vibration. The result would be additional eddy heating and added stress on the ring.

4.6 REFERENCES

1. B. V. Jayawant, Electromagnetic Levitation and Suspension Techniques, 1982.
2. G. J. Homer et al., "A New Method for Stable Levitation of an Iron Body Using Superconductors," J. Phys. D: Appl. Phys. 10, 879-886, 1977.
3. H. Joyce et al., "Some Initial Experimental Results for a New Form of Magnetic Suspension," IEEE Trans. Mag. Mag-17, 2154-2157, 1981.
4. J. J. Livingood, Principles of Cyclic Particle Accelerators, D. Van Nostrand, 1961.
5. M. S. Livingston and J. P. Blewett, Particle Accelerators, McGraw-Hill, 1962.

6. W. T. Scott, The Physics of Electricity and Magnetism, pp. 322-324, John Wiley and Sons, 1960.
7. S. W. Lee and R. Menendez, "Forces at low- and high-speed limits in magnetic levitation systems," J. Appl. Phys. 46, 422-425, 1975.
8. J. R. Powell and G. T. Danby, "Magnetic suspension for levitated tracked vehicles," Cryogenics 11, 192-204, 1971.
9. P. L. Richards and M. Tinkham, "Magnetic Suspension and Propulsion System for High-Speed Transportation," J. Appl. Phys. 43, 2680-2691, 1972.
10. Conference Report - p. 50, Cryogenics, 1977.
11. G. J. Homer et al., "A New Method for Stable Levitation of an Iron Body Using Superconductors," J. Phys. D: Appl. Phys. 10, 879-886, 1977.
12. J. T. Williams et al., "Modelling of Superconducting Screens for a New Form of Magnetic Suspension," IEEE Trans. Mag. 17, 2150-2153, 1981.
13. H. Joyce et al., "Some Initial Experimental Results for a New Form of Magnetic Suspension," IEEE Trans. Mag. 17, 2154-2157, 1981.
14. J. D. Jackson, Classical Electrodynamics, Problem 5.8, pp. 166-167, John Wiley & Sons, 1962.

4.7 PARTIAL BIBLIOGRAPHY OF MAGNETIC LEVITATION

- E. Abel, J. L. Mahtani, and R. G. Rhodes, "Linear Machine Power Requirements and System Comparisons," IEEE Trans. Magnetics MAG-14, 918-920, 1978.
- P. D. Agarwal, and T. C. Wang, "Evaluation of Fixed and Moving Primary Linear Induction Motor Systems," Proc. IEEE 61, 631-637, 1973.
- I. Akinbiya, P. E. Burke, and B. T. Ooi, "A Comparison of Ladder and Sheet Guideways for Electrodynamic Levitation of High Speed Vehicles," IEEE Trans. Magnetics MAG-12, 879-881, 1976.
- S. Aoki, "3-Dimensional Magnetic Field Calculation of the Levitation Magnet for HSSI by the Finite Element Method," IEEE Trans. Magnetics MAG-16, 725-727, 1980.
- D. L. Atherton, "Exact Solution of Coil Forces for Uniform Transverse Field Magnet," J. Appl. Phys. 39, 1411-1414, 1968.
- D. L. Atherton, "Shunt protection for superconducting Maglev Magnets," Cryogenics 19, 537-541, 1979.
- D. L. Atherton and A. R. Eastham, "Flat guidance schemes for magnetically levitated high-speed guided ground transport," J. Appl. Phys. 45, 1398-1405, 1974.
- D. L. Atherton and A. R. Eastham, "Limitations of Levitation by Iron-Cored Electromagnets," IEEE Trans. Magnetics MAG-10, 410-412, 1974.
- D. L. Atherton and A. R. Eastham, "Guidance of a High Speed Vehicle with Electrodynamic Suspension," IEEE Trans. Magnetics MAG-10, 413-416, 1974.
- D. L. Atherton and A. R. Eastham, "Canadian developments in superconducting Maglev and linear synchronous motors," Cryogenics 15, 395-402, 1975.
- D. L. Atherton and A. R. Eastham, "Superconducting Maglev and LSM Development in Canada," IEEE Trans. Magnetics MAG-11, 627-632, 1975.
- D. L. Atherton, A. R. Eastham, and K. Sturgess, "Passive secondary magnetic damping for superconducting Maglev vehicles," J. Appl. Phys. 47, 4643-4648, 1976.
- D. L. Atherton and A. R. Eastham, "Superconducting Magnetic Levitation and Linear Synchronous Motor Development- The Canadian Program," Adv. Cryogenic Eng. 21, 1-8, 1976.
- D. L. Atherton, A. R. Eastham, and R. E. Tedford, "Joints in Strips for Electrodynamic Magnetic Levitation Systems," IEEE Trans. Magnetics MAG-14, 69-75, 1978.

D. L. Atherton et al., "Forces and Moments for Electrodynamic Levitation Systems--Large-Scale Test Results and Theory," IEEE Trans. Magnetics MAG-14, 59-68, 1978.

D. L. Atherton, "A Magnetic Circuit Analysis of the Iron-Cored Homopolar Linear Synchronous Motor," IEEE Trans. Magnetics MAG-17, 1305-1310, 1981.

A. V. Baiko, K. E. Voevodskii, and V. M. Kochetkov, "Vertical unstable stability of electrodynamic suspension of high-speed ground transport," Cryogenics 20, 271-276, 1980.

P. B. Bailey and F. R. Norwood, "Stability of Magnets Moving Above a Conducting Plane," J. Appl. Phys. 41, 4890-4892, 1970.

G. Bohn and J. Langerholc, "Theoretical calculations of the electrodynamic properties of ferromagnetic levitation systems," J. Appl. Phys. 48, 3093-3099, 1977.

R. H. Borcherts, "Repulsive magnetic suspension research - US progress to date," Cryogenics 15, 385-393, 1975.

R. H. Borcherts and L. C. Davis, "Force on a Coil Moving over a Conducting Surface Including Edge and Channel Effects," J. Appl. Phys. 43, 2418-2427, 1972.

R. H. Borcherts and L. C. Davis, "Lift and Drag Forces for the Attractive Electromagnetic Suspension System," IEEE Trans. Magnetics MAG-10, 425-427, 1974.

R. H. Borcherts et al., "Baseline Specifications for a Magnetically Suspended High-Speed Vehicle," Proc. IEEE 61, 569-578, 1973.

J. Boulnois and J. Giovachini, "The fundamental solution in the theory of eddy currents and forces for conductors in steady motion," J. Appl. Phys. 49, 2241-2249, 1978.

W. Braunbek, "Freischwebende Körper im elektrischen und magnetischen Feld," Zeitschrift für Physik 112, 753-763, 1939.

W. Braunbek, "Freies Schweben diamagnetischer Körper im Magnetfeld," Zeitschrift für Physik 112, 764-769, 1939.

J. B. Breazeale, C. G. McIlwraith, and E. N. Dacus, "Factors Limiting a Magnetic Suspension System," J. Appl. Phys. 29, 414-415, 1958.

W. S. Brown, "The Effect of Long Magnets on Inductive Maglev Ride Quality," IEEE Trans. Magnetics MAG-11, 1498-1500, 1975.

W. Brzezina and J. Langerholc, "Lift and side forces on rectangular pole pieces in two dimensions," J. Appl. Phys. 45, 1869-1872, 1974.

P. E. Burke, "The Use of Stranded Conductors to Reduce Eddy Losses in Guideway Conductors of High Speed Vehicles," IEEE Trans. Magnetics MAG-11, 1501-1503, 1975.

P. E. Burke, "The Design of Reinforcing Steel Systems for Maglev Guideways," IEEE Trans. Magnetics MAG-15, 1497-1499, 1979.

P. E. Burke and T. Akinbiya, "The Design of Flat Ladder and Coil Guideway Systems for High Speed Trains," IEEE Trans. Magnetics MAG-12, 882-884, 1976.

D. C. Burnham, "Asymptotic Lift-to-Drag Ratios for Magnetic Suspension Systems," J. Appl. Phys. 42, 3455-3457, 1971.

H. T. Coffey, F. Chilton, and T. W. Barbee, Jr., "Suspension and Guidance of Vehicles by Superconducting Magnets," J. Appl. Phys. 40, 2161, 1969.

H. T. Coffey, F. Chilton, and L. O. Hoppie, "Magnetic Levitation of High Speed Ground Vehicles," Proc. Applied Superconductivity Conf. pp. 62-75, May, 1972.

G. T. Danby, J. W. Jackson, and J. R. Powell, "Force Calculations for Hybrid (Ferro-Nullflux) Low-Drag Systems," IEEE Trans. Magnetics MAG-10, 443-446, 1974.

G. Danby and J. Powell, "Integrated Systems for Magnetic Suspension and Propulsion of Vehicles," Proc. Applied Superconductivity Conf., pp. 120-126, May, 1972.

J. H. Dannon, R. N. Day, and G. P. Kalman, "A Linear-Induction-Motor Propulsion System for High-Speed Ground Vehicles," Proc. IEEE 61, 621-630, 1973.

L. C. Davis, "Drag force on a magnet moving near a thin conductor," J. Appl. Phys. 43, 4256-4257, 1972.

L. C. Davis and D. F. Wilkie, "Analysis of Motion of Magnetic Levitation Systems: Implications for High-Speed Vehicles," J. Appl. Phys. 42, 4779-4793, 1971.

G. E. Dawson, P. C. Sen, D. J. Clarke, and S. Lakhavani, "Linear Synchronous Motor Feedback Controls," IEEE Trans. Magnetics MAG-12, 885-888, 1976.

J. K. Dukowicz, "Theory of optimum linear induction motors," J. Appl. Phys. 47, 3690-3696, 1976.

S. Earnshaw, "On the nature of the molecular forces which regulate the constitution of the luminiferous ether," Trans. Camb. Phil. Soc. 7, 97-112, 1842.

A. R. Eastham, and R. M. Katz, "The Operation of a Single-Sided Induction Motor with Squirrel-Cage and Solid-Steel Reaction Rails," IEEE Trans. Magnetics MAG-16, 722-724, 1980.

J. File et al., "Stabilized, Levitated Superconducting Rings," J. Appl. Phys. 39, 2623-2626, 1968.

J. File et al., "Princeton Floating Multipole-Superconducting Ring Progress," J. Appl. Phys. 40, 2106-2108, 1969.

J. File et al., "Operation of a Levitated Superconducting Ring in a Plasma Physics Experimental Device," J. Appl. Phys. 42, 6-9, 1971.

H. J. Fink and C. E. Hobrecht, "Instability of Vehicles Levitated by Eddy Current Repulsion - Case of an Infinitely Long Current Loop," J. Appl. Phys. 42, 3446-3450, 1971.

R. L. Forgacs, "Evacuated Tube Vehicles Versus Jet Aircraft for High-Speed Transportation," Proc. IEEE 61, 604-616, 1973.

H. S. Fosque and G. Miller, "Electromagnetic Support Arrangement with Three-Dimensional Control. II. Experimental," J. Appl. Phys. 30, 240S, 1959.

R. H. Frazier, P. J. Gilinson, Jr., and G. A. Oberbeck, Magnetic and Electric Suspensions. MIT Press, 1974.

A. Grumet, "Penetration of Transient Electromagnetic Fields into a Conductor," J. Appl. Phys. 30, 682-686, 1959.

C. Guderjahn and S. L. Wipf, "Magnetically levitated transportation," Cryogenics 11, 171-178, 1971.

C. A. Guderjahn et al., "Magnetic Suspension and Guidance for High Speed Rockets by Superconducting Magnets," J. Appl. Phys. 40, 2133-2140, 1969.

T. R. Haller and W. R. Mischler, "A Comparison of Linear Induction and Linear Synchronous Motors for High Speed Ground Transportation," IEEE Trans. Magnetics MAG-14, 924-926, 1978.

J. R. Hogan and H. J. Fink, "Comparison and Optimization of Lift and Drag Forces on Vehicles Levitated by Eddy Current Repulsion for Various Null and Normal Flux Magnets with One or Two Tracks," IEEE Trans. Magnetics MAG-11, 604-607, 1975.

J. R. Hogan, and H. J. Fink, "Equilibrium Dynamics and Stability of Null-Flux, Brake-Flux, and Double-Track, Normal Flux Electrodynamic Levitation Systems," IEEE Trans. Magnetics MAG-15, 1354-1361, 1979.

G. J. Homer et al., "A new method for stable levitation of an iron body using superconductors," J. Phys. D: Appl. Phys. 10, 879-886, 1977.

L. O. Hoppie et al., "Electromagnetic Lift and Drag Forces on a Superconducting Magnet Propelled Along a Guideway Composed of Metallic Loops," Proc. Applied Superconductivity Conf. pp. 113-119, May, 1972.

J. P. Howell, J. Y. Wong, R. G. Rhodes, and B. E. Mulhall, "Stability of Magnetically Levitated Vehicles over a Split Guideway," IEEE Trans. Magnetics MAG-11, 1487-1492, 1975.

Y. Iwasa, "Magnetic Shielding for Magnetically Levitated Vehicles," Proc. IEEE 61, 598-601, 1973.

D. P. Jain and B. T. Ooi, "The Validity and the Limitations of the AC Impedance-Modeling Technique in Electrodynamic Levitation Systems," IEEE Trans. Magnetics MAG-15, 1169-1174, 1979.

B. V. Jayawant, Electromagnetic Levitation and Suspension Techniques, 1982.

- A. W. Jenkins and H. M. Parker, "Electromagnetic Support Arrangement with Three-Dimensional Control. I. Theoretical," J. Appl. Phys. 30, 2385, 1959.
- H. Joyce et al., "Some Initial Experimental Results for a New Form of Magnetic Suspension," IEEE Trans. Magnetics, MAG-17, 2154-2157, 1981.
- B. Z. Kaplan, "Estimation of mechanical transients in 'tuned-circuit' levitators by employing steady-state impedances," J. Appl. Phys. 47, 78-84, 1976.
- R. M. Katz et al., "Integrated Magnetic Suspension and Propulsion of Guided Ground Transportation Vehicles with a SLIM," IEEE Trans. Magnetics MAG-15, 1437-1439, 1979.
- U. Kawabe et al., "Rotary Electrical AC Generators Utilizing the Magnetic Shielding and Trapping by Superconducting Plates," J. Appl. Phys. 40, 4454-4457, 1969.
- H. Kimura et al., "Superconducting Magnet with Tube-Type Cryostat for Magnetically Suspended Train," IEEE Trans. Magnetics MAG-11, 619-622, 1975.
- R. Knowles, "Dynamic Circuit and Fourier Series Methods for Moment Calculation in Electrodynamic Repulsive Magnetic Levitation Systems," IEEE Trans. Magnetics MAG-18, 953-960, 1982.
- H. H. Kolm and R. D. Thornton, "Electromagnetic Flight," Sci. Am. 229(4), 17-25, Oct. 1973.
- H. H. Kolm et al., "The magneplane system," Cryogenics 15, 377-384, 1975.
- H. Kolm, P. Mongeau, and F. Williams, "Electromagnetic Launchers," IEEE Trans. Magnetics MAG-16, 719-721, 1980.
- M. N. Kreisler "How to Make Things Move Very Fast," Am. Sci. 70, 70-75, 1982.
- Y. Kyotani, "Development of superconducting levitated trains in Japan," Cryogenics 15, 372-376, 1975.
- E. R. Laithwaite and S. B. Kuznetsov, "Reactive Power Generation in High Speed Induction Machines by Continuously Occurring Space-Transients," IEEE Trans. Magnetics MAG-16, 716-718, 1980.
- J. Langerholc, "Torques and forces on a moving coil due to eddy currents," J. Appl. Phys. 44, 1587-1594, 1973.
- J. Langerholc, "Electrodynamics of a magnetic levitation coil," J. Appl. Phys. 44, 2829-2837, 1973.
- J. Langerholc, "Numerical computation of eddy-current effects in ferromagnetic maglev suspensions," J. Appl. Phys. 46, 5255-5258, 1975.
- S. W. Lee and R. Menendez, "Forces at low- and high-speed limits in magnetic levitation systems," J. Appl. Phys. 46, 422-425, 1975.

- S. D. Lindenbaum and M. S. Lee, "Lift, drag, and guidance forces on alternating polarity magnets, using loop guideways," J. Appl. Phys. 46, 3151-3159, 1975.
- N. Maki et al., "A Combined System of Propulsion and Guidance by Linear Synchronous Motors," IEEE Trans. Power App. Sys. PAS-96, 1109-1116, 1977.
- J. D. McHugh, "Magnetic Bearing Systems - A Comparison of Various Approaches," Proc. USAF-SwRI Aerospace Bearing Conf. pp. 253-277, Sept., 1964.
- P. H. Melville, "Magnetic propulsion for magnetically levitated trains," Cryogenics 13, 716-717, 1973.
- S. Nakamura, "Development of High Speed Surface Transport System (HSST)," IEEE Trans. Magnetics MAG-15, 1428-1433, 1979.
- S. Nakamura, Y. Takeuchi, M. Takahashi, "Experimental Results of the Single-Sided Linear Induction Motor," IEEE Trans. Magnetics MAG-15, 1434-1436, 1979.
- S. A. Nasar and L. del Cid, Jr., "Propulsion and Levitation in a Single-Sided Linear Induction Motor for High-Speed Ground Transportation," Proc. IEEE 61, 638-644, 1973.
- V. K. Neil and R. K. Cooper, "Magnetic Forces on a Coil Moving in a Conducting Tube," J. Appl. Phys. 41, 4619-4625, 1970.
- K. Oberretl and N. Kratki, "Transients and Oscillations in the Repulsive Magnetic Levitation System," IEEE Trans. Magnetics MAG-11, 1493-1494, 1975.
- F. Ohno, M. Iwamoto, and T. Yamada, "Characteristics of Superconductive Magnetic Suspension and Propulsion for High-Speed Trains," Proc. IEEE 61, 579-586, 1973.
- T. Ohtsuka and Y. Kyotani, "Superconducting Levitated High-Speed Ground Transportation Project in Japan," IEEE Trans. Magnetics MAG-11, 608-614, 1975.
- T. Ohtsuka and Y. Kyotani, "Superconducting Maglev Tests," IEEE Trans. Magnetics MAG-15, 1416-1421, 1979.
- E. C. Okress et al., "Electromagnetic Levitation of Solid and Molten Metals," J. Appl. Phys. 23, 545-552, 1952.
- B. T. Ooi, "Transverse Force in Magnetic Levitation with Finite Width Sheet Guideways," IEEE Trans. Power App. Sys. PAS-94, 994-1002, 1975.
- B. T. Ooi, "Electromechanical Dynamics in Superconducting Levitation Systems," IEEE Trans. Magnetics MAG-11, 1495-1497, 1975.
- B. T. Ooi, "Electromechanical Stiffness and Damping Coefficients in the Repulsive Magnetic Levitation System," IEEE Trans. Power App. Sys. PAS-95, 936-943, 1976.
- B. T. Ooi, "A Dynamic Circuit Theory of the Repulsive Magnetic Levitation System," IEEE Trans. Power App. Sys. PAS-96, 1094-1100, 1977.

B. T. Ooi and A. R. Eastham, "Transverse Edge Effects of Sheet Guideways in Magnetic Levitation," IEEE Trans. Power App. Sys. PAS-94, 72-80, 1975.

B. T. Ooi and O. P. Jain, "Moments and Force Densities of the Electrodynamic Levitation System," IEEE Trans. Magnetics MAG-15, 1102-1108, 1979.

B. T. Ooi and O. P. Jain, "Force Transients at Guideway Butt Joints in Repulsive Magnetic Levitation System," IEEE Trans. Power App. Sys. PAS-98, 323-329, 1979.

W. G. Pfann and D. W. Hagelbarger, "Electromagnetic Suspension of a Molten Zone," J. Appl. Phys. 27, 12-18, 1956.

J. R. Powell and G. I. Danby, "Magnetic suspension for levitated tracked vehicles," Cryogenics 11, 192-204, 1971.

J. H. Rakels, J. L. Mahtani, and R. G. Rhodes, "The Circular Form of the Linear Superconducting Machine for Marine Propulsion," IEEE Trans. Magnetics MAG-17, 127-129, 1981.

S. C. Rashleigh and R. A. Marshall, "Electromagnetic acceleration of macroparticles to high velocities," J. Appl. Phys. 49, 2540-2542, 1978.

R. Redlich, "Stability of Thin Metal Foils Levitated by ac Fields," J. Appl. Phys. 33, 231, 1962.

J. R. Reitz "Forces on Moving Magnets due to Eddy Currents," J. Appl. Phys. 41, 2067-2071, 1970.

J. R. Reitz and L. C. Davis, "Force on a Rectangular Coil Moving above a Conducting Slab," J. Appl. Phys. 43, 1547-1553, 1972.

P. L. Richards and M. Tinkham, "Magnetic Suspension and Propulsion Systems for High-Speed Transportation," J. Appl. Phys. 43, 2680-2691, 1972.

R. G. Rhodes and B. E. Mulhall, "The Wolfson magnetic levitation project," Cryogenics 15, 403-405, 1975.

A. G. Rubin, "Further Consideration of the Stability of Thin Metal Foils Levitated by ac Fields," J. Appl. Phys. 33, 2398, 1962.

M. S. Sarma and A. Yamamura, "Computer-Aided Analysis of Magnetic Fields in Nonlinear Magnetic Bearings," IEEE Trans. Magnetics MAG-14, 551-553, 1978.

D. Schieber, "Transient Eddy Currents in Thin Metal Sheets," IEEE Trans. Magnetics MAG-8, 775-779, 1972.

P. C. Sen, "On Linear Synchronous Motor (LSM) for High Speed Propulsion," IEEE Trans. Magnetics MAG-11, 1484-1486, 1975.

I. Simon, "Forces Acting on Superconductors in Magnetic Fields," J. Appl. Phys. 24, 19-24, 1953.

G. R. Slemmon, "The Canadian Maglev Project on High-Speed Interurban Transportation," IEEE Trans. Magnetics MAG-11, 1478-1483, 1975.

G. R. Slemon, P. E. Burke, and N. Terzis, "A Linear Synchronous Motor for Urban Transit Using Rare-Earth Magnets," IEEE Trans. Magnetics MAG-14, 921-923, 1978.

C. H. Tang, W. J. Harrold, and R. S. Chu, "A Review of the Magneplane Project," IEEE Trans. Magnetics MAG-11, 623-626, 1975.

K. Tendeloo, "Strong Eddy-Current Applications of Permanent Magnets," J. Appl. Phys. 30, 236S, 1959.

R. D. Thornton, "Design Principles for Magnetic Levitation," Proc. IEEE 61, 586-598, 1973.

R. D. Thornton, "Magnetic Levitation and Propulsion, 1975," IEEE Trans. Magnetics MAG-11, 981-995, 1975.

M. Tinkham, "ac losses in superconducting magnet suspensions for high-speed transportation," J. Appl. Phys. 44, 2385-2390, 1973.

O. Tsukamoto, Y. Iwata, and S. Yamamura, "Analysis of Ride Quality of Repulsive Type Magnetically Levitated Vehicles," IEEE Trans. Magnetics MAG-17, 1221-1233, 1981.

T. Umemori et al., "Study on Miniaturization of Electromagnet for dc Linear Motor," IEEE Trans. Magnetics MAG-16, 713-715, 1980.

L. Uranker, "Survey of Basic Magnetic Levitation Research in Erlangen," IEEE Trans. Magnetics MAG-10, 421-424, 1974.

K. E. Voevodskii and V. M. Kochetkov, "Theory of superconducting magnet suspension: main results survey," Cryogenics 21, 719-728, 1981.

A. K. Wallace, J. H. Parker, and G. E. Dawson, "Slip Control for LIM Propelled Transit Vehicles," IEEE Trans. Magnetics MAG-16, 710-712, 1980.

H. Weh, "Linear Synchronous Motor Development for Urban and Rapid Transit Systems," IEEE Trans. Magnetics MAG-15, 1422-1427, 1979.

J. T. Williams et al., "Modelling of Superconducting Screens for a New Form of Magnetic Suspension," IEEE Trans. Magnetics MAG-17, 2150-2153, 1981.

S. L. Wipf, "Propulsion of magnetically levitated trains," Cryogenics 16, 281-288, 1976.

C. H. Woods et al., "Stability Analysis of a Levitated Superconducting Current Ring Stabilized by Feedback and Eddy Currents," J. Appl. Phys. 41, 3295-3305, 1970.

P. F. Wuerker, H. M. Goldenberg, and R. V. Langmuir, "Electrodynamic Containment of Charged Particles by Three-Phase Voltages," J. Appl. Phys. 30, 441-442, 1959.

P. F. Wuerker, H. Shelton, and R. V. Langmuir, "Electrodynamic Containment of Charged Particles." J. Appl. Phys. 30, 342-349, 1959.

T. Yamada, M. Iwamoto, and T. Ito, "Levitation Performance of Magnetically Suspended High Speed Trains," IEEE Trans. Magnetics MAG-8, 634-635, 1972.

S. Yamamura, "Magnetic Levitation Technology of Tracked Vehicles Present Status and Prospects," IEEE Trans. Magnetics MAG-12, 874-878, 1976.

S. Yamamura and T. Ito, "Analysis of Speed Characteristics of Attracting Magnet for Magnetic Levitation of Vehicles," IEEE Trans. Magnetics MAG-11, 1504-1507, 1975.

K. Yoshida and S. Nonaka, "Levitation Forces in Single-Sided Linear Induction Motors for High-Speed Ground Transport," IEEE Trans. Magnetics MAG-11, 1717-1719, 1975.

5. SOURCES OF RING HEATING

It is important to limit the amount of heating that occurs in the moving ring. The primary reason for this limit is that if the superconducting ring gets too hot, then the superconducting current may go normal, resulting in one or more failure modes. It is also important to keep ring heating minimal for the sake of efficiency and economy. For the large refrigeration systems likely to be used in the MCKESR device, it takes approximately 500 W of electrical power to remove 1 W of heat from a source at 4 K to a heat sink at room temperature.

5.1 HEAT PRODUCTION FROM SKIN FRICTION

One of the primary sources of ring heating is frictional heating produced by contact between the rapidly rotating ring and the gas molecules in the tunnel. In the numerical examples in the following discussion, the tunnel gas is helium at 8 K. Some of the pertinent physical properties of helium are given in Table 5.1.

Table 5.1 Physical Properties of Helium

Property	Symbol	Value	Temperature (°C)	Reference
Viscosity	μ	1.97×10^{-5} Ns/m ²	25	1
Mean free path	L	1.9×10^{-7} m	25	2
Speed (rms)	u	1.26×10^3 m/s	25	3
Speed of sound	u_s	965 m/s	0	4
Density	ρ_g	0.1785 kg/m ³	25	5
Atomic mass	m	6.67×10^{-27} kg	-	-

Properties of helium at various temperatures are given in detail in Refs. 6 and 7.

According to the kinetic theory of gases, for an ideal gas:

- o μ , u, and u_s are independent of pressure, but proportional to $T^{1/2}$, where T is the temperature.
- o ρ_g is directly proportional to P/T, where P is the pressure.
- o L is directly proportional to T/P.

Assume a solid-ring design and examine the frictional heating due to momentum transfer parallel to the direction that the ring is moving (i.e., parallel to the ring surface). The amount of skin-friction power loss will

depend on the pressure and temperature of the helium in the tunnel. The types of analyses needed can be divided into two major regions, which are characterized by the Knudsen number

$$Kn = L / d , \quad (5.1)$$

where L is the mean free path of the molecules and d is a characteristic length of the problem. For a gas temperature of 8 K,

$$L_0 = 5.1 \times 10^{-9} \text{ m at } P_0 = 1 \text{ atm.}$$

5.1.1 Continuum Region (Kn < 0.01 to 0.1)

When $Kn < 0.01$ to 0.1 , the gas flow is that of a continuum and the Navier-Stokes equations should hold. For a characteristic length on the order of 1 cm, in order to get $Kn = 0.1$, a pressure P is needed, as follows:

$$P = \frac{P_0 L_0}{Kn d} = 5 \times 10^{-6} \text{ atm.} \quad (5.2)$$

The continuum-region assumption should be valid for pressures greater than this.

The force F per unit area A exerted on a plane moving with velocity v parallel to a stationary plane that is a distance d away is

$$F = \mu A v / d . \quad (5.3)$$

The power dissipated is $Q = F v$, or

$$Q = \mu A v^2 / d . \quad (5.4)$$

At 8 K, the viscosity is $\mu = 3.2 \times 10^{-6} \text{ Ns/m}^2$, according to ideal-gas behavior; according to Ref. 6, however, $\mu = 2.2 \times 10^{-6} \text{ Ns/m}^2$ at 10 K.

5.1.2 Free-Molecule Region (Kn > 5 to 10)

For $Kn > 5$ to 10 , the mean free path is longer than the characteristic length of the problem, and the Navier-Stokes equations will not hold. The ring surface and tunnel wall exchange molecules with each other, and the molecules suffer virtually no collisions with other molecules while in transit. For $d = 1 \text{ cm}$, this region is applicable whenever the pressure is less than about 10^{-7} atm .

The skin-friction heating can be calculated from an analysis of Couette flow⁸⁻¹⁰ with

$$Q = \frac{\sigma A \rho_g v^2 u_s}{2 \pi^{1/2}} , \quad (5.5)$$

where ρ_g is the gas density, u_s is the speed of sound, and σ is an accommodation coefficient. The accommodation coefficient is always less than or equal to 1; it is set equal to 1 in the following numerical calculations.

5.1.3 Accommodation Coefficient

The accommodation coefficient σ can be thought of in a simplistic fashion as the ratio of the number of molecules that stick to the surface to the number of molecules that strike the surface. (Those molecules that do not stick bounce off by way of specular reflection.) If a molecule reflects specularly from a surface, there is no tangential momentum imparted (i.e., no skin friction). This can be seen in Eq. 5.5, where if all the molecules striking a surface bounce off specularly, $\sigma = 0$, and hence $Q = 0$. It is clear that the MCKESR surface should be constructed so that σ is as low as possible.

In practice, the situation is somewhat more complicated than that just described. In order for a molecule to stick to the surface, enough of its momentum must be absorbed by the lattice of the solid that the molecule is stopped and can be captured in the attractive potential well at the surface. For molecules impinging at high velocities, capture is a rare event. The lattice simply cannot absorb enough momentum. Virtually all of the incident molecules bounce off. The accommodation coefficient σ is not zero, however, because many of the collisions are inelastic. Smooth surfaces should produce less momentum transfer than rough ones, because there will be fewer lattice molecules sticking out to intercept the incident molecules.

The energy of physisorption on a surface is roughly 3-10 times the van der Waals attraction energy. For helium-helium attraction, this energy is $E = 0.00088$ eV. The value $E = 0.01$ eV corresponds to $v = 700$ m/s.

The value of σ should decrease as the kinetic energy of the incident particle increases and as the angle of incidence approaches a path that is tangential to the surface. This behavior appears to have been seen in experiments¹¹. As a benchmark, a helium beam traveling at $v = 1770$ m/s, impinging on a $3 \mu\text{m}$ epitaxial layer of gold deposited on copper, had $\sigma = 0.2$ ¹². At $T = 8$ K and $v = 5000$ m/s, the molecules leaving or impinging upon the ring do so at an angle of about 1° to the surface tangent.

5.1.4 Transition Region ($0.1 < Kn < 5$)

For a pressure P corresponding to $0.1 < Kn < 5$ (10^{-7} atm $< P < 5 \times 10^{-6}$ atm), the analysis is complicated. For a first approximation, graphical interpolation can be used.

5.1.5 Results

We can factor the area out of Eqs. 5.4 and 5.5 to get the surface heating per area, $Q' = Q/A$:

$$Q' = \frac{\sigma \rho_g v^2 u_s}{2 \pi^{1/2}} \quad (5.6)$$

for the free-molecule region, and

$$Q' = \mu v^2/d \quad (5.7)$$

for the continuum region. The value of Q' is plotted as a function of tunnel pressure for several values of ring velocity in Fig. 5.1, with d chosen as $d = 1$ cm. The results presented in this figure can be used to calculate the expected values of skin-friction heating for different ring configurations. Values for several configurations are presented in Table 5.2 for the maximum ring velocity, using a 4 T magnetic field and ring current density of 10^4 A/cm². A pressure of 10^{-11} atm is assumed, $\sigma = 0.2$, and the ring height Z equals the ring width W .

Table 5.2 Skin-Friction Heating Q for Several Ring Configurations
($j = 10^4$ A/cm², $B = 4$ T, $P = 10^{-11}$ atm, $\sigma = 0.2$)

Radius, R (m)	Height, Z (= W) (m)	Density, ρ (kg/m ³)	Surface Area, A (m ²)	Velocity, v (m/s)	Power, Q (W)	Energy Stored, (MWh)
1,000	0.10	8,000	2,513	7,070	75	3,490
1,000	0.10	4,000	2,513	10,000	149	3,490
500	0.10	4,000	1,257	7,070	37	872
1,000	0.20	8,000	5,027	7,070	149	13,960

Inspection of Table 5.2 indicates that the ratio of skin heating to energy stored decreases with increasing ring radius R , ring height Z , and ring density ρ .

5.2 TUNNEL VACUUM

Skin-friction heating is directly proportional to the gas pressure around the ring; therefore, maintaining a good vacuum in the high-vacuum enclosure is necessary. The ability to maintain a high vacuum in this enclosure is greatly aided by the "self-pumping" action of the rotating ring, which makes the MCKESR very similar to the original Gaede molecular pumps¹³. In addition, a superconducting ring and tunnel wall result in a very good

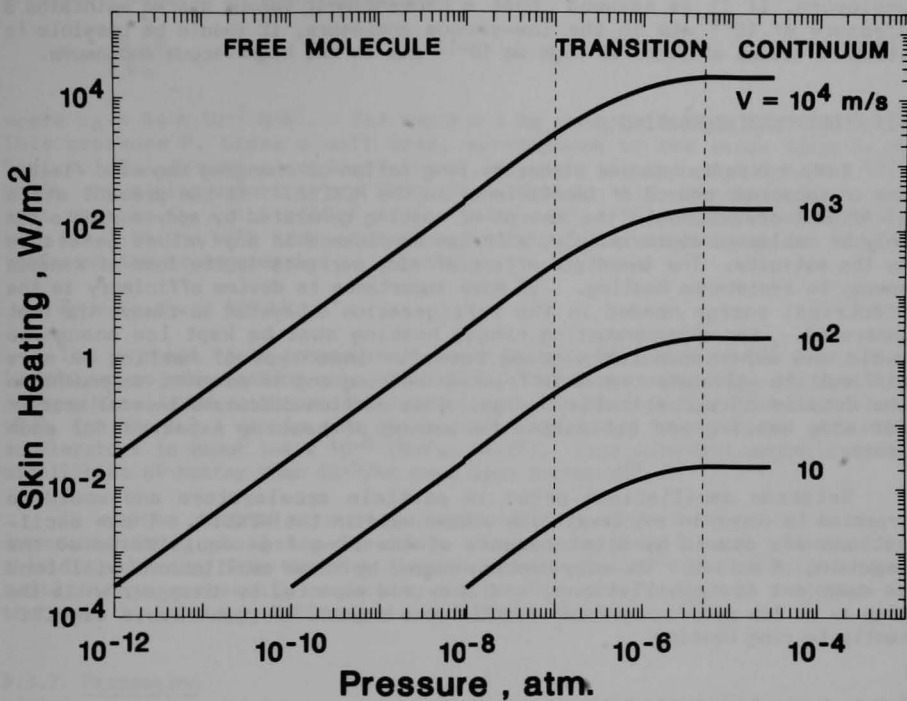


Fig. 5.1 Skin-Friction Heating as a Function of Pressure for Several Velocities

cryopump. With these two features, it should be relatively easy to produce a pressure ratio of 100,000 between the high-vacuum enclosure and the low-vacuum enclosure. If it is assumed that a conventional vacuum system maintains a pressure of 10^{-6} atm in the low-vacuum enclosure, it should be possible to attain a vacuum at least as high as 10^{-11} atm in the high-vacuum enclosure.

5.3 EDDY-CURRENT HEATING

Eddy currents, caused either by ring motion or changing magnetic fields, are an important source of inefficiency in the MCKESR. At the present state of MCKESR development, the amount of heating generated by eddy currents can only be estimated approximately, with low confidence in any values generated by the estimate. The immediate effect of eddy currents is the loss of kinetic energy to resistance heating. Of more importance to device efficiency is the electrical energy needed in the refrigeration subsystem to remove the heat generated. For superconducting rings, heating must be kept low enough to avoid the superconductor's going normal. This type of heating is more difficult to calculate than skin-friction heating and is somewhat dependent on the details of a particular design. This section discusses several sources for eddy heating and estimates the amount of heating expected for each source.

Betatron oscillations occur in particle accelerators and would be expected to occur in any levitation scheme used in the MCKESR. These oscillations are caused by displacements of the ring from equilibrium at the beginning of motion. The eddy heating caused by these oscillations will tend to damp out the oscillations, and they are expected to disappear while the ring is at low speed. Betatron oscillations should not contribute significantly to ring heating.

5.3.1 Levitation-Field Inhomogeneities

Ideally, the magnetic fields that levitate the MCKESR ring against centrifugal and gravitational forces should be homogeneous in the circumferential direction. Then, once betatron oscillations were damped out, there would be no eddy heating during coasting periods. In practice, there will always be some inhomogeneity in the circumferential direction, and this will cause heating when the ring moves. Eddy currents will be induced in the conducting skin of the ring and the normal conducting matrix of the superconductor.

The amount of heating generated can be estimated by treating the problem as the calculation of the drag force on a conducting track that is repulsively levitating a train containing a periodic magnetic field. (The conducting track is the skin of the ring, and the periodic magnetic field aboard the train is the inhomogeneity in the levitation magnetic field.) The analysis of Sec. 4.3.2, the high-speed, nonzero-track-thickness approximation, is appropriate.

Assume that the dominant field inhomogeneity can be represented by a mean amplitude of $\Delta B = 4 \times 10^{-4}$ T and a spatial period of $L = 10$ m. The mean pressure P exerted on the ring is then

$$P = \frac{2B \Delta B}{2 \mu_0}, \quad (5.8)$$

where $\mu_0 = 4\pi \times 10^{-7}$ N/A². For the $R = 1$ km example design, $P = 1270$ N/m². This pressure P , times a unit area, corresponds to the image force F_I of Sec. 4.3.2. Assume a conductivity of very pure aluminum at 4.2 K, $\sigma = 10^{11}$ mho/m, and a ring velocity, $v = 7000$ m/s. From Eq. 4.9, the drag force per unit area is $F_D = 4.8 \times 10^{-2}$ N/m². For a 10×10 cm ring cross-section, with $R = 1$ km and with eddy currents generated only on the top and bottom surfaces, the heat generated is given by

$$P_D = F_D A v = 420 \text{ kW}. \quad (5.9)$$

The average field inhomogeneity must be held to 1 part in 10^8 every 10 m to achieve an eddy heating rate of 40-50 W. This is a demanding, and possibly impossible, task with present technology. The average field inhomogeneity, $\Delta B/B$, for the 2-5 T dipole and quadrupole magnets of present day particle accelerators is about $1-4 \times 10^{-4}$ (Refs. 14-17). Time dependent magnetic field stabilities of better than 10^{-5} /hr have been achieved¹⁸.

It may be possible to reduce the heating rate further by using a superconducting shell for the ring. Such a shell may be more effective in shielding the ring from the high-frequency components of the field inhomogeneities than a normally conducting shell. This shield would be analogous to that used in shielding SMES magnets from field fluctuations¹⁹.

5.3.2 Precession

Section 4.5 discussed the problems associated with the Coriolis force acting on a large, rapidly moving ring. For a ring of $R = 1$ km traveling at $v = 7000$ m/s, it was found that the radial component of the levitational magnetic field must vary around the loop, providing a maximum differential force of 0.1 gravity. This corresponds to an image force $F_I = 1.0$ N/m², but now the spatial period is $L = 6280$ m. From the analysis of the previous section, the drag force is $F_D = 1.5 \times 10^{-6}$ N/m². With the same ring dimensions as in the previous section, this corresponds to an eddy-heating rate of $P_D = 13.2$ W.

5.4 REFERENCES

1. G. M. Barrow, Physical Chemistry, p. 21, 2nd Edition, McGraw-Hill, 1966.
2. Ibid, p. 48.
3. Ibid, p. 33.

4. CRC Handbook of Chemistry and Physics, 60th edition, p. E-47.
5. Ibid, p. B-82
6. F. E. Hoare, L. C. Jackson, and N. Kurti, Experimental Cryophysics, p. 362, Butterworths, 1961.
7. R. D. McCarty, "Thermophysical Properties of Helium-4 from 2 to 1500 K with Pressures to 1000 Atmospheres," NBS Report COM-75-10334, November, 1975.
8. S. A. Schaaf, "Rarefied Gas Dynamics," pp. 235-254 in Modern Developments in Gas Dynamics, ed. W. H. T. Loh, Plenum Press, 1969.
9. V. P. Shidlouskiy, Introduction to Rarefied Gas Dynamics, Elsevier, 1967.
10. M. N. Kogan, Rarefied Gas Dynamics, Plenum Press, 1969.
11. Rarefied Gas Dynamics, Proc. 9th International Symposium, Session E, 1974.
12. M. Seidl and E. Steinheil, "Measurement of Momentum Accommodation Coefficients on Surfaces Characterized by Auger Spectroscopy, SIMS and LEED," Paper E-9 in Rarefied Gas Dynamics, Proc. 9th International Symposium, 1974.
13. S. Dushman, Scientific Foundations of Vacuum Technique, p. 151-159, John Wiley & Sons, 1949.
14. H. E. Fisk, R. Peters, and R. Raja, "Room Temperature Harmonic Analysis of Superconducting Energy Saver Quadrupoles," IEEE Trans. Magnetics MAG-17, 420-423, 1981.
15. H. Hahn, "ISABELLE - a Progress Report," IEEE Trans. Magnetics MAG-17, 702-708, 1981.
16. R. A. Lundy, "State of the Energy Doubler," IEEE Trans. Magnetics MAG-17, 709-712, 1981.
17. Y. Okuma et al., "Measurements of the Inhomogeneities of Magnetic Fields in a Sector-Type SLIM Electromagnet," IEEE Trans. Magnetics MAG-17, 1234-1239, 1981.
18. H. R. Schneider and C. R. Hoffmann, "Independent Current Control in the Coupled Superconducting Coils of a Heavy-Ion Cyclotron Magnet," IEEE Trans. Magnetics MAG-17, 188-191, 1981.
19. T. Shintomi et al., "Construction of a Model Magnet for Shielded Pulsed Energy Storage," IEEE Trans. Magnetics MAG-17, 513-516, 1981.

6. RING-COOLING METHODS

Cooling of a superconducting ring that is moving at high velocity presents a formidable challenge. It is extremely unlikely that any solid connection can be made between the rapidly moving ring and the stationary tunnel. In addition, the high g-force due to centrifugal acceleration makes the design of moving parts on the ring very difficult. If the tunnel contains a high vacuum, the only way to transfer thermal energy from a rapidly moving ring to the tunnel wall is via radiation. Radiation transfer occurs at a very low rate at low temperatures.

Cooling of a nonsuperconducting ring has similar constraints, except that the ring surface is likely to be hot enough that radiative heat transfer is large. Of course, considerably more cooling is likely to be required for a nonsuperconducting ring than for a superconducting one.

This chapter discusses various possible methods to cool a moving superconducting ring. The most promising method is magnetic refrigeration, discussed in Sec. 6.3.

6.1 RADIANT COOLING

The primary method of cooling the rotating ring is to radiate energy from the ring surface to the tunnel walls. We assume that the tunnel walls are at approximately 5 K and are actively cooled. The power radiated by the ring to the tunnel is given by

$$P = \sigma A T^4, \quad (6.1)$$

where P is the power radiated, $\sigma = 5.67 \times 10^{-8} \text{ W m}^{-2} \text{ K}^{-4}$, A is the surface area of the ring, and T is the temperature of the ring surface in K. The emissivity of the ring surface is assumed equal to unity. The surface area is given by

$$A = 4 \pi R (Z+W), \quad (6.2)$$

where R is the ring radius, Z the ring height, and W the ring width. For our base case of one 10 by 10 cm ring with a radius of 1000 m, $\sigma A = 1.4 \times 10^{-4} \text{ W/K}^4$. The tunnel wall also radiates to the ring, but because the temperature of the tunnel wall is low, the amount radiated is small and is ignored in our calculations. Table 6.1 gives an indication of the power radiated from the ring for various ring surface temperatures.

The heat generated by skin friction and eddy currents is likely to be about 10-100 W. In order for the ring to dissipate most of this energy by radiation, the surface temperature must be significantly higher than the critical temperature of the superconducting wires. If the skin-friction heating energy is to be dissipated by radiation, good insulation is required between the ring surface and the ring conductors.

Table 6.1 Power Radiated from Ring Surface
($R = 1000 \text{ m}$, $Z = W = 10 \text{ cm}$)

Temperature (K)	Power (W)
10	1
20	11
30	113
40	358
50	875
80	5734
100	14,100

The power radiated from the ring could be increased by increasing the surface area of the ring. This could effectively be accomplished by projecting many radiating fins from the ring surface. The fins from the ring would interleave with similar fins attached to the tunnel wall. The tunnel-wall fins would be actively cooled. To significantly increase the ring surface area, many fins must be used and the fin thickness must be correspondingly small. The tunnel vacuum can be made high enough that skin-friction heating from the increased surface area will not be severe. However, two major problems are inherent with this cooling method. First, the fins must be made strong enough to withstand the large centrifugal forces. Second, the stability of the ring is more critical, because the ring fins must not contact the tunnel fins and their separation distance is small. If these problems can be solved, then radiative cooling of a superconducting ring is possible.

6.2 INERTIAL COOLING

Inertial cooling uses the heat capacity of the ring to maintain a sufficiently low temperature in the superconductors to prevent them from going normal. Heat generation in the superconducting part of the ring is minimized to allow the ring to spin as long as possible before recooling is necessary. The ring must be designed so that most of the heat generated on other parts of the ring is dissipated before it is transported to the superconducting part of the ring.

One procedure would be to initially cool the ring by pumping liquid helium through it. In the crudest form, one would attach hoses to the ring while the ring was stationary. After the ring had cooled to 4 K, one would detach the hoses, pump a good vacuum in the tunnel, and start the ring spinning. The ring would continue to rotate until it became hot, say at about 10 K. The ring would then be decelerated, stopped, and re-cooled. The cooling procedure would be as infrequent as possible (daily, at the worst).

The advantage of this method is that no helium has to be transferred to the ring while it is in flight, no refrigeration machinery need be located on the ring, and no radiation fins are required. This greatly simplifies ring design. The vacuum in the tunnel can be kept very high, because there is no deliberate outgassing from the ring. Pressure in the tunnel can be very low and the skin-friction thermal-cooling requirements consequently will also be low. A vacuum of 10^{-11} atm should be easy to obtain. The skin-friction heating for one 10 by 10 cm ring would be about 70 W.

6.2.1 Lattice Heat Capacity at Low Temperature

The problem with inertial cooling is that the heat capacity of most materials is very low at low temperature. The lattice heat capacity at low temperature is¹

$$C_L = 234 N k_B \left(\frac{T}{\theta_D}\right)^3, \quad (6.3)$$

where N is the number of atoms, $k_B = 1.38 \times 10^{-23}$ J/K is Boltzmann's constant, T is the absolute temperature, and θ_D is the Debye temperature. There is also a small additional heat capacity associated with the electronic motion; we will ignore this additional capacity.

For copper,

$$\rho = 8960 \text{ kg/m}^3,$$

$$N = (65 \text{ m}^3)(8960 \text{ kg/m}^3)(6 \times 10^{23}/63.5 \times 10^{-3} \text{ kg}) = 5.5 \times 10^{30},$$

$$C_L = (1.78 \times 10^{10} \text{ J/K})(T/\theta_D)^3.$$

For copper, $\theta_D = 310$ K, and $C_L = 596 T^3$.

The energy required to raise the ring from 5 K to 10 K is

$$\begin{aligned} E &= \int_5^{10} C_L dT \\ &= 1.40 \times 10^6 \text{ J}. \end{aligned} \quad (6.4)$$

If there is 30 W of heating on the average, the ring can spin for a time

$$t = 4.7 \times 10^4 \text{ s} = 13 \text{ h}.$$

Aluminum gives similar results.

If the ring is made of lead, $\rho = 11,350 \text{ kg/m}^3$, $N = 2.14 \times 10^{30}$, and $\theta_D = 88 \text{ K}$. We obtain a lattice heat capacity

$$C_L = 10,137 \text{ J}^3,$$

an increase by a factor of 17.

6.2.2 Magnetic Heat Capacity

At low temperatures the heat capacity of a magnetic material in an applied magnetic field is substantially higher than the lattice heat capacity. If a large fraction of the ring mass were magnetic material in good thermal (but not necessarily physical) contact with the superconductor, then the inertial cooling time would be at least an order of magnitude higher than that provided by the lattice heat capacity. An additional benefit is that once the ring approaches the critical temperature of the superconductor and must be powered down for recooling, the temperature of the magnetic material will decrease as the applied magnetic field decreases. A severe disadvantage of using a magnetic material is that the material will be attracted to the magnet supplying the field, and the equilibrium position will be unstable. This imposes an additional design constraint on the stability provided by the levitation system.

6.3 MAGNETIC REFRIGERATION

Probably the best way to refrigerate the ring is to use magnetic refrigeration. This technique has been used to obtain millikelvin temperatures in many low-temperature experiments. Magnetic refrigeration has the advantage of involving no moving parts and provides an efficiency very close to that of Carnot efficiency.

For the MCKESR, magnetic refrigeration would be coupled to a natural-convection thermal diode that connects the superconducting part of the ring with the magnetic material. This concept is illustrated schematically in Fig. 6.1, which shows the cross-section of a solid ring that includes the magnetic-refrigeration device. A similar scheme could be used with a modular ring. The refrigeration cycle is indicated in Fig. 6.2. The refrigerating magnetic field is provided by a separate set of magnets from that of the levitation field.

6.3.1 Thermal Diode

In Fig. 6.1 the superconducting material is shown surrounded by liquid helium at 4.2 K. The magnetic material is located far to the inside of the superconductor but is connected to it by the shell structure of the ring. Connecting passageways allow the helium to flow from the magnetic part of the ring to the superconducting part of the ring and vice versa. When the ring is moving, a strong acceleration exists toward the outside of the ring. If the magnetic material is colder than the superconductor, then natural convection will transport helium between the superconductor and the magnetic material.

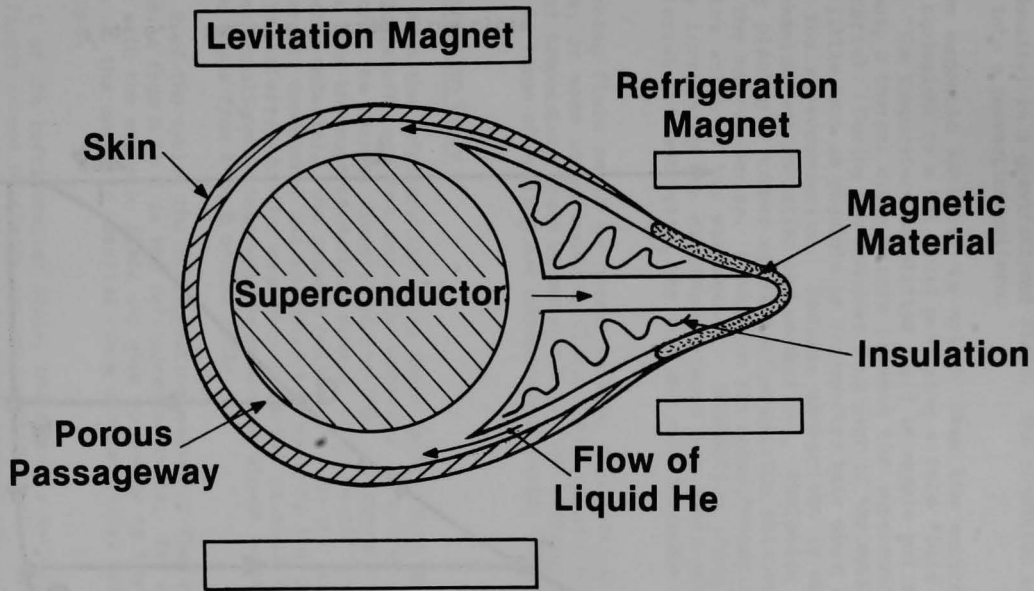


Fig. 6.1 Superconducting-Ring Cross-Section with Magnetic Refrigeration

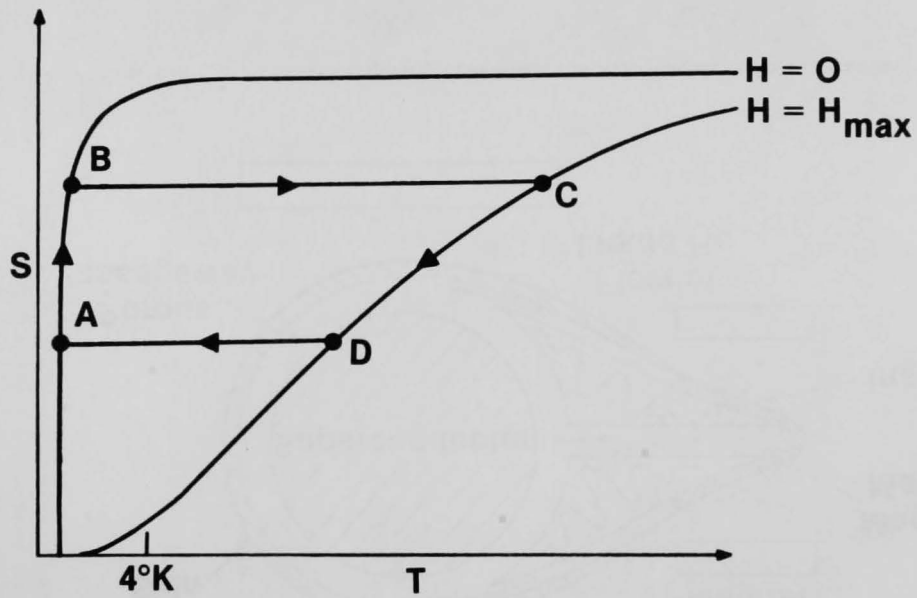


Fig. 6.2 Magnetic Refrigeration Cycle

The situation is equivalent to a hot fluid (low density) existing under a cold fluid (high density) in a gravitational field. The condition is unstable and destabilizes into a convection pattern.

When the magnetic material is hotter than the superconductor, the situation is equivalent to a hot fluid overlying a cold fluid in a gravitational field. The temperature-stratified fluid is stable and no convection is possible. Thus, a thermal diode exists between the superconductor and the magnetic material. During the nonconvecting part of the cycle, it is important that as little heat as possible be transported back along the temperature gradient to the superconductor. Because convection is suppressed, the transport mechanisms are radiation and conduction. Radiation can be easily minimized by placing a number of radiation shields between the magnetic material and the superconductor. Conduction can occur through the helium gas or through the walls of the passageway. Conduction along both paths is minimized by increasing the distance between the superconductor and the magnetic material and restricting the size and wall thickness of the passageways.

The working fluid could be normal helium, supercritical helium, superfluid helium, or some other working fluid. With superfluid helium, the superconductor temperature would be about 1.8 K. The refrigeration cycle will be described in terms of boiling and condensing of normal helium.

6.3.2 Refrigeration Cycle

At point A on the refrigeration cycle shown in Fig. 6.2, the refrigerating magnetic field is off, and the magnetic material is colder than the 4.2 K superconductor. The thermal diode is convecting. As energy is transferred to the liquid He from the superconductor, some of it boils off and is convected to the magnetic material. The gaseous helium gives up its latent heat to the magnetic material, condenses, and is convected back to the superconductor. Entropy is transferred to the magnetic material as some of the magnetic dipoles become nonaligned. This process occurs at almost constant temperature as the system moves from A to B on the cycle.

At point B of the cycle, the refrigerating magnetic field is turned on. The system moves from B to C in the refrigeration cycle. The magnetic dipoles are lined up with the magnetic field and give up energy to the lattice. The temperature of the magnetic material rises substantially, and the convection of helium stops.

At point C of the refrigeration cycle, the magnetic material is hot enough that a significant amount of energy can be radiated to the tunnel walls, which are kept at 4.2 K by circulation of liquid He through the walls. The entropy of the magnetic material decreases as the lattice energy is radiated away. The system moves from point C to point D in the refrigeration cycle.

At point D, the temperature of the magnetic material has decreased so much that the amount of energy radiated to the tunnel walls is not enough to keep the ring cold. At this point the refrigerating magnetic field is turned off, and the system moves from D to A in the refrigeration cycle. The magnetic material is once again colder than the 4.2 K superconductor, and the convection of He starts once again.

A candidate magnetic salt is gadolinium sulfate. The calculated entropy- vs.-temperature diagram for this salt is shown in Fig. 6.3. The diagram for gadolinium hydroxide, another candidate, is shown in Fig. 6.4. Inspection of these two figures indicates that a temperature of 30 K should be readily attainable.

6.3.3 Other Features

Should the refrigeration process fail for some reason, the ring has enough inertial cooling capacity to keep it cool during the "power-down" process. When the magnetic material is in the strong magnetic field, it will exist in unstable equilibrium. However, the forces near equilibrium are small and a restoring force is provided by the levitational field acting on the superconductor, as both parts of the ring are rigidly coupled.

Magnetic materials exist that can provide magnetic refrigeration in any temperature range, from room temperature down to below 1 K²⁻⁵. With a rotating magnetic-refrigeration device, cycle times of much less than a second have been reported². The same reference claims that a single liter of paramagnetic gadolinium can provide approximately 1 kW of refrigeration in the temperature range of interest for the MCKESR.

If the thermal-diode heat-transfer efficiency is not impaired by short cycle times, then the refrigerating magnets need not necessarily extend all the way around the loop and can remain on continually. Otherwise, the refrigerating magnets would have to be pulsed, possibly with a cycle time of several minutes, which would complicate the design and lower the overall efficiency. When the magnets are left on continually, the refrigeration is analogous to the rotating device described in Ref. 2.

The ring shell around the magnetic material should have a large surface area in order to radiate away as much energy as possible. This could be facilitated by projecting from the ring many fins containing magnetic material. These fins could interleave with actively cooled fins from the tunnel wall. Presumably, several stages could be coupled together in series if the maximum temperature from a single stage were not sufficient to radiate away enough energy. Neon could be used as the transport fluid in a second stage.

6.4 THERMOELECTRIC OR THERMOMAGNETIC COOLING

One possible method of cooling the ring is to use thermoelectric or thermomagnetic cooling to keep the superconductors cold while letting the ring surface attain a relatively high temperature. Cooling of the ring is then achieved by radiation to the tunnel wall. The amount of power radiated for a given ring surface temperature was given in Table 6.1.

ENTROPY OF GADOLINIUM SULFATE OCTAHYDRATE

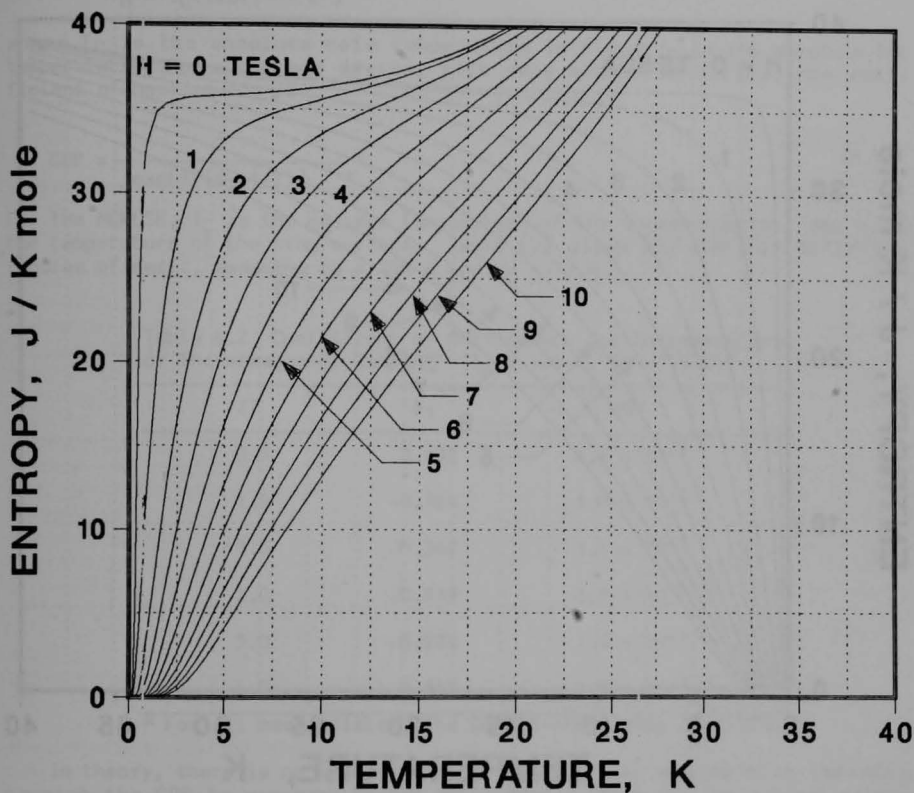


Fig. 6.3 Entropy vs. Temperature for Gadolinium Sulfate Octahydrate for Several Applied Magnetic-Field Strengths

ENTROPY OF GADOLINIUM HYDROXIDE

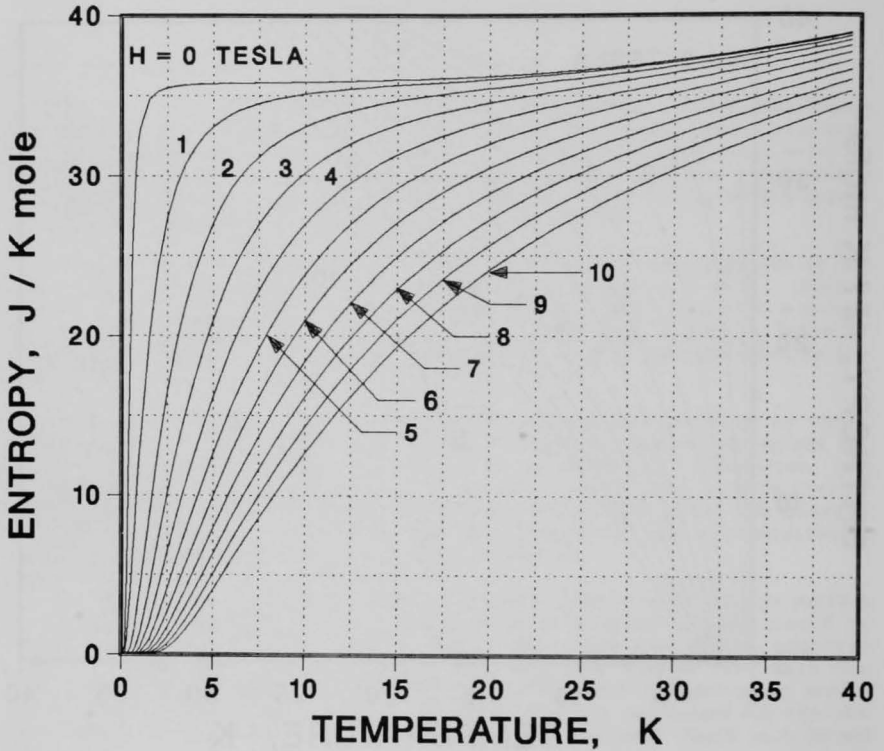


Fig. 6.4 Entropy vs. Temperature for Gadolinium Hydroxide for Several Applied Magnetic-Field Strengths

Thermoelectric and thermomagnetic refrigerators are characterized by a figure of merit ZT^6 . The coefficient of performance (COP) for a single stage device is given by

$$\phi_1 = \frac{T_C (1+ZT)^{1/2} - T_H/T_C}{T_H - T_C(1+ZT)^{1/2} + 1}, \quad (6.5)$$

where T_C is the absolute cold temperature in K and T_H is the absolute hot temperature. For a cascade device, with many stages in series, the coefficient of performance is

$$\text{COP} = \frac{1}{\exp[1/(\phi_1+1/2)] - 1}. \quad (6.6)$$

For the MCKESR, T_C is the maximum temperature of the superconductor, and T_H is the temperature of the ring surface. Table 6.2 gives the COP for different figures of merit, assuming $T_H = 100$ K and $T_C = 15$ K.

Table 6.2 Coefficient of Performance for Thermoelectric or Thermomagnetic Cooling ($T_H = 100$ K, $T_C = 15$ K)^a

ZT	ϕ_1	COP
0.5	0.432	4.4×10^{-7}
1.0	-0.384	1.8×10^{-4}
1.5	-0.347	1.4×10^{-3}
2.0	-0.319	4.0×10^{-3}
3.0	-0.274	1.2×10^{-2}
4.0	-0.242	2.1×10^{-2}

^a For all cases listed, the Carnot efficiency is 0.176.

In theory, there is no upper limit to ZT , with ZT approaching infinity causing the COP to approach Carnot efficiency. There are theoretical considerations that indicate thermomagnetic cooling will produce higher ZT at low temperature than will thermoelectric cooling. Production of the required magnetic field is certainly no problem with the MCKESR. In practice, a ZT of 1.0 has been attained for thermoelectric elements from 80 K to 700 K. Work on thermomagnetic cooling has received less research support, but a ZT of 0.5 was obtained in the early 1960s in a 1.5 T field⁶, with ZT still increasing with the field strength. It seems reasonable to assume that a ZT of 1.0 can readily be obtained in thermomagnetic cooling for temperatures from 15 K to 100 K. It does not seem reasonable that ZT s greater than 2.0 can be easily obtained. It may be difficult to obtain high ZT s at low temperature (15 K), because at the present state of the art it is not possible to tune the material's band structure to the required small energy gaps⁷.

6.5 STIRLING-CYCLE REFRIGERATORS

One possible refrigeration method is to actively cool the superconducting part of the ring with a Stirling-cycle (or some other cycle) refrigerator. Heat is pumped away from the superconductor to the outer part of the ring. Electrical power to run the refrigerator is inductively coupled into the ring. Although this scheme is possible, the moving parts of the refrigerator must function reliably under very high acceleration. There is very little experience with this type of design.

6.6 TRANSFER OF LIQUID HELIUM

Another possible method of actively cooling the ring is to squirt liquid helium from the inside of the tunnel wall to the moving ring. The helium is then transported passively through the ring by the high centrifugal acceleration and exits on the outside of the ring to the outer tunnel wall. The problem with this concept arises from the large ring velocity. A slug of liquid helium striking the ring wall could possibly ablate the wall and cause more heating than cooling. It is difficult to accelerate the helium up to the ring velocity (on the order of 5000 m/s) without the helium losing its cooling value. Another problem associated with this concept is the loss of vacuum due to helium outgassing from the transfer.

A similar possibility is the technique of in-flight refueling. In this concept, a tanker module is accelerated up to the ring velocity. Hot helium gas is pumped out of the ring to the tanker while cold helium from the tanker replaces it. The need for a separate tunnel and magnet system for the tanker, as well as the difficulty of docking at such high speeds and g-forces, makes this method seem unfeasible at this time.

6.7 REFERENCES

1. F. E. Hoare, L. C. Jackson, and N. Kurti, Experimental Cryophysics, Butterworth's, London, 1961.
2. W. A. Steyert, "Rotating Carnot-Cycle Magnetic Refrigerators for use Near 2 K," J. Appl. Phys. 49, 1227-1231, 1978.
3. G. V. Brown, "Magnetic Heat Pumping Near Room Temperature," J. Appl. Phys. 47, 3673-3680, 1976.
4. T. Hashimoto, T. Numasawa, M. Shino, and T. Okada, "Magnetic Refrigeration in the Temperature Range from 10 K to Room Temperature: The Ferromagnetic Refrigerants," Cryogenics 21, 647-653, 1981.
5. W. P. Pratt, Jr, S. S. Rosenblum, W. A. Steyert, and J. A. Barclay, "A Continuous Demagnetization Refrigerator Operating Near 2 K and a Study of Magnetic Refrigerants," Cryogenics 17, 689-693, 1977.
6. H. J. Goldsmid, Thermoelectric Refrigeration, Plenum Press, 1964.
7. C. Kooi, Private Communication, 1983.

7. POWER INPUT AND OUTPUT

7.1 SYNCHRONOUS MOTOR

For power input and output (I/O) to and from the MCKESR, the ring may be considered equivalent to the rotor of an induction motor/generator, and a number of well known designs are possible. There has been an impressive amount of research conducted on superconducting alternators and generators. The need to keep ring heating to a minimum suggests that a synchronous motor design is the most promising. Such a design, illustrated in Fig. 7.1, employs a set of current slabs embedded in the ring. A magnetic field follows each current slab synchronously around the loop. The magnetic field acting on the ends of the slabs produces the acceleration or deceleration, with the phase of the applied field changed by 180° to change the direction of the force. Because the current slab encounters a uniform field as it travels around the loop, eddy-current heating in the ring is minimized.

If the ring is composed of modules, then the current slab for power I/O can be identical with the currents used for constraint. One possible design is indicated in Fig. 4.3, where the power-I/O magnets sit between the dual synchrotron confinement magnets. In this design, only half of the ring volume is occupied by the modules. During acceleration and deceleration, the modules are kept in position around the loop by the synchrotron resonance principle. Any module that is lagging (leading) the equilibrium position automatically gets an increased (decreased) kick from the power magnets. During coasting periods, the ends of each module repel the ends of its neighbors.

In order to achieve low eddy-current heating, it is desirable to have the current in the slab as high as possible and the applied magnetic field as low as possible. Based on experience at Argonne National Laboratory with large pulsed magnets¹, the fraction of power dissipated in a circuit is proportional to $B \, dB/dt$, with 10 T/s corresponding to a fractional energy loss of 10^{-3} for $B = 1$ to 5 T.

To put 1000 MW of power into a ring traveling at a speed of 2000 m/s, a total force of 5×10^5 N must be generated. If there are 100 slabs in the ring, then a force of 2500 N must be generated on each 10-cm-long end. A current of 2.5×10^5 A in the slab will result in a required B of 0.1 T. To first order, the flux change in the loop is zero, but a second-order flux change results from magnetic field inhomogeneities. If it is assumed that 0.001% of the dB/dt for the magnets is imposed on the ring, with a frequency of 100 Hz (100 loops at 1 Hz), then $dB/dt = 10^{-3}$ T/s. The fractional energy loss is 10^{-8} . At 1000 MW of power insertion or extraction, the eddy heating is then 10 W. The design of the MCKESR power-I/O magnets is likely to be considerably different than that of the pulsed magnets of Ref. 1; however, the numbers used in the above calculation can serve as a first estimate until a more detailed design is available.

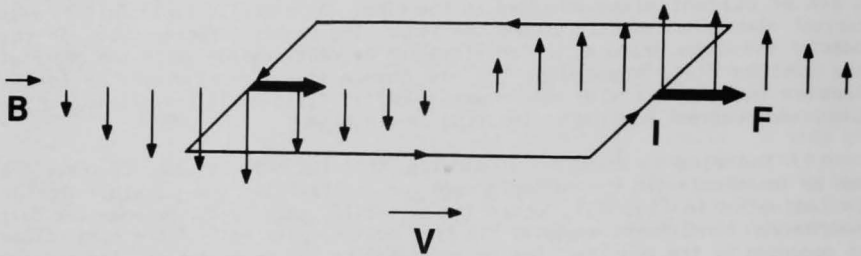


Fig. 7.1 Relationship between Applied Magnetic Field and Current Slab in Synchronous-Motor Power I/O Method (To first approximation, the net magnetic flux contained in the current slab is zero, resulting in low eddy heating.)

At a maximum field of 0.1 T, the power-I/O magnets need not be superconducting, but for purposes of estimating losses, the analysis of the previous paragraph can be applied. The fraction of energy lost in the magnets is 10^{-4} , and at a refrigeration factor of 500, this loss will require 50 MW of cooling. If the slab current is 10^6 A, then the magnets need only generate a field of 0.025 T, and the cooling requirements are then only 3.1 MW. This would also reduce the amount of ring heating to less than 1 W.

7.2 POWER CONDITIONING

The power-I/O magnets would be connected to the utility grid through a cycloconverter. Design of cycloconverters is relatively straightforward², although none as large as the one proposed here has been built. If a 3.5:1 frequency ratio is assumed as the operating range of the converter, then the speed of the MCKESR ring will range from 2000 m/s to 7000 m/s, and the MCKESR will be able to deliver 92% of the stored kinetic energy to the grid.

7.3 REFERENCES

1. S. H. Kim; S. T. Wang, and M. Lieberg, "Operating Characteristics of a 1.5 MJ Pulsed Superconducting Coil", Advances in Cryogenic Engineering 25, 90-97, 1979.
2. B. R. Pelly, Thyristor Phase-Controlled Converters and Cycloconverters, Wiley-Interscience, 1971.

8. CONTROL OF PERSISTENT CURRENTS

The control of the persistent superconducting-ring currents is one of the more challenging technical problems associated with the MCKESR. It is relatively easy to establish a persistent current in a stationary ring. However, as the ring spins, the persistent current is subject to degradation. Therefore, it seems desirable to control the persistent current without physical contact.

8.1 MAGNETIC INDUCTION

One method of controlling the ring currents is by magnetic induction, using the flux of the tunnel magnets that is linked with the ring superconductor. As the ring speeds up, the tunnel magnetic field must increase in order to balance the increased centrifugal force. If the ring is continuous, this increase in magnetic field induces a current in the ring. The sign of the current change is such that the ring current increases with increasing field, a stable situation to first order.

An inherent difficulty with control of the ring current by induction is that the ring is of finite width. More magnetic flux is linked with the outside of the ring than with the inside, and the current density of the outside of the ring will tend to increase faster than that of the inside as the ring speed increases. Unless the applied magnetic field is very carefully controlled, this differential increase in the current density will lead to instability; the outer portion of the ring will tend to flip up relative to the inner portion. A method to surmount this difficulty is to wind the superconducting cables helically around the ring, so that within one "stiffness length," the amount of magnetic flux linked to each cable is identical. The cables must be wound anyway for cryogenic stability, but until more detailed designs are considered, it is not clear whether the requirements of kinetic stability and cryogenic stability will be compatible.

For a modular ring, the magnetic flux linking each module is zero (to first order). Inductive control of the ring current must then be accomplished by changing the magnetic field at the fringes of the confinement magnets.

8.2 FLUX PUMP

An extremely attractive method of controlling the persistent ring currents without physical contact is by the use of a flux pump^{1,2}. Flux pumps have been built that are capable of controlling more than 1 kA of current with high efficiency. Application of the flux pump to the MCKESR would require that each superconducting cable in the ring come outside of the ring shell at some point so that the flux-pump magnet could interact with it. An example design is illustrated in Fig. 8.1. The flux pump must be carefully designed so that magnetic-field inhomogeneities at the current-control portion of each cable and ring heating induced by the flux-pump magnet are held to a minimum.

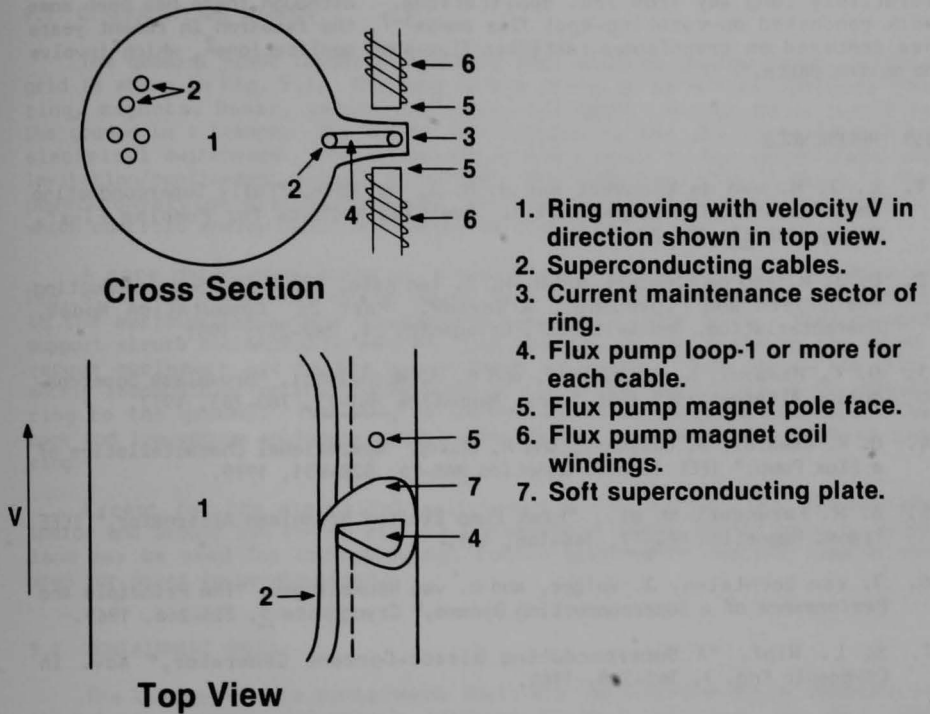


Fig. 8.1 Flux-Pump Method of Creating and Maintaining Persistent Current in a Superconducting Ring

While the flux pump appears to be an attractive technique for the MCKESR, research investigations carried out to date still leave the flux pump a relatively long way from real applications. Although there has been some work conducted on rotating-spot flux pumps³⁻⁷, the research in recent years has centered on transformer-rectifier flux-pump applications², which involve no moving parts.

8.3 REFERENCES

1. L. J. M. van de Klundert and H. H. J. ten Kate, "Fully Superconducting Rectifiers and Fluxpumps. Part 1: Realized Methods for Pumping Flux", *Cryogenics* 21, 195-206, 1981.
2. L. J. M. van de Klundert and H. H. J. ten Kate, "On Fully Superconducting Rectifiers and Fluxpumps. A Review. Part 2: Commutation Modes, Characteristics, and Switches", *Cryogenics* 21, 267-277, 1981.
3. O. K. Mawardi, S. A. Muelder, and R. A. Michelotti, "Brushless Superconducting Alternators," *IEEE Trans. Magnetics* MAG-13, 780-783, 1977.
4. O. K. Mawardi, A. Gattozzi, and H. Chung, "Operational Characteristics of a Flux Pump," *IEEE Trans. Magnetics* MAG-15, 828-831, 1979.
5. A. M. Ferendeci et al., "Flux Pump Excited Brushless Alternator," *IEEE Trans. Magnetics* MAG-17, 146-148, 181.
6. J. van Suchtelen, J. Volger, and D. van Houwelingen, "The Principle and Performance of a Superconducting Dynamo," *Cryogenics* 5, 256-266, 1965.
7. S. L. Wipf, "A Superconducting Direct-Current Generator," *Adv. in Cryogenic Eng.* 9, 342-348, 1964.

9. PLANT DESIGN

9.1 GENERAL PLANT DESIGN

The general plant layout of a MCKESR that would be coupled to the utility grid is shown in Fig. 9.1. The loop is the circular path that includes the ring, magnets, Dewar, vacuum enclosure, and support struts and is buried in the ground in a trench. The MCKESR is connected to the utility grid via an electrical switchyard. The switchyard provides power to the vacuum pumps and levitation/confinement magnets as needed. The switchyard also connects to the power-conversion station (probably a thyristor-controlled cycloconverter), which controls energy input and output to the rotating ring.

A more detailed diagram of a possible MCKESR tunnel design is shown in Fig. 9.2. The outer wall of the tunnel is a low-vacuum enclosure, connected to the surrounding ground (competent rock) with rock bolts. Warm-to-cold support struts mechanically connect the low-vacuum enclosure to the high-vacuum enclosure and to the magnet Dewar enclosure. These struts are ultimately responsible for the transmission of the centrifugal force of the moving ring to the ground. The ring is located in the high-vacuum enclosure. The rock and low-vacuum enclosure contain the MCKESR, and the magnets confine the ring.

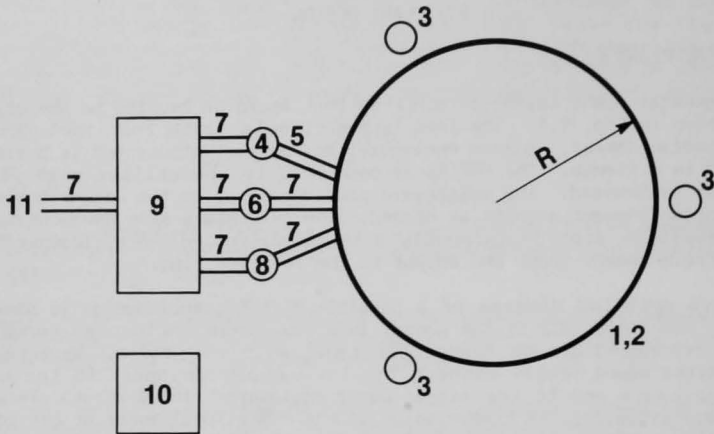
Except for the electrical switchyard and buildings, the land surface inside and around the tunnel will be undisturbed after construction. This land may be used for crop growing, cattle grazing, or whatever else it was used for prior to construction.

9.2 CONTAINMENT SHELL

The design of the containment shell and the transmission of pressure to the outside ground is essentially identical to that necessary for SMES, and the excellent work conducted for that technology¹⁻⁶ can be adopted almost directly for the MCKESR. The system is constructed in an excavated trench, and the pressure from the cold Dewar wall is transmitted to the warm bedrock via epoxy-fiberglass struts.

9.2.1 Dewar-Wall Heat Loss

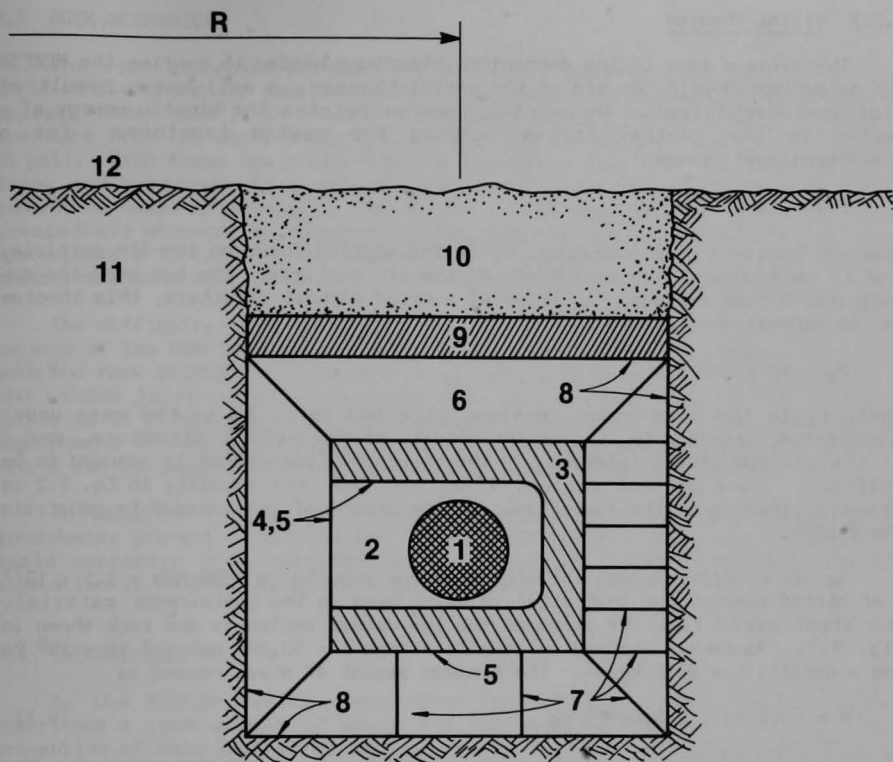
The space containing the pressure struts is evacuated and filled with superinsulation, and one or more actively cooled barriers are attached to the pressure struts to minimize heat leakage from the warm surface to the Dewar and to minimize the total room-temperature refrigeration load. For a structure the size of the MCKESR, the Dewar heat leakage contributes a large fraction of the total refrigeration load and is proportional to the total force needed to constrain the ring, independent of the device size. If the optimized design of the SMES research¹ is used and a refrigeration factor of 500 W of electricity per watt of heat removed is assumed, the estimated refrigeration power needed for a 7000 MWh device is 2.0 MW. This figure is proportional to the maximum energy stored and inversely proportional to the radius of the device.



- | | |
|--|--------------------------------|
| 1. Trench and Tunnel | 7. Power Transmission Lines |
| 2. Confining Magnets and Moving Ring | 8. Magnet Power Station |
| 3. Vacuum Pump Stations | 9. Electrical Switchyard |
| 4. Refrigeration Plant | 10. Control and Maintenance |
| 5. Refrigerant Leads | 11. Utility Transmission Lines |
| 6. Power Conversion Station
– Ring KE I/O | |

R is Typically ~ 1 km

Fig. 9.1 General MCKESR Plant Layout



- | | |
|---|--------------------------------|
| 1. Ring | 6. Low Vacuum Region |
| 2. High Vacuum Region | 7. Cold-to-warm Support Struts |
| 3. Confinement Magnets
Levitation Magnets
Power IO Coils
Refrigerant | 8. Low Vacuum Enclosure |
| 4. High Vacuum Enclosure | 9. Tunnel Cover |
| 5. Dewar Enclosure | 10. Backfill |
| | 11. Original Rock or Earth |
| | 12. Grade |

Fig. 9.2 Trench Cross-Section

9.2.2 Virial Theorem

The minimum mass of the mechanical structure needed to confine the MCKESR can be estimated with the aid of the virial theorem, a well-known result of classical mechanics⁷. The virial theorem relates the kinetic energy of a system to the central forces holding the system together. For a one-dimensional system,

$$E = -1/2 \sum_i \overline{F_i r_i}, \quad (9.1)$$

where E is the kinetic energy, F_i is the applied force on the i th particle, and r_i is the position coordinate of the i th particle. The bar over the sum indicates a time average. In terms of a solid support structure, this theorem may be expressed in the form

$$M_t - M_c \geq \rho E / \bar{\sigma}, \quad (9.2)$$

where M_t is the mass under tension, stressed to σ , M_c is the mass under compression, stressed to σ , ρ is the density of the support structure, and $\bar{\sigma}$ is the minimum stress tolerable in the structure (the stress is assumed to be uniform). In a perfect design, if $M_c = 0$ and the equality in Eq. 9.2 is assumed, then M_t is the lower limit to the amount of mass needed to constrain the system.

As an example, assume the stored energy amounts to 7000 MWh = 2.5×10^{13} J of stored energy, and that steel is being used as the containment material. The steel would take the place of the low-vacuum enclosure and rock shown in Fig. 9.1. Assume a maximum allowable stress $\sigma = 50,000$ psi = 3.45×10^8 Pa and a density $\rho = 8000$ kg/m³. The minimum amount of steel needed is

$$M = (\rho / \sigma) E = 5.8 \times 10^8 \text{ kg}. \quad (9.3)$$

If a cost of \$1.00/kg for the steel is assumed, a minimum cost for the containment structure is \$580 million. Comparison with the cost calculation of Sec. 10.2 indicates that this "perfect" design for the containment structure would more than double the total cost of the plant. Using aluminum instead of steel results in a similar cost. This calculation leads one to the economic constraint, identical to the case for SMES¹, that a containment structure of steel, aluminum, etc. is prohibitively expensive. Therefore, a low-cost material for the structure must be chosen, which will dictate that the device be placed in the ground. It must be emphasized that the virial theorem is a fundamental constraint⁸. No amount of clever design, where forces in one direction cancel forces in another direction, can avoid the minimum-confining-mass constraint of Eq. 9.2.

9.3 ROCK MECHANICS

The rock-mechanics problems for MCKESR are almost identical to those for SMES. While there are some unique design considerations, none of the problems appears formidable⁹. In the $R = 1$ km design example used in this report, the pressure from the outer Dewar wall to the rock is about 4×10^5 Pa (4 atm, or 60 psi). With these low pressures, the excavation does not have to go very deep, and numerous sites are available. The low-cost, open-trench type of excavation seems adaptable to the MCKESR. For comparison, note that compressed-air storage, or deep-buried SMES options, exert pressures on the rock approximately 10 to 50 times higher. If the rock formation allows higher pressures than 4 atm, then possibly a smaller Dewar vessel can be used.

The difficulty of determining rock loading stems from the fact that, because of the MCKESR doughnut shape, the tunnel wall will intersect the joint sets and rock principle stresses at every conceivable angle. Both systematic and random joints divide the rock mass, and the mechanical effect of these joints is to reduce stiffness and strength. However, once a probabilistic assignment of mechanical properties is made, the rock mechanics for a given MCKESR can be assessed with various finite-element computer programs.

An important parameter of the rock structure is the amount and type of groundwater present. Water contact with the Dewar wall should be minimized to avoid corrosion and undesired icing. Preventing excessive seepage into the excavation is another important design task.

9.4 THERMAL CONTRACTION

As the MCKESR device cools down from ambient temperature, it will experience a contraction of about 3 m for each kilometer of radius. The prevention of this contraction may place an intolerable mechanical stress on a device designed to operate at room temperature. SMES designs have solved the same contraction difficulties by rippling both the magnet conductors and the Dewar wall in the radial direction¹. As contraction progresses, the ripples straighten out, placing a minimal stress on the structure.

The MCKESR can use the same strategy for the Dewar, and possibly the magnet conductors could be rippled in the vertical direction; however, the task of minimizing field inhomogeneities then becomes enormous. A more promising approach would be to design the tunnel magnets and ring in modules. As the temperature decreased, the design would constrain the modules to contract in the circumferential direction. A small set of secondary tunnel magnets would be necessary to ensure a homogeneous magnetic field in the gaps.

9.5 SAFETY

The safety aspects of a large energy-storage device such as the MCKESR will be of paramount concern to any potential user. As would be true for a large massive flywheel, the potential for damage resulting from mechanical or magnetic failure is enormous if massive objects fly off at high velocity. The damage can be separated into two types: damage to the world outside of the

facility, and damage to the facility. The MCKESR must be surrounded by enough mass to confine the ring under normal operation. As for a SMES device, the most cost-effective method of accomplishing this is to bury the device in the ground. It should be possible to design the containment structure and ring so that upon catastrophic failure the ring vaporizes before it travels a significant distance. Although the magnetic energy associated with the ring current is a small fraction of the kinetic energy, it is sufficiently large to significantly raise the temperature of the ring if the superconducting current goes normal. If the containment structure can add more heat (e.g., by mechanical-friction or skin-friction heating due to increased gas pressure), then the ring or ring pieces should melt or vaporize before they leave the vicinity of the plant. A detailed analysis of the possible failure modes would have to be made before a plant were commissioned.

No utility will want to purchase a capital-intensive facility in which the risk of loss is significant. It is therefore important to design the MCKESR with a high degree of reliability from the very beginning. To minimize the cost of the stored energy, simple designs (such as the solid outer-wall levitation scheme illustrated in Fig. 1.2) are desired. However, the MCKESR concept is flexible enough that a large amount of redundancy can be incorporated. (The catcher magnet illustrated in Fig. 1.1 is an example.)

9.6 REFERENCES

1. R. W. Boom et al., Wisconsin Superconductive Energy Storage Project, Vol. I, July 1974.
2. R. W. Boom, et al., Wisconsin Superconductive Energy Storage Project, Vol. II, January 1976.
3. R. W. Boom ed., Proc. U.S.-Japan Workshop on Superconductive Magnetic Energy Storage, Madison, October 1981.
4. R. W. Boom, "Superconductive Energy Storage for Diurnal Use by Electric Utilities," IEEE Trans. Magnetics MAG-17, 340-343, 1981.
5. E. Hoffmann et al., "Design of the BPA Superconducting 30 MJ Energy Storage Coil," IEEE Trans. Magnetics MAG-17, 521-524, 1981.
6. J. D. Rogers, "Magnetic Energy Storage," IEEE Trans. Magnetics MAG-17, 330-335, 1981.
7. H. Goldstein, Classical Mechanics, pp. 69-71, Addison-Wesley (1950).
8. Y. M. Eyssa and R. W. Boom, "Considerations of a Large Force Balanced Magnetic Energy Storage System," IEEE Trans. Magnetics MAG-17, 460-462, 1981.
9. B. C. Haimson "Rock Mechanics Studies for SMES," pp. 228-237, Proc. U.S.-Japan Workshop on SMES, Madison, 1981.

10. PERFORMANCE ANALYSIS

10.1 EFFICIENCY

Overall efficiency is an important parameter in determining the cost of stored energy for the MCKESR. In this chapter a rough calculation for a prototypical 7000 MWh device, assuming no outage, is presented. The device is also assumed to be capable of receiving or transmitting power at 1000 MW. Many of the values (e.g., power lead losses) have been adapted from SMES research^{1,2}, as discussed below. A summary of the losses is presented in Table 10.1.

Table 10.1 Estimated Daily Losses for a 7000 MWh, 1000 MW MCKESR Plant Operating on a Diurnal Basis (R = 1 km)

Type of Loss	Energy Loss (MWh)
Dewar Loss	48
Magnet Current Leads	5.8
Power-I/O Leads	2.8
Magnet Losses (self)	2.0
Magnet Losses (due to ring)	48
Ring Losses	96
Bridge Connection to Grid	140
Power-I/O Magnet Losses	22
Total (at 300 K)	365

The average power loss is 15.2 MW, and the daily efficiency is 94.8%. The bridge connection to the grid does not require cooling, so a refrigerator rated at 9.4 MW at the compressor will handle the cooling load.

The Dewar heat loss was estimated from Sec. 9.2. The heat loss for the power-I/O leads was estimated directly from SMES research for a similarly sized storage unit. The heat loss for the magnet current leads was arbitrarily taken as twice the power-I/O loss. Because the MCKESR magnets are more than an order of magnitude smaller than the SMES magnets and may operate in persistent mode during coasting periods, this estimate is probably too high. The self-magnet losses consist of magnetic hysteresis, mechanical hysteresis, and eddy-current heating during charge and discharge periods. These losses were estimated as 0.067 those of a SMES system. The heating of the tunnel magnets due to motion of the ring was arbitrarily estimated at 8 kW, resulting in 2 MW of room-temperature refrigeration power. The ring heating, as discussed in Chapter 5, was estimated at 200 W. A refrigeration factor of 20,000 was assumed--a factor of 500 to go from 4 K in the tunnel wall to 300 K at the compressor, a factor of 20 to go from 2 K at the ring superconductor to 40 K at the ring heat-rejecting sector, and a factor of 2 for the ring refrigerator's efficiency. The loss for the bridge connection to the electric-power grid was taken as 2% of the maximum power rating. The cooling requirements for the power-I/O magnets were based on the discussion of Chapter 7.

Although the numbers in Table 10.1 are only approximate and are subject to revision once a more detailed design is available, it is reasonable to expect that if the MCKESR proves technically feasible, it will have an efficiency of 90% or better.

10.2 COST ANALYSIS

It is rather premature to suggest a cost for a technology that is still in the conceptual stages; however, a cost estimate is necessary to determine the attractiveness of such a device for potential users. This cost analysis, therefore, assumes that all technological problems have been solved. This analysis is based on figures developed for SMES devices¹⁻⁴. The results of this exercise are summarized in Table 10.2.

The calculated total capital requirement translates into a capital cost of \$66/kWh of energy storage. The cost of the conductor, magnet support structure, and vacuum enclosure was taken as 0.05 times that of a SMES unit of equivalent capacity. All other costs were taken as equivalent to that of a SMES unit. It must be noted that no cost optimization of the MCKESR design was attempted. The analysis also assumes a solid-ring design, with a relatively high on-site construction cost. If a modular ring is feasible, then more of the fabrication can be done at the factory, and the total cost should drop. The cost of the power-conditioning equipment is a large fraction of the total cost. It was assumed that the cost of an equivalently rated cyclo-converter is equivalent to a similarly rated Graetz bridge used in a SMES plant.

If only the basic total cost in Table 10.2 is used, a common procedure to make a technology seem cost-effective, the capital cost is \$42/kWh. As indicated by the comparison in Fig. 2.1, either cost makes the MCKESR extremely attractive when compared with existing energy-storage technologies. MCKESR has the advantage over pumped hydroelectric storage in that a mountain is not necessary. The advantage over compressed air is that fossil fuels do not have to be burned on discharge. In our cost analysis, we have not included the financial benefits inherent in a high-efficiency device. Use of the high-efficiency MCKESR (90+%) will result in less needed baseload capacity than a lower-efficiency pumped hydroelectric or compressed-air (70%) plant. No credit for this displacement was taken in the cost analysis.

Inspection of Table 10.2 indicates that the power-conditioning equipment constitutes more than one-third of the total cost. This cost component scales directly with the power rating of the device. For larger-radius units, power conditioning becomes the dominant cost factor. This is clearly an area for research on cost reduction and development of alternatives to thyristors.

The cost of a MCKESR with a nonsuperconducting ring, using attractive levitation as discussed in Sec. 4.4, can be similarly determined. With 4 T tunnel magnets and a 1.5 T ring, the ring cross-section needs to be approximately ten times larger to achieve the same amount of stored energy as in the superconducting-ring example. In Table 10.2, the conductor cost should be multiplied by about three and the magnet support structure cost by about ten. The cooling requirements should be about the same, with any increased eddy heating of the ring compensated by a gain of a factor of 40 in the removal of

Table 10.2 Capital Cost Estimate of 7000 MWh, 1000 MW
MCKESR Facility (R = 1 km)

Item	Cost (\$10 ⁶)
Preconstruction (mostly engineering design, 5% of direct cost)	14
Conductor (ring and magnets)	19
Magnet-Support Structure	12
Power-Conditioning System	100
Vacuum Enclosure	3
Refrigeration System	30
Struts	9
Thermal Shields	9
Helium Vessel	14
Construction	
Direct Cost	44
Indirect Cost (65%)	29
Miscellaneous Expense	<u>10</u>
Basic Total Cost	293
Contingency (25%)	<u>73</u>
Total Plant Investment	366
Allowance for Funds during Construction	64
Land and Inventory	<u>30</u>
Total Capital Requirement	460

the magnetic-refrigeration system. All of the other costs should be roughly the same. The basic total cost is then \$439 million, the total plant investment \$549 million, and the total capital requirement \$643 million. This translates into a capital cost of \$92/kWh of energy storage.

By the time that the MCKESR is ready for commercialization, 10 T (or higher) magnets made from Nb_3Sn should be available⁵. If instead of a 10 by 10 cm superconducting ring, a 20 by 20 cm magnetic-material ring is used, the 10 T magnets will give the same energy-storage density as that calculated here for the superconducting ring. The amount of conductor in the tunnel magnets should cost about the same, and the cost of the ring will be less. The Dewar, refrigerators, etc. should be about the same. Once the Nb_3Sn technology becomes available, the total cost for a MCKESR with a nonsuperconducting ring should be roughly equivalent to the costs indicated in Table 10.2.

An important item to remember is that the present cost analysis is based on an initial design example and not on a design that has been optimized.

10.3 REFERENCES

1. R. W. Boom et al., Wisconsin Superconductive Energy Storage Project, Vol. I, July 1974.
2. R. W. Boom, et al., Wisconsin Superconductive Energy Storage Project, Vol. II, January 1976.
3. B. M. Winer and J. Nicol, "An Evaluation of Superconducting Magnetic Storage," IEEE Trans. Magnetics MAG-17, 336-339, 1981.
4. S. T. Lee, R. S. Albert, and D. T. Imamura, "Evaluation of Superconducting Magnetic Energy Storage Systems," Report EPRI EM-2861, Feb. 1983.
5. C. R. Spencer, et al., "Production of Nb_3Sn by the In-Situ Process," IEEE Trans. Magnetics MAG-17, 257-260, 1981.

11. FUTURE DEVELOPMENT

A large amount of research and development will be necessary before the MCKESR passes from its present conceptual stage to commercialization. There is no reason to conclude that a MCKESR device in some form will not be technically feasible. As pointed out earlier in this report, magnetically levitated trains with velocities of 100 m/s are a present-day reality. Clearly, a large MCKESR running at this velocity can be made. The question that needs to be addressed is how far technology can be pushed in order to make a cost-effective MCKESR device that runs at 7000 m/s. Several avenues that extend technology toward this goal have been explored in this report. Sec. 11.1 discusses some of the key research areas that need to be addressed before a cost-effective MCKESR is found to be technically feasible. The discussion is limited to needs that are unique to MCKESR and unlikely to be developed in research on other technologies. Sec. 11.2 discusses specialized applications that might be suitable for MCKESR while it is still in the developmental stages.

11.1 CRITICAL RESEARCH NEEDS

It is not clear that this report has exhausted all of the major design options available to MCKESR. An important research task is to identify the remaining options, and to examine the critical research needs associated with each option. This task will require input from many diverse technologies.

Many of the laboratory experiments will benefit from access to a rotating environment. Experiments on different MCKESR components could be performed in a centrifuge, rather than in a small, specially built version of a MCKESR. The centrifuge must be able to contain cryogenic experiments that occupy approximately the cross-section of the ring (10-20 cm). To avoid a significant influence from centrifuge curvature, the radius of the centrifuge should be approximately 1 m. To produce the equivalent centrifugal force that would be encountered in the MCKESR base design, the centrifuge should be capable of 5000 gravities, although experiments conducted at relatively lower g-forces should be acceptable for some purposes. Adaptation of several existing experimental cryogenic alternators or generators for this task seems possible.

As was discussed in Chapter 6, a workable magnetic refrigerator is the most viable option for continuously cooling the rotating superconducting ring. A refrigerator of this type has never been built, and the determination of its feasibility is an important research need.

Control of the persistent superconducting-ring current, independent of the applied external magnetic field, is desirable in order to ensure dynamic stability of the ring. The ability to cool the ring is limited, so this control must be accomplished with a minimal amount of ring heating. A homopolar-type flux pump¹ appears to be the best way to achieve contactless control of the ring currents. A prototype device could be designed and investigated experimentally using the centrifuge, establishing and changing a superconducting current on a rotating conductor. Several design iterations would determine whether a flux pump with sufficiently low ring heating is feasible.

It is necessary to keep ring heating to a minimum in order to keep the demands on the ring-cooling system low. Eddy-current heating of the moving ring is the most uncertain, and probably the largest, fraction of the ring's heating load. The major eddy heating modes for the most likely MCKESR designs (both superconducting and nonsuperconducting rings) need to be investigated, both theoretically and experimentally. The best methods for obtaining good tunnel-magnet field homogeneity need to be identified. A theoretical and experimental investigation of the use of thin superconducting shields on the ring and tunnel wall to minimize the eddy heating is also important.

The requirement that the ring contain a persistent superconducting current imposes a severe design constraint on the MCKESR, since contactless cooling of the ring is difficult to achieve at the rate of heat transfer calculated as necessary. An alternative approach is to use a nonsuperconducting ring that is composed of a magnetic material (e.g., iron). In this case, the ring temperature is allowed to float, and any heat generated in the ring is eventually radiated to the tunnel walls, where it is relatively easy to remove. Most designs of this type do not yield sufficiently high energy-storage densities to make the cost of storage very attractive. A possible exception is the attractive levitation of a magnetic ring using a superconducting shield in the tunnel wall to provide vertical stabilization. This method was illustrated in Fig. 4.2 and discussed briefly in Sec. 4.4. Because the magnetic material will saturate, this design is not likely to achieve as high an energy-storage density as a MCKESR with a superconducting ring. However, the storage density is high enough that the simplicity of the ring design should make the storage costs attractive, especially if the higher magnetic fields associated with Nb_3Sn superconductors become available for the tunnel magnets.

The use of superconducting shields for this design is desirable in that associated drag forces should be very low. An alternative that should not be ruled out is to provide vertical levitation by the use of a small, inhomogeneous field acting on a conductor located on the ring. The vertical forces are small compared with the radial forces, so the associated drag force may be tolerable. Even active feedback for stabilization of this attractive levitation scheme needs to be investigated.

Other research areas, such as rock mechanics, refrigeration design, and power I/O, also need to be investigated, but these areas are not as critical as the ones discussed above. Also, further advances in these areas are likely to be made in the investigation of other technologies (e.g., SMES).

11.2 POSSIBLE TECHNOLOGICAL NICHES

New technologies, such as the MCKESR, are usually expensive during the early developmental stages and cannot compete with existing, in-place technologies. Very often a new technology must find some small use or "technological niche" to keep it in existence while it is developed and improved. The steam engine is a case in point.

For MCKESR, the need to find a technological niche is especially acute. Most of the early developmental work will consist of laboratory experiments on a rather small scale. Unfortunately, it is not clear that results from experiments on a small scale can be extrapolated reliably to large-size devices. The large amount of resources necessary to build several intermediate-size devices before a 1 km device is built may be difficult to justify for such a risky technology as the MCKESR. It is imperative that a niche be found for a medium size ($R = 20$ m) MCKESR if the progress to utility-size devices is to be made smoothly.

Some of the alternative applications for MCKESR were mentioned in Sec. 1.2. Another utility application that might be appropriate for a smaller-sized MCKESR is the damping of low-frequency instabilities in large, high-voltage power-transmission lines. A 30 MJ SMES unit with a 10 MW converter is operated for this purpose by the Bonneville Power Administration³. Another possible utility application is as a suppression system for voltage fluctuation and flicker⁴.

One very appealing niche would be the construction of a small ($R = 5$ -20 m) MCKESR in the form of a user facility for scientists. Experiments in many diverse fields could be conducted at the facility. Examples are (1) production of very-high-quality vacuums and (2) high-velocity monoenergetic molecular beams for materials studies. The 7000 m/s ring velocity for the example design in this report is only a factor of 70 higher than the 100 m/s velocity of magnetically levitated trains in commercial operation. A small MCKESR might find a niche as an advanced test facility for maglev-train concepts. It can be expected that more exciting and viable ideas along these lines will emerge as preliminary work on the MCKESR progresses and more people become familiar with its potential.

A side benefit that a MCKESR facility might exhibit is the provision of pulsed power to very-high-field (100 T) magnets used for materials studies⁴. Capacitors are presently used in this application, but because of the low energy-storage density inherent in capacitors, only very short pulses (ms) have been available.

11.3 REFERENCES

1. J. E. C. Williams, Superconductivity and Its Applications, pp. 156-160, Pion Limited, 1970.
2. R. E. Gomory, "Technology Development," Science **220**, 576-580, 1983.
3. E. Hoffmann et al., "Design of the BPA Superconducting 30 MJ Energy Storage Coil," IEEE Trans. Magnetics **MAG-17**, 521-524, 1981.
4. T. Shintomi and M. Masuda, "Pulse Superconductive Energy Storage," Proc. U.S.-Japan Workshop on SMES, pp. 442-454, Madison, 1981.

Distribution for ANL-84-19Internal:

J. W. Allen	J. J. Roberts
J. Asbury	G. S. Rosenberg
L. Burris	W. W. Schertz (15)
B. C. Chen	A. Schriesheim
R. L. Cole	W. T. Sha
E. Croke	R. S. Zeno
A. J. Gorski	ANL Patent Dept.
J. R. Hull (40)	ANL Contract File
R. L. Kustom	ANL Libraries (3)
A. I. Michaels	TIS Files (6)
P. A. Nelson	

External:

DOE-TIC, for distribution per UC-94b (150)

Component Technology Division Review Committee:

- D. Anthony, General Electric Company, Schenectady
- A. Bishop, U. of Pittsburgh
- B. Boley, Northwestern U.
- F. Buckman, Wood-Leaver & Associates, Monroeville, PA
- R. Cohen, Purdue U.
- J. Weisman, U. of Cincinnati
- R. Boom, U. Wisconsin, Madison
- R. A. Leacock, Iowa State U.
- K. Lofstrom, Launch Loop, Portland, OR
- W. McClain, Pioneer Hybrid, Johnston, IA
- J. Purcell, General Atomic, San Diego, CA
- R. Smith, Fermi National Accelerator Laboratory
- H. Sparks, MTS Corporation, Minneapolis, MN

ARGONNE NATIONAL LAB WEST
3 4444 00024037 4 X

ARGONNE NATIONAL LAB WEST
3 4444 00024037 4 X

ARGONNE NATIONAL LAB WEST
3 4444 00024037 4 X

ARGONNE NATIONAL LAB WEST
3 4444 00024037 4 X

ARGONNE NATIONAL LAB WEST
3 4444 00024037 4 X

ARGONNE NATIONAL LAB WEST
3 4444 00024037 4 X

ARGONNE NATIONAL LAB WEST
3 4444 00024037 4 X

ARGONNE NATIONAL LAB WEST
3 4444 00024037 4 X

ARGONNE NATIONAL LAB WEST
3 4444 00024037 4 X

ARGONNE NATIONAL LAB WEST
3 4444 00024037 4 X